

1

A UNIFIED METHOD FOR PREDICTING THE PERFORMANCE OF SUBSONIC DIFFUSERS OF SEVERAL GEOMETRIES

AD642497

BY

A. B. COCANOWER, S. J. KLINE, and J. P. JOHNSTON

PREPARED UNDER FINANCIAL SUPPORT OF
GENERAL ELECTRIC COMPANY
GENERAL MOTORS RESEARCH LABORATORIES
CONTRACT AF 49(638)-1278
MECHANICS DIVISION, AIR FORCE OFFICE OF SCIENTIFIC RESEARCH

CLEARINGHOUSE FOR FEDERAL SCIENTIFIC AND TECHNICAL INFORMATION			
Hardcopy	Microfiche		
3,00	165	108	PP WS
1 ARCHIVE COPY			



REPORT PD-10

THERMOSCIENCES DIVISION
DEPARTMENT OF MECHANICAL ENGINEERING
STANFORD UNIVERSITY
STANFORD, CALIFORNIA

DDC
NOV 30 1966
AW

MAY 1965

Department of Mechanical Engineering
Stanford University
Stanford, California

July 15, 1965

ERRATA (incomplete)

for Report PD-10 by Cocanower, Kline and Johnston

Page 16, line 17: $\frac{dR}{dx} R(x)$ should read $\frac{dR}{dx} / R(x)$.

Page 19, eq. (18) should read:

$$A_e(x) = \pi R^2(x) - 2\pi R(x)\delta^*(x)$$

A UNIFIED METHOD FOR PREDICTING
THE PERFORMANCE OF SUBSONIC DIFFUSERS OF SEVERAL GEOMETRIES

by

A. B. Cocanower, Research Assistant

S. J. Kline, Professor

J. P. Johnston, Associate Professor

Prepared under financial support of
General Electric Company
General Motors Research Laboratories
Contract AF 49(638)-1278 for
Mechanics Division, Air Force Office of Scientific Research

Report PD-10

Thermosciences Division
Department of Mechanical Engineering
Stanford University
Stanford, California

May 1965

ACKNOWLEDGMENTS

The authors wish to acknowledge the comments and suggestions of Professor J. K. Vennard.

The grant of computer time (refer NSF-GP948) by the Stanford University Computation Center and the financial support of the continuing Internal Flow Program by the General Motors Corporation, the General Electric Company, and the Air Force Office of Scientific Research are gratefully acknowledged.

Finally, Mrs. Betty Jane Emory and Miss Sarah Mitchell, who typed the report, are also gratefully acknowledged.

ABSTRACT

→ A unified performance prediction method has been developed for class A diffusers. Class A diffusers are those diffusers which have the following flow and geometry restrictions:

Flow restrictions

1. Subsonic, i.e., $0 \leq M_1 \leq M_{\text{choking}}$,
2. Inlet Reynolds number, $Re \geq 25,000$,
3. Symmetric inlet velocity profile,
4. Unstalled,
5. The flow is divisible into an effective core flow plus turbulent boundary layers. (An effective core flow is that flow with a uniform velocity profile and a flow area equal to the diffuser cross-sectional area minus the flow blockage area.)

Geometric restrictions

6. General,
 - a. Symmetric,
 - b. Non-turning,
7. Structural,
 - a. Two-dimensional,
 - b. Three-dimensional, i.e., a diffuser with rectangular cross-section and plane walls that diverge in both directions normal to the flow direction,
 - c. Conical,
 - d. Annular.

The prediction method is a system of linear, first order differential equations. These equations embody the momentum equation, continuity equation, and two empirical correlation equations. The correlation equations, due to von Doenhoff and Tetervin, are known to be less than totally adequate for boundary layer calculations. However, they appear to be sufficient for the present purpose since prediction of

diffuser performance is insensitive to the boundary layer calculation method.

In addition to the prediction method, two parameters have been developed to characterize inlet conditions and separation respectively: B_1 is defined as the ratio of the inlet boundary layer blockage area to the total inlet area; $B_1 \leq 0.05$ indicates those flows which can be divided into an effective core flow plus turbulent boundary layers. β^* is a correlation of first appreciable stall in a diffuser; it provides a means to terminate analytical calculations.

The predicted results include:

1. Performance charts; i.e., contours of constant pressure recovery on a plane of area ratio versus non-dimensional length;
2. Predicted effects of Reynolds number, Mach number, wall contour, corners, and diffuser geometry on pressure recovery for class A diffusers.

BLANK PAGE

TABLE OF CONTENTS

	Page
Acknowledgments	111
Abstract.	iv
Table of Contents	vii
List of Figures	viii
Nomenclature.	ix
Glossary.	xii
Chapter 1 - Introduction.	1
A. General Remarks	1
B. Objective	1
C. Historical Survey of Diffuser Research.	4
D. Closing Remarks	7
Chapter 2 - Analysis.	10
A. Flow Model Motivation	10
B. Developing Equations for the Flow Model	14
C. Development of Parameters for Blockage and Stall; Relations among Performance Parameters	21
Chapter 3 - Comparison of Data and Predictions.	27
A. Objective of Comparison between Data and Predictions	27
B. Input Data Requirements for Flow Model.	27
C. Results of the Comparison between Data and Predictions	29
D. Conclusions of Comparison between Data and Predictions	40
E. β^* Data Comparison	41
Chapter 4 - Predicted Results	43
A. Performance Charts.	43
B. Additional Calculated Effects	46
C. General Conclusions	50
Chapter 5 - Conclusions	51
References.	79
Appendix A - Detailed Flow Equations.	83
Appendix B - Corner Boundary Layer Correction	91
Appendix C - Letter of Permission from Ingersoll-Rand Company.	93
Appendix D - Suggested Critical Experiments	94

Figure	LIST OF FIGURES	Page
1	Diffuser flow regimes as established by Fox and Kline [1962] for two-dimensional diffusers	52
2	Diffuser geometries with nomenclature.	53
3	Coordinate system used in developing the two-dimensional boundary layer equations	55
4	Relation of "a" to the bounding streamline	55
5	Coordinate system used in developing the axisymmetric boundary layer equations.	55
6	Comparison between theory and Carlson's [1965] data for a two-dimensional diffuser.	56
7	Comparison between theory and Sprenger's [1959] data for a conical diffuser.	57
8	Comparison between theory and Sovran and Klomp's [1964] data for an annular diffuser.	58
9	Comparison between theory and Copp's [1951] data for compressible flow in a conical diffuser .	59
10	Comparison between theory and Johnston's [1959] data for compressible flow in an annular diffuser.	60
11	Comparison between theory and Nelson and Popp's [1949] data for compressible flow in an annular diffuser	61
12	Comparison of measured and theoretical recovery. .	63
13	Comparison among contours of $\beta^* = 0.48$, line a-a, and maximum pressure recovery for two-dimensional diffusers.	64
14	Comparison between contours of $\beta^* = 0.48$ and maximum pressure recovery of several researchers for conical diffusers.	65
15	Comparison between contours of $\beta^* = 0.48$ and maximum pressure recovery for annular diffusers. .	66
16	The effect of H_1 on contours of $\beta^* = 0.48$ for two-dimensional diffusers.	67
17	Performance charts for two-dimensional diffusers .	68
18	Performance charts for three-dimensional diffusers	70
19	Performance charts for conical diffusers	72
20	Performance charts for annular diffusers	74
21	The predicted effects of inlet boundary layer shape parameter, H_1 , on two-dimensional diffuser performance.	76
22	The predicted effect of B_1 on pressure recovery at constant area ratios for class A diffusers. . .	78

NOMENCLATURE

- a - distance used to define the rate of divergence of the core flow of a diffuser (see Eqn. 7)
- AR - diffuser area ratio, A_2/A_1
- AR(x) - local area ratio, $A(x)/A_1$; $1 \leq AR(x) \leq AR$
- AS - diffuser aspect ratio, b/W_1
- $A_e(x)$ - effective core area (local cross-sectional area minus the local boundary layer blockage area)
- A_{δ^*} - boundary layer blockage area
- B(x) - the ratio of the boundary layer blockage area to the total area
- B_1 - B(0) or inlet blockage (see table on page 23)
- b - distance between parallel walls of a two-dimensional diffuser, or the longer of the two inlet dimensions for a three-dimensional diffuser
- C_p - static pressure recovery, $\frac{\bar{P}_2 - \bar{P}_1}{\bar{q}_1}$
- $C_p(x)$ - local value of pressure recovery in a passage
 $\frac{\bar{P}(x) - \bar{P}_1}{\bar{q}_1}$
- \bar{C}_p - static pressure recovery, $\frac{\bar{P}_2 - \bar{P}_1}{q_1}$, based on the centerline dynamic head q_1 (without overscore)
- C_{p1} - ideal static pressure recovery based on one-dimensional, inviscid flow
- \hat{D} - characteristic length for Reynolds number
 W_1 for two-dimensional and three-dimensional diffusers
 R_1 for conical diffusers
 $\Delta R_1 = R_{O,1} - R_{I,1}$ for annular diffusers
- Eu - local Euler number
- H - boundary layer shape parameter, δ^*/θ
- L - diffuser wall length
- M(x) - local Mach number
- N - axial length of a diffuser

- \hat{N} - non-dimensional axial diffuser length
 N/W_1 for two-dimensional and three-dimensional diffusers
 N/R_1 for conical diffusers
 $N/\Delta R_1$ for annular diffusers
- P - static pressure
- \bar{P} - average static pressure at the cross-section. For the data taken at Stanford, \bar{P} is the arithmetic average of the static pressure measurements
- q - dynamic head, $(1/2)\rho U^2$
- \bar{q} - dynamic head based on \bar{U} , $(1/2)\rho \bar{U}^2$
- r - inlet radius ratio for annular diffusers, $R_{I,1}/R_{O,1}$
- R - radius
- ΔR_1 - difference between the inlet radii for an annular diffuser, $R_{O,1} - R_{I,1}$
- Re - Reynolds number, $\frac{\bar{U}_1 \hat{D}}{\nu}$
- Re_θ - Reynolds number based on momentum thickness, $\frac{U_1 \theta}{\nu}$
- u, v, w - local mean velocity
- U - core flow velocity or maximum velocity
- \bar{U} - mass average velocity
- W - width of two-dimensional diffuser between diverging walls, or the shorter of the two inlet dimensions for a three-dimensional diffuser
- x - axial and flow directions measured from the throat
- \hat{x} - non-dimensional axial coordinate
 x/W_1 for two-dimensional and three-dimensional diffusers
 x/R_1 for conical diffusers
 $x/\Delta R_1$ for annular diffusers
- y - distance normal to the wall
- Z(x) - effective wall shape (see Figure 4)
- z - distance transverse to the flow
- α - parameter in wall shape equation for wall fairing calculations
- β^* - a parameter that indicates the probable inception of stall

- δ - boundary layer thickness
- δ^* - boundary layer displacement thickness, $\int_0^{\delta} (1 - \frac{u}{U}) dy$
- δ_3^* - the corner interference boundary layer displacement thickness (see Appendix B)
- θ - boundary layer momentum thickness, $\int_0^{\delta} \frac{u}{U} (1 - \frac{u}{U}) dy$
- η - diffuser effectiveness, C_p/C_{p_1}
- $\bar{\eta}$ - diffuser effectiveness based on the centerline pressure recovery, \bar{C}_p/C_{p_1}
- ϕ - half angle of the diffuser
- ν - kinematic velocity
- ρ - fluid density
- τ - shear stress in the boundary layer
- $\bar{\tau}_w$ - the particular wall shear correlation in Eqn. 21

Subscripts

- 1 - diffuser entrance or throat
- 2 - diffuser exit
- d - diverging walls
- d_a, d_b - distinguishes the diverging walls in a two-dimensional diffuser with unequal inlet boundary layer
- d_1, d_2 - the two divergence directions for a three-dimensional diffuser
- p - parallel walls
- p_a, p_b - distinguishes the parallel walls in a two-dimensional diffuser with unequal inlet boundary layers
- O, I - outer and inner surface of an annular diffuser
- w - wall

GLOSSARY

B_1 - The parameter, B_1 , is defined as the ratio of the inlet boundary layer blockage area to the total inlet area. For "normal" profiles, the blockage area is essentially the boundary layer displacement thickness times the inlet perimeter. This parameter is a measure of the inlet boundary layer thickness.

β^* - The parameter, β^* , is a correlation of the line a-a, the line of first appreciable stall in a diffuser. When the value of β^* decreases to 0.48, then first appreciable stall is probable in the diffuser.

Class A diffusers - Class A diffusers are those diffusers whose flows and geometries are restricted as follows:

Flow restrictions

1. Subsonic,
2. $Re \geq 2.5 \times 10^4$,
3. Symmetric inlet velocity profiles,
4. Unstalled,
5. $B_1 \leq 0.05$;

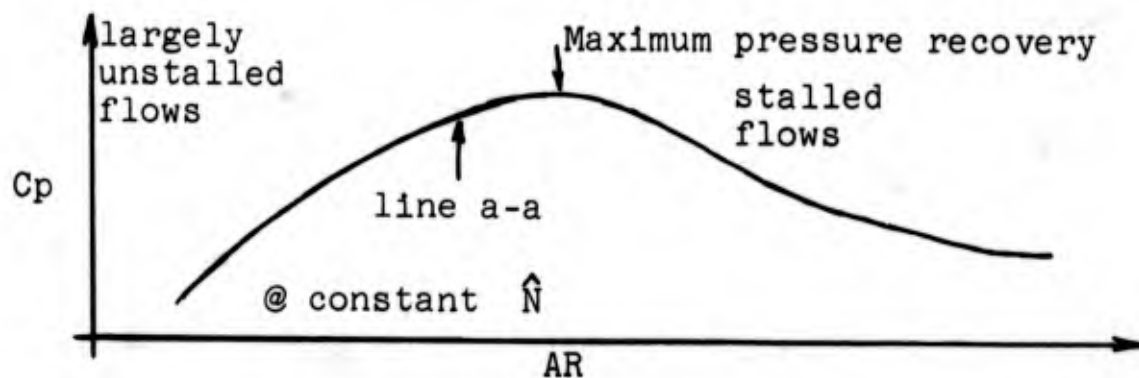
Geometric restrictions

6. General,
 - a. symmetric,
 - b. non-turning,
7. Structural,
 - a. two-dimensional,
 - b. three-dimensional,
 - c. conical,
 - d. annular.

Effective core area - The effective core area is the local diffuser cross-sectional area minus the local blockage area.

Three-dimensional diffusers - That class of diffuser geometries which have a rectangular cross-section and walls that diverge in both directions normal to the flow direction are denoted three-dimensional diffusers.

Maximum pressure recovery - The pressure recovery for a series of diffusers with constant non-dimensional length but different total area ratios varies as indicated in the following diagram:



The peak in pressure recovery is denoted the maximum pressure recovery.

The following brief descriptions of the major states of stall in a diffuser (see Figure 1) are quoted from Reneau [1964].

1. No Appreciable Stall

This flow regime is confined to small angles and area ratios; it is shown as the crosshatched region below line a-a in Figure 1. The flow is steady, and although the boundary layers may become thick, at most only small areas of stall are observed. The pressure and velocity profiles are essentially symmetrical about the center plane and are relatively constant in time. Geometries in the vicinity of line a-a contain a small amount of stall near the exit; the stall is generally seen in a corner.

The definition of line a-a is that selected by Fox and Kline [1962]. At line a-a, $1/5$ of the wall height b of

one wall is stalled at times.

2. Large Transitory Stall[†]

This region lies between line a-a and line b-b in Figure 1. The flow is very erratic and gross fluctuations of the whole flow pattern are observed. Stalled regions constantly form and wash out of the diffuser. This causes relatively large pressure fluctuations throughout the diffuser.

3. Two-Dimensional Stall[‡]

For geometries in the region just above line b-b a two-dimensional stall exists. It can exist up to line c-c, but between lines c-c and d-d jet flow can also exist. The zone between line c-c and line d-d is a hysteresis region.

In two-dimensional stall, the flow separates near the throat and follows one wall; a steady, fixed stall covers the other diverging wall. The flow is steady except for the intense turbulence in the mixing zone between the stall and the through flow. The stall is bi-stable; that is, the stall is stable on either diverging wall.

4. Jet Flow

Jet flow is always observed above line c-c and may exist down to line d-d.

In the jet flow pattern, the incoming stream separates from both diverging walls at or very near the throat and proceeds straight down the diffuser; a large, fixed stall covers each diverging wall. Jet flow is much steadier than the large transitory stall.

[†]Sometimes called three-dimensional stall in the literature.

[‡]Sometimes referred to as fully-developed stall in the literature.

CHAPTER 1

INTRODUCTION

A. General Remarks

A diffuser is a device for converting the momentum of an incoming flow represented by the velocity into an increase in static pressure. Thus, fluid diffusion is often denoted a pressure recovery process.

The pressure recovery process is easily described by Bernoulli's equation for the ideal or reversible case; for steady flow of an incompressible fluid along a streamline: $p + 1/2 \rho U^2 = \text{constant}$, i.e., a decrease in velocity is accompanied by an increase in pressure. The details of the actual process are difficult to describe or predict because real fluid effects lead not only to a complicated coupling between the boundary layer growth and the adverse pressure gradient in the diffuser, but also to several kinds of flow separation which may be transient and three-dimensional in nature.

As a consequence of these difficulties, many researchers have investigated the diffuser pressure recovery process with the following three objectives:

1. To measure the pressure recovery;
2. To determine the effect, if any, of the various flow and geometric parameters on the pressure recovery process;
3. To determine the overall flow patterns.

The major results of this long research effort are summarized in a brief historical survey in Section C below. The objective of this work is given in the following section.

B. Objective

The objective of this work is the development of a prediction method for the pressure recovery of diffusers. The effort has been successful to the extent that a method is given which can predict the pressure recovery for one large

group of diffusers. This group is called "class A"; it is subject to the following set of flow and geometric restrictions:

Flow restrictions

1. Subsonic flow, i.e., the inlet Mach number, M_1 , ranges from 0 to choking;
2. Inlet Reynolds number, $Re \geq 2.5 \times 10^4$;
3. Symmetric inlet velocity profiles;
4. Unstalled flow, i.e., no appreciable boundary layer separation in the diffusing flow. The amount of boundary layer separation in diffusers can be summarized with a flow regime chart where the flow regimes are defined as functions of area ratio and a non-dimensional length. For example, the flow regime chart for two-dimensional diffusers is reproduced from Fox and Kline [1962] in Figure 1. The unstalled regime is crosshatched, and this is the flow regime where the theory applies. The line a-a, the line of first appreciable stall, is the upper bound for this regime; a parameter, β^* , has been developed which correlates line a-a and, hence, provides a means to terminate analytical calculation of the pressure recovery;
5. The flow must be divisible into an effective core flow plus turbulent boundary layers. To provide a means to indicate when a flow can be so divided, another parameter, B_1 , has been defined as the ratio of the inlet boundary layer blockage area to the total inlet area. When $B_1 \leq 0.05$ and the inlet flow is nearly symmetric, the requisite division is an adequate flow model;

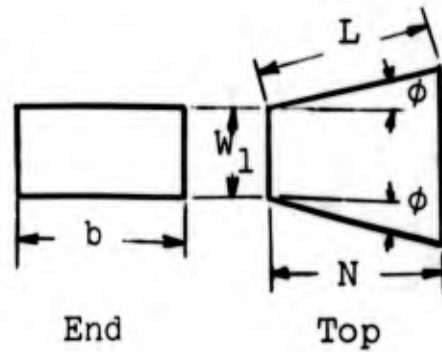
Geometric restrictions

6. Non-turning;
7. Symmetric.

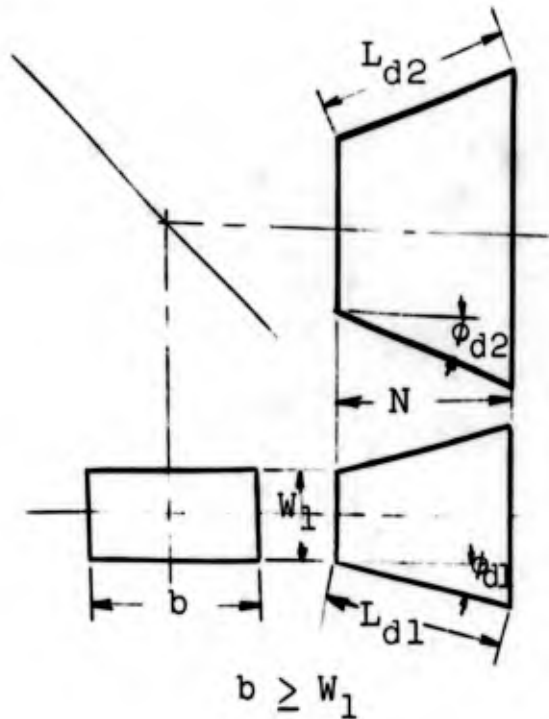
The method to predict the pressure recovery of a diffuser

has been applied to diffusers with the following geometries:

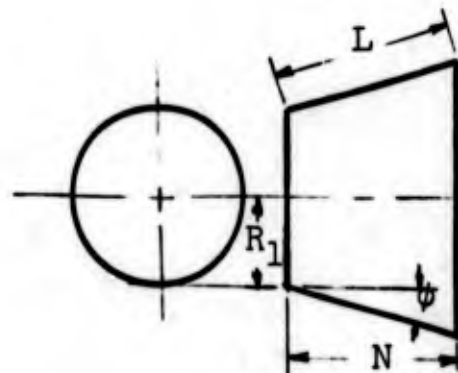
1. Flat, two-dimensional diffusers with straight and contoured walls.
(See Figure 2a, repeated from Reneau [1964].)



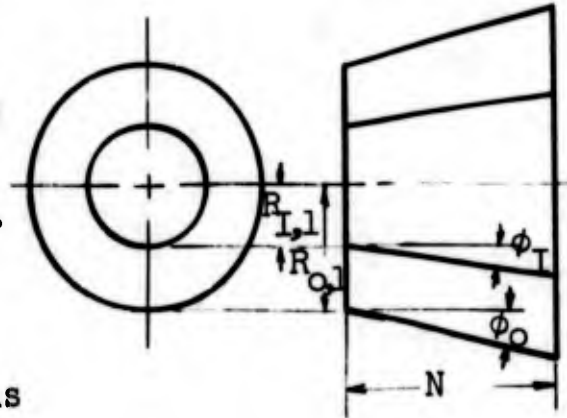
2. Three-dimensional (divergence in both principle directions normal to the flow direction) rectangular cross-section diffusers with straight walls. (Square diffusers are a subset of this class; see Figure 2b.) For convenience, this diffuser class will be denoted three-dimensional and a particular diffuser of this class will be denoted $2\phi_{d1}$; $2\phi_{d2}$; AS; 3D where ϕ_{d1} and ϕ_{d2} are the divergence half angles, AS is the aspect ratio and 3D denotes the class.



3. Conical diffusers with straight and contoured walls; (see figure 2c).



4. Annular diffusers with straight walls; (see figure 2d). For convenience, a particular diffuser of this class will be denoted by ϕ_o ; ϕ_I ; r . where ϕ_o and ϕ_I are the outer and inner cone divergence half angles respectively and r is the inlet radius ratio, $R_{I,1}/R_{O,1}$.



For convenience, diffusers described by the above set of flow and geometry restrictions and with two-dimensional, three-dimensional, conical, and annular geometries are denoted class A diffusers.

C. Historical Survey of Diffuser Research

The first recorded, quantitative diffuser research was conducted in the late 18th century by Venturi [1797] and contemporaries. They sought to answer the then academic question, "What are the geometric specifications for the most efficient diffuser?" Venturi's answer was, "A straight, conical diffuser with a total divergence angle of $4^{\circ}27'$."

In the early 19th century, the technological problem of increasing the overall performance of hydraulic turbines stimulated more diffuser research. This research was directed specifically toward providing an acceptable means to solve the design problem that confronted the turbine builders. When the quantitative research results indicated that actual pressure recoveries were much smaller than ideal recoveries, researchers began seeking means to improve diffuser pressure recovery. Their efforts were only marginally successful in that a few devices were found that would increase the pressure

recovery of very specific diffusers, but they did not improve all diffusers.

Around 1900, diffuser research was still centered on the design problem, but the effect of some parameters on pressure recovery were being measured. For example, pressure recovery was found to be essentially independent of Reynolds number. Gibson [1910, 1912, 1913] correlated pressure recovery with divergence angle for a fixed area ratio.

With new applications (notably wind tunnels, pumps, and ejectors) developing by the nineteen-twenties, more fundamental studies of diffuser processes were conducted. The major conclusion was that boundary layer separation in internal flow could be correlated with the diffuser geometry. The early correlations (for example, Nikuradse [1929]) were based on one parameter of geometry, which later proved inadequate. Peters [1934] qualitatively determined the effect of inlet boundary layer thickness and tailpipes on pressure recovery. He showed that pressure recovery decreases as the inlet boundary layer thickness is increased, but increases with the addition of a tailpipe. The tailpipe also stabilizes the exit flow in some situations. In 1938, Patterson [1938] surveyed all the then available diffuser data, and deduced general rules for diffuser design within the limits of available data.

In the nineteen-forties, more details of the diffuser pressure recovery process were determined. First, Polzin [1940] correctly suggested that the boundary layer separation in internal flows could be correlated with two parameters of geometry, say, area ratio and non-dimensional length, but did not construct the correlation due to a lack of data. The graphical representation of the correlation between the diffuser geometry and the amount of boundary layer separation can be called a flow regime chart. Later in response to the jet engine development (where diffusers are part of the air

intake system), the effect of Mach number on pressure recovery was investigated (for example, Young and Green [1944]). For subsonic flows, this effect is small until the diffuser chokes.

Beginning in the mid-fifties and continuing to the present, S. J. Kline and co-workers at Stanford University have engaged in several aspects of diffuser research. First the areas on the flow regime chart (see Figure 1) were established with greater confidence over a wider range of geometries as reported in Moore and Kline [1958] and Fox and Kline [1962]. The basis for the added confidence was the recognition that a spectrum of stall states exists (see Kline [1959]). The major regimes of stall indicated in Figure 1 are: no appreciable stall, large transitory stall, two-dimensional stall, and jet flow. These regimes are briefly defined in the glossary; more complete definitions appear in Fox and Kline [1962]. The concept of a spectrum of stall states has been related to flow steadiness and the occurrence of maximum pressure recovery at constant length (see Kline [1962]).

The effects of inlet boundary layer thickness and the inlet velocity profile distortions on the diffuser flow pattern and pressure recovery have been reported in Waitman, Reneau, and Kline [1960]. In particular, the pressure recovery decreases as the inlet boundary layer thickness increases and as the inlet velocity profile is distorted from a uniform profile. In Kline, Abbott, and Fox [1959], the diffuser design problem was defined in terms of four optima:

1. Minimum total head loss per unit actual pressure rise or equivalently, the maximum effectiveness;
2. Optimum recovery for a given area ratio;
3. Optimum recovery for a given length;
4. Best optimum for any geometry.

Reneau [1964] presented a rational method for designing non-turning, two-dimensional diffusers. The method is summarized with data maps and a survey of the effects of the many flow

and geometric parameters on diffuser performance. Reneau also specifically provides data over an exceptionally wide range of geometries and inlet conditions as a basis for checking prediction methods.

Recently, the pressure recovery has been predicted for some diffusers (Ackeret [1958], Schlichting and Gersten [1961], Reneau [1964]). The two major disadvantages of all these prediction methods are: (i) they apply only to unstalled flow, but provide no reliable means to indicate when the flow may be stalled; (ii) each was applied to only one diffuser shape. Reneau did suggest a detachment criterion based on a maximum value of the axial gradient of the momentum thickness, $d\theta/dx > 0.012$, as a means to terminate calculations. However, this criterion does not correlate the line of first appreciable stall, instead it conservatively estimates the line of maximum pressure recovery which occurs after first appreciable stall. Moreover, additional calculations show it does not work well for units with other than straight walls.

The major results of diffuser research have been indicated in this brief history. These results plus the place of this work in terms of these results will be considered in the following section.

D. Closing Remarks

The brief historical summary indicates the progress in understanding the diffuser pressure recovery process from the first efforts to determine the geometry of the most efficient diffuser to developing methods that predict the pressure recovery of arbitrary diffusers. During this long period of research, it has gradually become clear that the important factors affecting diffuser pressure recovery are inlet velocity profile and the amount of boundary layer separation in the diffuser. In particular, the pressure recovery of a diffuser decreases as the inlet boundary layer

thickness increases and as the inlet velocity profile is distorted from a uniform velocity profile. With all other things equal, the pressure recovery decreases with appreciable boundary layer separation. In addition, the effects of Reynolds number on pressure recovery is small for the Reynolds number range of most applications, and the effect of Mach number is also small until the flow chokes. Similarly, cross-sectional geometry and aspect ratio are unimportant except in the most extreme limits.

Quantitative and qualitative understanding of the above effects allow rational design of diffusers. For two-dimensional class A diffusers, the design problem has been reduced to selecting the appropriate data map in Reneau [1964]. For the remaining class A diffusers, the data are not sufficient to allow construction of detailed data maps.

The data maps for the remainder of the class A diffusers could be constructed by an extensive experimental program similar to that undertaken for two-dimensional diffusers. However, this would be a long and expensive process. The alternate approach is to use the experience gained in predicting the pressure recovery for two-dimensional diffusers as a basis for construction of analytical methods to predict the pressure recovery for the remaining class A diffusers. The latter approach does not completely replace an experimental program; but, if successful, it will greatly reduce the scope of the experimental program required. In this approach, only the pressure recovery of a few diffusers must be measured to verify the calculated pressure recoveries and to determine the useful range of the theory.

This work does provide an analytical method for predicting the pressure recovery of the remaining class A diffusers.

The analytical methods, which are developed in Chapter 2, are based on the momentum equation and the continuity equation for a simple, quasi-one-dimensional flow model and on two

correlations - the von Doenhoff and Tetervin [1943] two-dimensional shape factor correlation and the Ludwig and Tillman [1950] wall shear correlation. These basic equations plus the two correlations are combined to produce a system of linear differential equations which represent the change in integral boundary layer parameters. These differential equations are solved numerically, and the resulting information is sufficient to determine the pressure recovery of the diffuser.

In Chapter 3, the predicted pressure recoveries are compared to measured pressure recoveries from the widest possible selection of published sources. No experimental work was undertaken by the author, but all available data have been used as appropriate to check the theory. The pressure recovery for class A diffusers and several other calculated effects are presented in Chapter 4. In Appendix D, a few additional experiments are suggested to check the present theory in extreme cases for which data do not presently exist.

CHAPTER 2

ANALYSIS

Ideally an analytical method to predict diffuser performance would produce numerical pressure recovery values for all possible inlet conditions and all diffuser geometries. In this sense, the method presented below is far from ideal. Only class A diffusers can be simulated with the diffuser flow model to be developed in this chapter; they represent perhaps half of the cases encountered in technical applications.

A. Flow Model Motivation

Before the generalized equations which model the flows in class A diffusers are derived, the following discussion is presented to motivate the flow model of an effective core plus boundary layers. Experimentally, the pressure recovery, \bar{C}_p , of a diffuser may be determined by measuring the average pressure difference across the diffusing section, then non-dimensionalizing the pressure difference by the centerline, inlet dynamic head

$$\bar{C}_p = \frac{\bar{P}_2 - \bar{P}_1}{q_1} \quad (1)$$

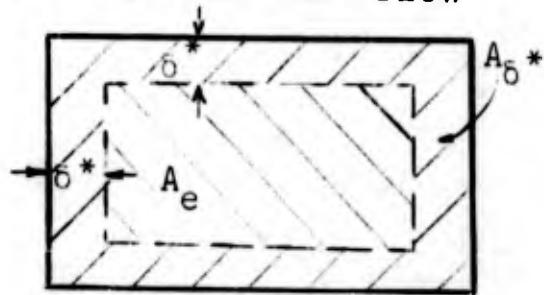
Provided the flow in the central region has only a small stream-normal pressure gradient and is without appreciable dissipation, equation (1) can be combined with Bernoulli's equation to give for incompressible flow

$$\bar{C}_p = 1 - \left(\frac{U_2}{U_1} \right)^2 \quad (2a)$$

The compressible case is easily expressed in slightly more complex form under the same assumptions

$$C_p = \frac{\left(\frac{1.0 + \frac{k-1}{2} M_1^2}{1.0 + \frac{k-1}{2} M^2(x)} \right)^{k/k-1} - 1.0}{\left(1.0 + \frac{k-1}{2} M_1^2 \right)^{k/k-1} - 1.0} \quad (2b)$$

In equation (2a), the pressure recovery is expressed in terms of the centerline velocity ratio. If the velocity ratio can be determined, then the pressure recovery can be calculated. The velocity ratio can be determined indirectly from an effective diffuser flow. The effective flow is that flow with a uniform velocity profile and an effective flow area equal to the actual flow area minus the boundary layer blockage area (see sketch). Now, the velocity ratio can be determined by applying the continuity equation to the effective flow and the pressure recovery can be expressed



$$A_e = A - A_{\delta^*}$$

where

- A = actual flow area
- A_{δ^*} = boundary layer blockage area
- A_e = effective core area

$$\bar{C}_p = 1 - \left(\frac{A_{e,1}}{A_{e,2}} \right)^2 \quad (3)$$

In equation (3), A_e is the effective core area.

The above example demonstrates that the pressure recovery of a diffuser can be determined by measuring the boundary layer displacement thickness since the core area can be calculated once the boundary layer displacement thickness is known. In general, the boundary layer measurement method for determining pressure recovery is not as operationally convenient as the usual pressure measurement method. To repeat, under the conditions considered here, the pressure recovery of a diffuser is known once the boundary layer growth

in the diffuser is known. This idea suggest a reasonable approach for analytical prediction of diffuser pressure recovery; that is, to predict the boundary layer growth in the diffuser and hence, determine the pressure recovery.

The problem of predicting the pressure recovery for a diffuser has now been reduced to predicting the boundary layer growth. Here again, the ideal solution would be to predict the boundary layer growth for all inlet conditions and all diffuser geometries. The basic obstacle to the ideal goal is predicting the growth of a turbulent boundary layer in an arbitrary, adverse pressure gradient. This problem has not been fully solved, nor is a new solution attempted here. Instead, the diffuser problem is solved with one of the many semi-empirical correlaticns which have been developed to estimate the growth of a turbulent boundary layer in an adverse pressure gradient in terms of the boundary layer integral parameters, δ^* and θ . These semi-empirical methods are known to be less than totally satisfactory, but they are the best tools available.

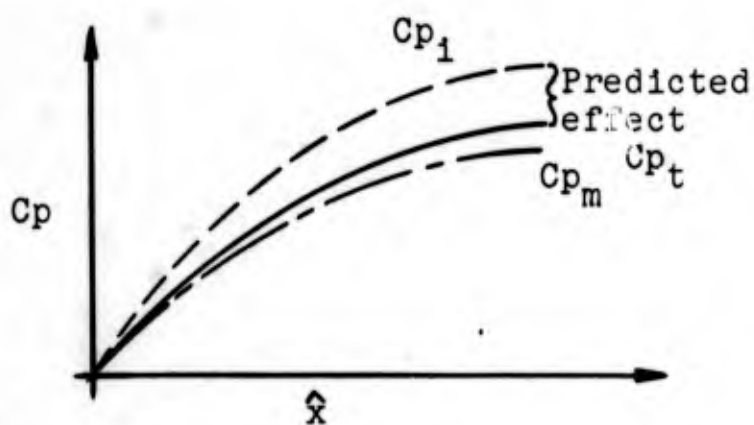
One approach developed for external flows is to combine the integrated, boundary layer momentum equation with a wall shear correlation and a shape factor correlation. When the external pressure gradient is also specified, the problem is well posed, and the change in the integral boundary layer parameters can be estimated.

An approach as general as the above has stimulated many researchers to develop a "better" method. Rotta [1962] summarizes most of these methods, and indicates that one particular method can solve one problem well, but in general, all methods that have been developed do about equally well (or poorly) for general problems.

To apply the boundary layer calculation methods of external flows to the internal flow in a diffuser, the class of diffuser flows must be restricted. The two major differences

between internal and external flows with respect to boundary layer calculation methods are: (i) the pressure gradient is not known a priori in an internal flow, (ii) the boundary layer on one wall of a diffuser can have a large influence on the boundary layer on the opposite wall. One means to avoid both of these difficulties is to consider only those flows which can be divided into an effective core plus boundary layers. For these flows, the pressure gradient can be determined in a stepwise manner from a differential form of the continuity equation applied to the effective core as the calculation proceeds down a given diffuser. In addition, as long as an effective core exists in which the total boundary layer thicknesses on opposite walls do not overlap and the flow is unstalled, the boundary layers can be assumed independent of mutual interaction. Hence, for the present calculations, the scope of the possible diffuser flows is limited to those that can be divided into an effective core flow plus boundary layers.

In terms of the overall problem of predicting the pressure recovery for diffusers, the above result is one of two key reasons for expecting the proposed calculating method to succeed for class A diffusers. The other reason is the insensitivity of the predicted result (i.e., the pressure recovery) to a particular means for calculating the growth of the boundary layer. The calculation method predicts the difference between the ideal pressure recovery and the theoretical value; this is a small quantity relative to the total value of the pressure recovery as indicated in the following sketch:



- Cp_1 - ideal pressure recovery
- Cp_t - theoretical pressure recovery
- Cp_m - measured pressure recovery
- \hat{x} - non-dimensional diffuser length

Hence, a large percentage error in calculating the boundary layer parameters gives a much smaller percentage error in pressure recovery.

A restatement of the above result is that this work is not an endorsement of the von Doenhoff and Tetervin boundary layer calculation method. In fact, any reasonable boundary layer calculation method could have been used in the method to predict the performance of class A diffusers.

B. Developing Equations for the Flow Model

Having motivated the flow model of an effective core plus boundary layers by the above example, the generalized mathematical expressions for the model will be developed. The equations are of two types - basic principles and correlations. For this development, the basic principles are the boundary layer momentum equation and the continuity equation; the correlations are the von Doenhoff and Tetervin [1943] shape factor correlation for turbulent flows and the Ludwig and Tillman [1950] wall shear correlation for turbulent flows. The necessary equations will be developed in parallel for the two subclasses (with regard to boundary layer types) of Class A diffusers - two-dimensional and axisymmetric.

The two-dimensional case was developed completely by Reneau [1964]; it is summarized here with the motivation and the resulting equations. The axisymmetric case is developed

in greater detail.

The momentum equation is considered first. For the two-dimensional case, Reneau started with the time averaged, differential boundary layer momentum equations (the turbulence terms were neglected since they are small and their general behavior cannot yet be predicted in an adverse pressure gradient)

$$u \frac{\partial u}{\partial x} + v \frac{\partial u}{\partial y} = - \frac{1}{\rho} \frac{dp}{dx} + \nu \frac{\partial^2 u}{\partial y^2} \quad (4)$$

and the full continuity equation (the $\frac{\partial w}{\partial z}$ term accounts for streamline divergence, Pierce [1961, 1964])

$$\frac{\partial u}{\partial x} + \frac{\partial v}{\partial y} + \frac{\partial w}{\partial z} = 0 \quad (5)$$

Combining equations (4) and (5) into the usual momentum integral form produces the following equation

$$\frac{d\theta}{dx} = \frac{\tau_w}{2q} - \theta \left[\frac{1}{a} + (H + 2) \frac{1}{U} \frac{dU}{dx} \right] \quad (6)$$

Equation (6) is valid for collateral flow down the centerline of a diffuser wall, (see Figure 3). Equation (6) contains the usual boundary layer integral parameters plus the $\frac{1}{a}$ term. This term represents a correction to the equation resulting from the boundary layer interaction with the ideal streamline divergence in a diffusing flow. The length represented by "a" is the distance a source flow should be located upstream to produce streamlines tangent to the local effective wall shape, (see Figure 4). The magnitude of "a" can be determined from the effective wall shape via

$$\frac{1}{a} = \frac{\frac{dz}{dx}}{Z(x)} \quad (7)$$

The effective wall shape can be written in terms of the actual wall shape and the boundary layer displacement thickness.

For the axisymmetric case, consider the case where the boundary layer thickness, δ , is small relative to the radius of the diffuser. The time-averaged, differential, boundary layer momentum equation is the same as equation (4). Equation (4) is combined with the axisymmetric continuity equation

$$\frac{\partial(uR)}{\partial x} + \frac{\partial(vR)}{\partial y} = 0 \quad ; \quad R = R(x) \quad (8)$$

The momentum integral form becomes

$$\frac{d\theta}{dx} = \frac{\tau_w}{2q} - \theta \left[\frac{\frac{dR}{dx}}{R(x)} + (2 + H) \frac{1}{U} \frac{dU}{dx} \right] \quad (9)$$

Equation (9) applies to collateral flow down an element of an axisymmetric surface, (see Figure 5). The integral boundary layer parameters in equation (9) have the two-dimensional definition. The two-dimensional and axisymmetric definition of the boundary layer parameters differ by less than 2% for $B_1 \leq 0.02$. This difference is within the experimental uncertainty of measuring boundary layer parameters. For a more fully developed flow with $B_1 = 0.15$, the differences are about 23%. Also note that the $\frac{dR}{dx} R(x)$ term in equation (9) is analogous to the $\frac{1}{a}$ term in equation (6) and can be considered a streamline divergence correction in the same sense as $\frac{1}{a}$.

In addition to the momentum integral equations (6) and (9), the continuity equation is needed separately to provide both the velocity change in the effective core as well as to express the pressure gradient in a differential form.

Since the effect of compressibility[†] will be considered

[†]The compressible flow case is modeled by a compressible core flow plus incompressible boundary layers. To justify this model note the empirical result that diffuser inlets choke for $M_1 \sim 0.7$ to 0.9 and that the local Mach number decreases monotonically in a diffuser. Then knowing that Mach number is less than 0.9 at all points in the diffuser; the difference

for the core flow, the continuity equation will be considered in full generality. The incompressible case is determined by letting the Mach number approach zero. To obtain the effective core velocity change, consider the continuity equation in the form

$$(\rho U A_e)_1 = \rho U A_e \quad (10)$$

Solving for $U(x)$

$$U(x) = U_1 \frac{\rho_1 A_{e,1}}{\rho(x) A_e(x)} \quad (11)$$

Assuming the core flow to be reversible and adiabatic, the density ratio can be written in terms of Mach number and the ratio of specific heats, k ; equation (11) becomes

$$U(x) = U_1 \frac{A_{e,1}}{A_e(x)} \left[\frac{1 + \frac{k-1}{2} M^2(x)}{1 + \frac{k-1}{2} M_1^2} \right] \quad (12)$$

or

$$U(x) = U_1 \frac{A_{e,1}}{A_e(x)} \left[\frac{1 + 0.2 M^2(x)}{1 + 0.2 M_1^2} \right]; \quad k = 1.4 \quad \ddagger$$

between the compressible and incompressible integral boundary layer parameters is less than the uncertainty in determining them and the ratio of the friction coefficients is

$$1.0 \geq \frac{C_{f_c}}{C_{f_1}} \geq 0.95 \quad \left(C_f = \frac{\tau_w}{\frac{1}{2}\rho U^2} \right) \quad \text{for } M \leq 0.9 \quad (\text{from Figure B13, Schubauer and Tchen [1961]}).$$

[‡]The only compressible flow data available are for air ($k = 1.4$) at moderate temperatures; this result forms the basis for setting $k = 1.4$. However, the theory is not limited to this value of k .

Equation (12) does not express the velocity at the downstream station uniquely, but the local Mach number dependence is small for subsonic flows and two or three iterations are sufficient to determine the velocity with errors of the order of 0.001%. For the incompressible case, letting M_1 and M go to zero gives

$$U(x) = U_1 \frac{A_{e,1}}{A_e(x)} \quad (13)$$

The pressure gradient term $\frac{1}{U} \frac{dU}{dx}$ is developed from another form of the continuity equation

$$\rho U A_e = \text{constant} \quad (14)$$

Differentiation with respect to x gives

$$\frac{1}{U} \frac{dU}{dx} = - \frac{1}{A_e} \frac{dA_e}{dx} - \frac{1}{\rho} \frac{d\rho}{dx} \quad (15)$$

Again, using the isentropic flow relationships, equation (15) can be written

$$\frac{1}{U} \frac{dU}{dx} = - \left[\frac{1}{1 - M^2(x)} \right] \frac{1}{A_e(x)} \frac{dA_e}{dx} \quad (16)$$

The incompressible form is obtained by letting M go to zero

$$\frac{1}{U} \frac{dU}{dx} = - \frac{1}{A_e(x)} \frac{dA_e}{dx} \quad (17)$$

The geometry has not been specified in equations (12), (13), (16), or (17). This omission has been deliberate to indicate the general development of the analytical method. The explicit expressions are readily obtained for any desired geometry by recalling the definition of the effective core area, A_e , which is the local diffuser cross-sectional area minus the local boundary layer blockage area. For example, the effective core area in a conical diffuser is

$$A_e(x) = \pi R^2(x) - \pi[R(x) - \delta^*(x)]^2 \quad (18)$$

and equation (17) becomes

$$\frac{1}{U} \frac{dU}{dx} = - \frac{2 \left[\delta^*(x) \frac{dR}{dx} + [R(x) - \delta^*(x)] \frac{d\delta^*}{dx} \right]}{R^2(x) - [R(x) - \delta^*(x)]^2} \quad (19)$$

Equations (6) or (9), (12) or (13), and (16) or (17) are combined with two correlations and one definition to make the problem well posed mathematically. The two correlations are: (i) the von Doenhoff and Tetervin shape factor correlation

$$\frac{dH}{dx} = e^{4.68(H-2.975)} \left[- \theta \frac{2}{U} \frac{dU}{dx} \frac{2q}{\bar{\tau}_w} - 2.035(H - 1.286) \right] \frac{1}{\theta} \quad (20)$$

which includes the apparent wall shear, $\bar{\tau}_w$, which is expressed by the Squire and Young [1938] formula

$$\frac{2q}{\bar{\tau}_w} = [2.558 \ln(4.075 Re_\theta)]^2 \quad (21)$$

and (ii) the Ludweig and Tillman wall shear correlation

$$\frac{\bar{\tau}_w}{2q} = 0.123 e^{-1.561H} (Re_\theta)^{-0.268} \quad (22)$$

The two wall shear correlations do not represent weak analytical logic. The Ludweig and Tillman correlation represents the measured values better in an adverse pressure gradient while the Squire and Young correlation is part of the original von Doenhoff and Tetervin shape factor correlation. Use of both in appropriate places gives more accurate results.

The final expression needed to complete the mathematical description is a relationship between the boundary layer parameters

$$H = \frac{\delta^*}{\theta} \quad (23)$$

With equations (6) or (9), (12) or (13), (16) or (17), (20), (22), and (23), the flow in a class A diffuser can be represented mathematically. To represent an explicit diffuser geometry, the equations for the effective core flow, equations (12) or (13) and (16) or (17), are combined with the boundary layer equations, equations (6) or (9), (20), (22), and (23), for each separate diffuser surface. This combination of equations provides a system of at least five linear, first order differential equations with non-linear coefficients. The following class A diffusers have been represented mathematically in this fashion (the equation details are tabulated in Appendix A):

A. INCOMPRESSIBLE FLOW

1. Two-dimensional
 - a. straight walls, Reneau [1964]
 - b. contoured walls, Reneau [1964]
 - c. correction for corner boundary layer
 - d. inlet boundary layer of unequal thickness on opposite walls (this case does not satisfy the symmetric inlet velocity distribution assumption; however, the effect of small differences in inlet boundary layer displacement thicknesses can be studied)
2. Three-dimensional, straight walls
3. Conical
 - a. straight walls
 - b. contoured walls
4. Annular, straight walls

B. COMPRESSIBLE FLOW

1. Two-dimensional, straight walls
2. Conical, straight walls
3. Annular, straight walls

For the class A diffusers considered, analytic solutions for the describing systems of equations are not known. Solutions were obtained numerically with either an Euler

integration method or an Adams integration method. Both integration methods were quite stable and converged well as long as the real diffuser would not have been stalled. Also, pressure recovery values calculated independently by each integration method differed by less than 0.01%.

In summary, the pressure recovery of a class A diffuser can be determined from the boundary layer growth in the diffuser. In these cases, the boundary layer growth can be estimated with a combination of the momentum equation, the continuity equation, a wall shear correlation, and a shape factor correlation. Hence, the pressure recovery of these diffusers can be predicted.

C. Development of Parameters for Blockage and Stall; Relations among Performance Parameters

Before the predicted pressure recovery values are compared with measured values, three more analytical developments will be considered:

1. Development for a measure of the inlet boundary layer thickness in terms of a parameter denoted B_1 ;
 2. Development of a means to indicate the probable inception of stall in the diffuser by a parameter denoted β^* ;
 3. Development of relationships between diffuser performance factors.
1. Development of B_1

First consider the development of the parameter, B_1 , which characterizes the inlet boundary layer thickness. As shown by Peters [1934], Waitman, Reneau, and Kline [1960], and others, pressure recovery decreases as the inlet boundary layer thickness increases. For a particular class A diffuser geometry, the inlet boundary layer thickness, δ^* , is sufficient to describe the difference between inlet boundary layers in so far as pressure recovery is concerned. However, the

displacement thickness alone is not sufficient when the pressure recoveries of diffusers with different geometries are compared. A more universal parameter is desired. A parameter based on the inlet effective flow area should be sufficient to characterize the inlet boundary layer since a flow model of an effective flow plus boundary layers has been assumed to be sufficient to predict the pressure recovery of class A diffusers. In more general terms, a parameter based on the effective flow area should be sufficient to characterize the flow at any cross-section in the diffuser.

Since a parameter is desired to characterize the boundary layer thickness, consider the ratio of the boundary layer blockage area, i.e., the local cross-sectional area minus the effective flow area, to the local cross-sectional area for a section of unit depth from a two-dimensional diffuser of infinite aspect ratio

$$B = \frac{W \times 1 - (W - 2\delta^*) \times 1}{W \times 1}$$

or

$$B(x) = \frac{2\delta^*(x)}{W(x)} \quad (24)$$

$B(0)$ represents the inlet boundary layer blockage and is denoted B_1 . For the above example, B_1 is expressed by

$$B_1 = \frac{2\delta_1^*}{W_1} \quad (25)$$

The form of B_1 for various geometries of class A diffusers is listed in the following table:

DIFFUSER GEOMETRY		B_1
Two-dimensional	$\frac{2}{W_1} \left[\delta_{d,1}^* + \frac{\delta_{p,1}^*}{AS} \right]$	$;$ $\frac{2\delta_1^*}{W_1} \left[1 + \frac{1}{AS} \right]$
	if $\delta_{d,1}^* = \delta_{p,1}^*$	
Three-dimensional	$\frac{2}{W_1} \left[\delta_{d1,1}^* + \frac{\delta_{d2,1}^*}{AS} \right]$	$;$ $\frac{2\delta_1^*}{W_1} \left[1 + \frac{1}{AS} \right]$
	if $\delta_{d1,1}^* = \delta_{d2,1}^*$	
Conical	$\frac{2\delta_1^*}{R_1}$	
Annular	$\frac{2(R_{O,1} \delta_{O,1}^* + R_{I,1} \delta_{I,1}^*)}{R_{O,1}^2 - R_{I,1}^2}$;	
	$\frac{2\delta_1^*}{R_{O,1} - R_{I,1}}$ if $\delta_{O,1}^* = \delta_{I,1}^*$	

The geometric parameters are indicated in Figures 2a, b, c, and d.

To repeat, B_1 is defined as the ratio of the inlet boundary layer blockage area to the inlet cross-sectional area.

2. Development of β^*

Next consider the development of the parameter, β^* . Since the analytical method developed here is for unstalled diffusers, some means should be provided to indicate when the calculated pressure recovery no longer corresponds to a unstalled diffuser. The parameter, β^* has been formulated to estimate stall inception. β^* has not been developed from basic principles; it is a correlation of the line of first appreciable stall, line a-a, for two-dimensional diffusers (Fox and Kline [1962]; see Figure 1). The form of the correlation parameter is assumed to be

$$\beta^*(x) = \frac{B_1^a}{\left(\frac{A_{\delta^*}(x)}{A_{e,1}}\right)} \frac{\hat{x}}{\left(\frac{A(x)}{A_1}\right)^2} \quad (26)$$

where $\hat{x} = x/W_1$ for two- and three-dimensional diffusers,
 $= x/R_1$ for conical diffusers,
 $= x/\Delta R_1$ for annular diffusers.

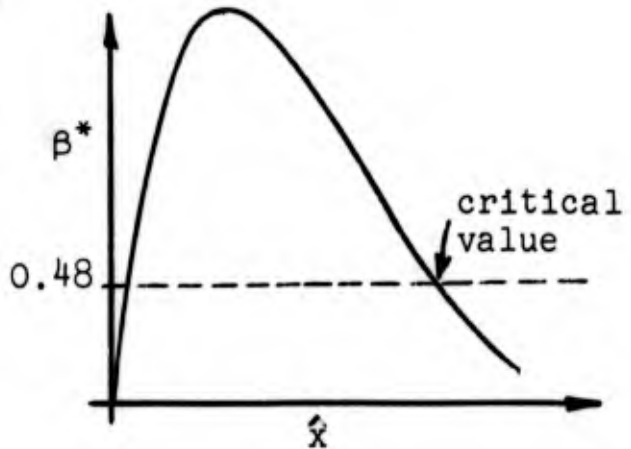
The power "a" was chosen so that one contour of β^* equal to a constant would coincide with the line of first appreciable stall, line a-a, from Fox and Kline [1962]. The value is:

$$a = 0.536$$

with

$$\beta_{crit}^* = 0.48$$

The value of the parameter, β^* , is zero at the inlet of a diffuser. Proceeding downstream of the inlet, the value rapidly increases to a peak, then decreases as indicated in the sketch. (Note that the value of β^* at any given x-station depends on the predicted flow at that station. Hence, the value of β^* cannot be determined independently of a diffuser calculation.) The data show that first appreciable stall is probably when the value of β^* decreases to 0.48. These data are considered in Chapter 3.



The parameter, β^* , is satisfactory for terminating pressure recovery calculations for two-dimensional diffusers. Similar parameters are desired for the remainder of the class A diffusers. Reliable line a-a data comparable to that reported in Fox and Kline [1962] are not available for the remaining class A diffusers. Hence, for the present, it is

assumed that the parameter, β^* , applies to the other geometries of the class A diffusers with the appropriate change in the non-dimensional length. In Chapter 3, indirect evidence will be presented to suggest that this assumption is reasonable.

3. Development of relations between performance parameters

The last relationships to be developed are between diffuser performance parameters. Diffuser performance can be specified in many ways; (Sprenger [1959] gives a very detailed discussion). At the beginning of this chapter, the diffuser performance was indicated by the pressure recovery based on the centerline dynamic head

$$\bar{C}_p = \frac{\bar{P}_2 - \bar{P}_1}{q_1} \quad (27)$$

Another measure of performance, the diffuser effectiveness, is the ratio of the actual pressure recovery \bar{C}_p given by equation (27) to the ideal pressure recovery, C_{p_1}

$$\bar{\eta} = \frac{\bar{C}_p}{C_{p_1}} \quad (28)$$

$C_{p_1} = 1 - \frac{1}{AR^2}$ for an incompressible fluid. However, the centerline dynamic head is not always known or easily determined. Usually, the mass-averaged inlet dynamic head is known since the flow rate and the inlet cross-sectional area are known. The ratio of the pressure difference to the mass-averaged inlet dynamic head defines C_p (without overscore). Thus

$$C_p = \frac{\bar{P}_2 - \bar{P}_1}{\bar{q}_1} \quad (29)$$

The comparable effectiveness is

$$\eta = \frac{C_p}{C_{p_1}} \quad (30)$$

The difference in definition of the two pressure recoveries is the inlet dynamic head employed in the denominator. The ratio of the two dynamic heads for class A diffusers is

$$\frac{\bar{q}_1}{q_1} = (1 - B_1)^2 \quad (31)$$

Therefore

$$\bar{C}_p = C_p(1 - B_1)^2 \quad (32)$$

and

$$\bar{\eta} = \eta(1 - B_1)^2 \quad (33)$$

CHAPTER 3

COMPARISON OF DATA AND PREDICTIONS

A. Objective of Comparison between Data and Predictions

Before the model, developed in Chapter 2, can be accepted as representative of physical reality, the calculated pressure recoveries must be compared with measured values. The comparison consists of two parts:

1. Comparison with data that satisfy all the assumptions of the theory to determine if the theory is adequate;
2. Comparison with data that do not quite satisfy the assumptions of the theory to determine the maximum useful range of the theory.

Satisfactory results from the first comparison provides a domain where the model is established and allows interpolation between measured pressure recovery values. The second comparison indicates the limits for extrapolating beyond the region where the pressure recovery has been measured.

The results of the comparison will be considered in Section C. In the following section, the input data requirements for the flow model will be considered.

B. Input Data Requirements for Flow Model

In principle, the theory can immediately be compared with experimental results. The flow model starts with the inlet flow and simulates the diffuser. The necessary description of the inlet flow is given by the overall flow parameters - core velocity and kinematic viscosity - and the boundary layer parameters - displacement thickness, momentum thickness, and shape parameter. In addition, the diffuser geometry must be specified including inlet dimensions, and divergence angles. In all reported data, the geometry and overall flow parameters are either stated or can be inferred from other information given. However, the inlet boundary layer information usually has not been reported.

The available reports can be classified into four groups as follows:

GROUP	INLET BOUNDARY LAYER INFORMATION REPORTED	THEORY SHOULD APPLY
1	yes	yes
2	no	yes
3	yes	no
4	no	no

Reports in group 1 provide the most critical test of the theory since large differences in the predicted and measured pressure recovery values would invalidate the theory. As shown below, the adequacy of the theory is clearly indicated by comparisons of this type.

A very large fraction of available data fall in group 2 (class A conditions, but inlet boundary layer not measured). The information in these reports can still be compared to the theory by careful estimation of the inlet boundary layer parameters. The estimation is based either on reported estimates of the boundary layer thickness or on a fitting technique. The fitting technique assumes that the inlet conditions are essentially constant for a given series of diffuser tests. The pressure recovery of one diffuser in the series is predicted by adjusting the values of the boundary layer parameters at the inlet[†] until good agreement is obtained between the calculated and measured pressure recoveries. These fitted values of the boundary layer parameters are assumed to be correct for the remainder of the diffusers in that particular apparatus. In this connection, both Copp [1951] and Nelson and Popp [1949] reported that the inlet boundary layer parameters remained essentially constant as the Mach number is increased. This result provides the basis

[†] Usually by assuming $H_1 = 1.4$ and varying δ_1^* .

for assuming that the inlet boundary layer parameters are independent of Mach number.

The third group of reports allow the maximum useful range of the theory to be determined. Hence, these reports define definite bounds for extrapolation beyond the theoretically justifiable limits of the analysis.

C. Results of the Comparison between Data and Predictions

The theory has been compared with published data for all known class A diffusers. The following table relates each geometry with the data source used in the following discussion:

A. INCOMPRESSIBLE FLOW

1. Two-dimensional diffusers
 - a. straight walls; Reneau [1964], Carlson [1965]
 - b. contoured walls; Carlson [1965]
 - c. asymmetric inlet flow; Norbury [1959]
2. Three-dimensional diffusers, straight walls; Hudimoto [1952]
3. Conical diffusers, straight walls; Copp [1951], Sprenger [1959], Squire [1953]
4. Annular diffusers, straight walls; Ainley [1952], Nelson and Popp [1949], Sovran and Klomp [1964]

B. COMPRESSIBLE FLOW

1. Two-dimensional diffusers, straight walls; Young and Green [1944]
2. Conical diffusers, straight walls; Copp [1951], Johnston [1959]
3. Annular diffusers, straight walls; Johnston [1959], Nelson and Popp [1949]

In the following discussion, the code in the margin indicates the particular item of the above outline being discussed; for example, A3 in the margin indicates that the adjacent paragraphs refer to conical diffusers with straight walls.

To indicate which data are expected to compare favorably with the theory, the following table relates reports, diffuser geometry, and the group number indicating the amount of boundary layer information reported:

Report	Diffuser Geometry	Group	Comments
Reneau [1964]	2D	1,3	
Carlson [1965]	2D	1,3	contoured walls
Norbury [1951]	2D	1	asymmetric inlet flows
Young and Green [1944]	2D	2,4	$0 \leq M_1 \leq M_{\text{choking}}$
Hudimoto [1952]	square	2,4	
Copp [1951]	conical	1,3	$0 \leq M_1 \leq M_{\text{choking}}$
Sprenger [1959]	conical	1	
Squire [1953]	conical	2	
Ainley [1952]	annular	1,3	
Nelson and Popp [1949]	annular	1	$0 \leq M_1 \leq M_{\text{choking}}$
Sovran and Klomp [1964]	annular	2,4	estimate of B_1 given
Johnston [1959]	annular & conical	2,4	$0 \leq M_1 \leq M_{\text{choking}}$

A1.a) For incompressible flow in two-dimensional diffusers with straight walls, Reneau [1964] has shown that the theory satisfactorily predicts pressure recovery for B_1 in the range 0.0075 to 0.03. For $B_1 \geq 0.05$, deviations can be as high as 20%. In Figure 6, the pressure recovery distribution for a two-dimensional diffuser with $N/W_1 = 18.0$, $AR = 2.4$, $B_1 = 0.043$, $Re = 1.5 \times 10^5$, Group 1 is compared with the data measured by Carlson [1965]. The agreement is within 4% at the diffuser exit.

A1.b) The effect of wall contour on the pressure recovery of a two-dimensional diffuser was considered analytically by Reneau [1964]; he predicted the effect to be small. Carlson [1965] has investigated the effect of wall contour experimentally. Carlson's data basically agree with the results predicted by Reneau.

In the following table, the effect of contouring on pressure recovery is presented for a diffuser with $N/W_1 = 18.0$, $AR = 2.4$, $B_1 = 0.043$, $Re = 1.5 \times 10^5$, $Cp_1 = 0.827$:

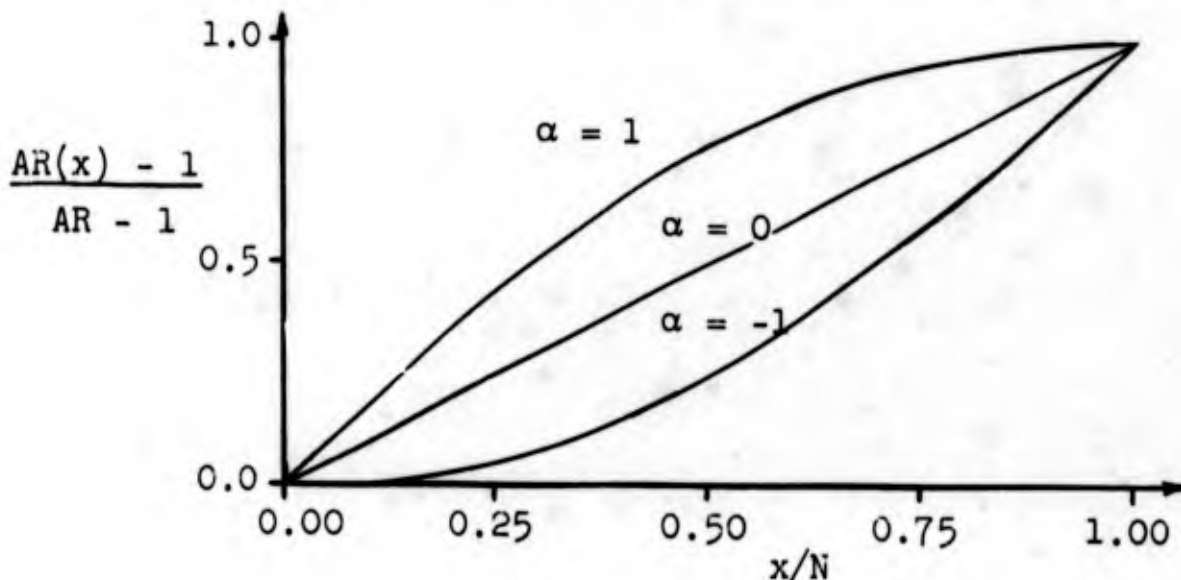
contour parameter [†]	Cp_m	Cp_t	Group
$\alpha = + 1.0$	0.700	0.733	1
$\alpha = 0.0$	0.679	0.706	1
$\alpha = - 1.0$	0.589	0.637	1

Both theory and experiment indicate that the highest pressure recovery occurs when the largest fraction of the pressure drop occurs while the boundary layer is

[†]The area ratio family considered is given by

$$AR(x) = 1 + (AR - 1) \frac{x}{N} \left[1 + \alpha \left(1 - \frac{x}{N} \right) \right]$$

The effect of α is indicated in the following sketch:



still thin. Quantitative agreement between data and theory is, however, only adequate.

Al.c) Next consider two-dimensional diffusers with inlet boundary layers of different thicknesses. The analytical method developed above does not strictly apply to this case. However, the asymmetry modification can be considered a perturbation of the symmetric case.

The motivation for considering the effect of asymmetry is that most inlet flows are asymmetric. For example, Norbury [1959] reports the inlet boundary layer parameters plus their change for a slightly contoured, two-dimensional diffuser.[†] The inlet boundary layers on the parallel walls differed in thickness from 20% to 70%. In the following table, the measured ratio of displacement thickness on one parallel wall to the opposite wall is compared with the calculated ratio:

x/W_1	$\delta_{p_a}^*/\delta_{p_b}^*$ measured	$\delta_{p_a}^*/\delta_{p_b}^*$ calculated
0.0	1.219	1.219
2.0	1.138	1.162
4.0	1.151	1.128
6.0	1.136	1.105
8.0	1.100	1.082

The measured and calculated ratios agree within 3% for an initial unbalance of 22%. For greater initial unbalance, the agreement is poor. For example, with an initial unbalance of 70%, the ratios differ by as much as 100%. Of greater importance than the ratio of displacement thicknesses is the difference between

[†]For the calculations, the contour was approximated by two straight lines. This approximation produced a diffuser with straight walls that had an abrupt change in divergence at $x/W_1 = 2.4$.

measured and calculated pressure recoveries. The difference is less than 3% as indicated in the following table:

$$N/W_1 = 8.0, AR = 2.0, B_1 = 0.043,$$

$$Re = 5.35 \times 10^6, Cp_1 = 0.750:$$

	Cp
measured	0.643
predicted using measured δ^* 's	0.624
predicted using average δ^* 's	0.623

This comparison indicates that the effect of slightly (20% difference) asymmetric inlet boundary layers can be calculated. Indeed, the pressure recovery can be calculated from the average values of the inlet boundary layer parameters.

- A2) Only two sources of data are known for three-dimensional diffusers. These are the reports of Gibson [1910, 1912, 1913] and Hudimoto [1952] both of whom consider square cross-section diffusers. The data from Gibson cannot be compared with the theory for two reasons: (i) the inlet boundary layer thickness is estimated to be in the order $B_1 \approx 0.05$, (ii) the effect of the tailpipe is unknown. Hudimoto's data contain only one case that can be compared to the theory. Reneau estimated Hudimoto's inlet boundary layer thickness to be $B_1 \approx 0.02 - 0.03$. For $B_1 = 0.03$ the values of the measured and predicted pressure recovery are listed in the following table:

$$N/W_1 = 6.9, AR = 2.98, B_1 = 0.03,$$

$$Re = 6.0 \times 10^4, Cp_1 = 0.887:$$

	Cp
measured	0.733
predicted	0.746

A3) Straight-wall, conical diffusers have been studied extensively; several researchers have reported inlet boundary layer parameters. The data from three reports will be considered here.

Sprenger [1959] studied several diffusers with many inlet boundary layer thicknesses. The measured pressure recovery distribution (Fig. 19b, Sprenger; $N/R_1 = 14.3$, $AR = 4.0$, $B_1 = 0.035$, $Re = 5.2 \times 10^5$, Group 1) is compared with the predicted pressure recovery distribution in Figure 7. The agreement is good. The remainder of the comparison is summarized in the following table:

N/R_1	AR	B_1	H_1	Re	Cp_m	Cp_t	Cp_1	Group
14.3	4.0	0.0465	1.398	3.6×10^5	0.765	0.796	0.937	1
14.3	4.0	0.0121	1.987	3.6×10^5	0.870	0.849	0.937	1
2.8	1.44	0.0102	1.97	5.2×10^5	0.469	0.469	0.518	1
2.8	1.44	0.0349	1.47	5.2×10^5	0.424	0.433	0.518	1
2.8	1.44	0.0921	1.331	5.2×10^5	0.397	0.446	0.518	3

The last entry in the table indicates the large difference that occurs between theory and data for nearly fully-developed inlet flows. The generally good agreement between Sprenger's data and the theory indicates that the theory satisfactorily predicts diffuser pressure recovery for $B_1 \leq 0.047$.

Copp [1951] reported the inlet boundary layer parameters for his conical diffuser study. The range of

Mach number for this study was 0.23 to choking. The data comparison for low Mach number is presented in the following table:

N/R_1	AR	B_1	Re	M_1	C_{p_m}	C_{p_t}	C_{p_i}	Group
4.75	2.0	0.012	1.45×10^6	0.237	0.666	0.669	0.750	1
4.75	2.0	0.012	2.0×10^6	0.355	0.660	0.660	0.770	1
4.75	2.0	0.056	1.45×10^6	0.247	0.558	0.589	0.750	3
4.75	2.0	0.056	1.85×10^6	0.327	0.547	0.580	0.767	3

For $B_1 = 0.056$, the difference in pressure recovery values is about 7%, again indicating that for B_1 much greater than 0.05 the predictions deviate significantly from measurements.

Squire [1953] reports pressure recovery data for several diffusers having an area ratio of 4.0 but with different divergence angles. The inlet boundary layer parameters were not reported, but the inlet conditions for one series of tests were constant; only the diffusers were changed. Hence, the boundary layer parameters were determined by fitting one test of the series as described above. The measured and predicted pressure recoveries are compared in the following table:

N/R_1	AR	B_1^\dagger	Re	C_{p_m}	C_{p_t}	C_{p_i}	Group
28.6	4.0	0.0075	5×10^5	0.854	0.834	0.937	2
22.8	4.0	0.0075	5×10^5	0.854	0.837	0.937	2
18.9	4.0	0.0075	5×10^5	0.850	0.838	0.937	2
14.3	4.0	0.0075	5×10^5	0.831	0.838	0.937	2
11.4	4.0	0.0075	5×10^5	0.822	0.840	0.937	2

[†]Fitted to one run and assumed constant for remainder.

A4) Ainley [1952] measured pressure recoveries for annular diffusers. The inlet velocity profile was reported which allowed the inlet boundary layer parameters to be calculated. The measured and predicted pressure recovery values are presented in the following table:

$N/\Delta R_1$	AR	B_1	Re	C_{p_m}	C_{p_t}	C_{p_1}	Group
19.25	3.19	0.019	1.12×10^5	0.786	0.779	0.902	1
14.75	3.19	0.019	1.12×10^5	0.808	0.778	0.902	1

Nelson and Popp [1949] studied the effect of Mach number of pressure recovery for two diffusers. The effect of the centerbody struts was neglected because the struts were well streamlined and located at least one third of the diffuser length from the inlet. The measured and predicted values of pressure recovery agree to 4% or better as indicated in the following table:

$N/\Delta R_1$	AR	B_1	Re	M_1	C_{p_m}	C_{p_t}	C_{p_1}	Group
10.0	1.75	0.015	3.82×10^5	0.225	0.618	0.617	0.681	1
10.0	1.75	0.015	5.1×10^5	0.300	0.599	0.613	0.689	1
20.4	1.75	0.015	3.69×10^5	0.217	0.621	0.590	0.681	1
20.4	1.75	0.015	4.73×10^5	0.278	0.620	0.591	0.688	1

Sovran and Klomp [1964] measured the performance of many annular diffusers to determine design information related to maximum pressure recovery at a constant length. The authors estimated $B_1 = 0.03$ for all diffusers with an inlet radius ratio of 0.7. Predicted and measured pressure recovery distributions are compared in Figure 8 for an annular diffuser with $N/\Delta R_1 = 12.4$, AR = 2.20, $B_1 = 0.03$, Re = 6.5×10^5 , Group 2. The remainder of the data comparison is

summarized in the following table:

$N/\Delta R_1$	AR	B_1	Re	Cp_m	Cp_t	Cp_1	Group
3.43	1.68	0.03	6.5×10^5	0.544	0.555	0.646	2
3.43	2.05	0.03	6.5×10^5	0.544	0.576	0.762	2
8.5	3.26	0.015	6.5×10^5	0.786	0.801	0.906	2

In addition to considering the incompressible flow in a diffuser, the effects of compressibility were determined with a flow model based on a compressible core flow plus incompressible boundary layers (see footnote, page 16). In the following paragraphs the pressure recovery values calculated with this flow model will be compared to measured pressure recovery value for Mach number from 0.1 to choking. For compressible flow, the pressure recovery is defined as:

$$\bar{C}_p = \frac{P_2 - P_1}{P_0 - P_1} \quad (34)$$

where P_0 is the inlet stagnation pressure.

Equation (34) reduces to the pressure recovery based on the centerline inlet dynamic head for incompressible flow, i.e., for $M_1 \leq 0.3$.

- B1) First, the experimental results of Young and Green [1944] for two-dimensional diffusers will be considered. The boundary layer parameters were not measured for these diffusers. However, the total boundary layer thickness was reported to be less than one-quarter inch. Hence, the value of B_1 was chosen to be 0.03 with $H_1 = 1.4$. In the following table, the predicted and measured pressure recovery values are compared:

N/W_1	AR	B_1	Re	M_1	Cp_m	Cp_t	Cp_1	Group
21.5	4.0	0.03	2.87×10^5	0.2	0.890	0.865	0.937	2
21.5	4.0	0.03	5.74×10^5	0.4	0.880	0.857	0.945	2
21.5	4.0	0.03	8.60×10^5	0.6	0.848	0.848	0.952	2
21.5	4.0	0.03	10.0×10^5	0.7	0.775 [†]	0.840	0.955	4
11.8	4.0	0.03	2.87×10^5	0.2	0.840	0.858	0.937	2
11.8	4.0	0.03	5.74×10^5	0.4	0.837	0.851	0.945	2
11.8	4.0	0.03	8.60×10^5	0.6	0.818	0.836	0.952	2
11.8	4.0	0.03	10.8×10^5	0.75	0.745 [†]	0.821	0.957	4

The difference between theory and experiment is less than 3% until the diffuser inlet begins to choke (indicated by †).

B2) Copp [1951] reported the pressure recovery values for conical diffusers as a function of Mach number. The boundary layer parameters were measured and did not depend on Mach number. The measured and predicted effect of Mach number on pressure recovery is presented in Figure 9. The agreement is very good for $B_1 = 0.012$, but only fair for $B_1 = 0.056$.

Johnston[‡] [1959] considered the effect of Mach number on pressure recovery for both conical and annular diffusers. The inlet boundary layer parameters were not measured, but the inlet was similar for both the conical and annular studies. The values of $B_1 = 0.0075$, $H_1 = 1.4$ were determined by fitting for the conical diffusers. The corresponding value of displacement thickness, δ^* , was assumed to be a reasonable estimate for the values of the annular displacement thicknesses, δ_o^* and δ_I^* . The boundary layer parameters were

[‡]Ingersoll-Rand Company has given permission for this data, taken from their internal report TN 71, to be published here; see letter in Appendix C. Their generosity is appreciated.

assumed to be independent of Mach number. The measured and predicted values of pressure recovery are compared in the following table for Johnston's conical diffusers:

N/W_1	AR	B_1	Re	M_1	C_{p_m}	C_{p_t}	C_{p_1}	Group
15.25	4.0	0.0075	3.17×10^5	0.3	0.874	0.840	0.941	2
15.25	4.0	0.0075	6.34×10^5	0.6	0.854	0.845	0.950	2
15.25	4.0	0.0075	8.97×10^5	0.85	0.840	0.841	0.962	2

The difference is 5% or less.

B3) Before the annular pressure recovery data of Johnston can be compared with predicted values of pressure recovery, the effect of the centerbody struts near the inlet must be considered. The struts were 0.04 inch thick sheet metal and were not streamlined. The correction considered here is to add a fraction of the frontal area of the strut to the inlet boundary layer displacement area. The apparent boundary layer displacement thicknesses for the inner and outer surface of the annulus were assumed to be equal and their value determined to give the necessary blockage area. In Figure 10, the measured pressure recoveries for two different annular diffusers are compared to predicted pressure recoveries where 75% and 100% of the strut frontal area has been added to the boundary layer blockage area. (The predicted curves have been labeled 75% and 100% to indicate how much of the strut frontal area has been added.) The agreement is good; this suggests that the effect of struts near the inlet of an annular diffuser is similar to that of increasing the inlet blockage.

Nelson and Popp [1949] considered the effect of Mach number on pressure recovery. The measured pressure recovery is compared to predicted pressure recovery in Figure 11. The difference is less than 5%.

In the above paragraphs, the results of the data comparison have been summarized. In the next section the conclusions resulting from the data comparisons are considered.

D. Conclusions of Comparison between Data and Predictions

The pressure recovery values measured by several researchers for diffusers with incompressible flow have been compared with predicted pressure recovery values. The agreement has been satisfactory as long as $B_1 \leq 0.05$. The quality of the agreement is shown in the verification plot of Figure 12. The root mean square percentage difference between measured and predicted pressure recovery values is 3.2%. Also, the effect of compressibility can be determined for subsonic flows up to choking for $B_1 \leq 0.05$.

For several of the diffusers considered, the parameter, β^* , has indicated the probable inception of stall (i.e., the value of β^* has decreased to a value less than 0.48). Yet the pressure recovery has been predicted within 4.0% in all cases. This result does not mean that this theory can predict the pressure recovery of stalled diffusers, nor does it imply that the parameter, β^* , is inadequate for predicting the inception of stall.

This apparent paradox can be resolved by considering the meaning of "inception of stall" and its relation to fully-developed stall. The inception of stall has been defined to describe the state of a boundary layer when a fixed fraction of the layer has separated. Fully-developed stall does not immediately follow the inception of stall; in a mild adverse pressure gradient, which is the case for most of the above diffusers, the initial rate of growth of the stall is small. Hence, the initial effect of the stall on the pressure recovery is small.

E. β^* Data Comparison

To conclude the chapter on data comparison, the parameter, β^* , will be compared with line a-a data and lines of maximum pressure recovery. In Figure 13, contours of $\beta^* = 0.48$ for $0.0075 \leq B_1 \leq 0.05$ are compared with the line a-a of Fox and Kline [1962]. The deviation between line a-a and the β^* contours is less than the reported uncertainty of line a-a ($\pm 1.0^\circ$). The line of maximum pressure recovery at constant N/W_1 is included on Figure 14 to indicate its relative position with respect to line a-a.

Since stall data equivalent to line a-a are not available for the remaining class A diffusers, the value of the correlation parameter $\beta^* = 0.48$ was assumed to indicate the probable inception of stall for the remaining class A diffusers with the appropriate changes in the non-dimensional length term, \hat{x} , indicated in Chapter 2. This assumption has been compared with available data. For conical and annular geometries, contours of $\beta^* = 0.48$ are compared to lines of maximum pressure recovery determined by several researchers[†]; Figure 14 is a comparison for conical diffusers; Figure 15 is for annular diffusers. The contours of $\beta^* = 0.48$ lie below lines of maximum pressure recovery. This result agrees with the expected behavior in that appreciable stall must occur before the pressure recovery decreases. The relation is similar to that found for two-dimensional diffusers as would be expected if the criterion is valid, (see Figure 13). The stalled conical diffuser geometries studied by Robertson and Fraser [1960] are plotted on Figure 15; they lie above the contours for $\beta^* = 0.48$ providing a further check on the criterion.

[†]The effect of the tailpipe on Gibson's data was compensated by lowering the line 2° in total divergence angle as suggested by Reneau [1964].

The available data are consistent with the parameter, β^* . In addition, a comparison among β^* and several other stall criteria such as maximum shape factor, maximum momentum thickness gradient, and minimum wall shear by Carlson [1965] indicates that β^* correlates stall more consistently than the others. These results will be reported in detail by Carlson. However, more stall data are required before the correlation parameter, β^* , can be considered as a well-established criterion for indicating the probable inception of stall for all class A diffusers.

The last item to be considered is the effect of the initial value of the shape factor[†] on the parameter, β^* . The initial value of the shape factor has a very small effect on the location of the $\beta^* = 0.48$ contours as indicated in Figure 16.

[†]The β^* correlation was developed with $H_1 = 1.4$.

CHAPTER 4

PREDICTED RESULTS

A flow model for class A diffusers has been developed (Chapter 2); predicted pressure recovery values have been compared with measured pressure recovery values (Chapter 3). The resulting diffuser flow model of an effective core plus turbulent boundary layers satisfactorily predicts pressure recovery values for class A diffusers. Having defined the region of validity for the diffuser flow model, performance charts (maps with contours of constant pressure recovery) have been prepared by crossplotting the predicted pressure recovery values for these regions. These charts plus a few other calculated results will be presented in this chapter.

A. Performance Charts

Performance charts were prepared for all the class A diffusers. For the performance charts, each of the class A diffusers can be adequately described with the area ratio, AR , and the non-dimensional length, \hat{N} †. For straight wall two-dimensional and conical diffusers, the geometry is uniquely determined when the area ratio and non-dimensional length are specified. However, for three-dimensional and annular diffusers, the geometry is not uniquely determined from these data alone. Two more constraints are needed in both cases; for three-dimensional diffusers, they are aspect ratio, AS , and one of the two divergence angles; for annular

† Recall that:

$$\begin{aligned}\hat{N} &= N/W_1 && \text{for two- and three-dimensional diffusers} \\ &= N/R_1 && \text{for conical diffusers} \\ &= N/\Delta R_1 && \text{for annular diffusers}\end{aligned}$$

diffusers, they are inlet radius ratio, r , and one of the two divergence angles. Nevertheless, the calculated results in the following table indicate that area ratio and B_1 also are sufficient to determine pressure recovery values to a good first approximation for unstalled three-dimensional or annular diffusers:

Aspect ratio effect on three-dimensional diffusers

diffuser type	AS	N/W_1	AR	B_1	Cp_t
3.0;3.0;1.0;3D	1	3.95	2.00	0.015	0.668
3.0;3.0;10.0;3D	10	8.05	2.00	0.015	0.666

Divergence angle effect on three-dimensional diffusers

diffuser type	AS	N/W_1	AR	B_1	Cp_t
3.0;0.0;1.0;3D	1	9.50	2.00	0.015	0.647
3.0;3.0;1.0;3D	1	3.95	2.00	0.015	0.668

Radius ratio effect on annular diffusers

diffuser type	$N/\Delta R_1$	AR	B_1	Cp_t
15.0;15.0;0.3	2.5	1.72	0.015	0.606
15.0;15.0;0.8	12.25	1.73	0.015	0.589

Divergence angle effect on annular diffusers

diffuser type	$N/\Delta R_1$	AR	B_1	Cp_t
10.0;10.0;0.7	8.50	1.53	0.015	0.516
10.0;0.0;0.7	2.4	1.53	0.015	0.530
10.0;-10.0;0.7	1.5	1.53	0.015	0.519

The above discussion justifies plotting pressure recovery contours on AR , \hat{N} planes for all the class A diffusers without concern for the unique specification of a particular

geometry in the three-dimensional or annular diffuser geometries.

In Chapter 3, the effect of the inlet boundary layer thickness on pressure recovery has been indicated. In all cases the boundary layer thickness has been represented by B_1 . However, a given value of B_1 does not uniquely represent one boundary layer displacement thickness. The effect of the component values of displacement thickness in B_1 on the pressure recovery is indicated in the following table; the effect is very small in selected extreme cases which have been calculated which include two-dimensional, three-dimensional, and annular cases. Consider:

Three-dimensional case

diffuser type	$\delta_{d1}^*/\delta_{d2}^*$	N/W_1	AR	B_1	Cp_t
3.0;3.0;1.0;3D	2.0	3.95	2.0	0.015	0.664
3.0;3.0;1.0;3D	1.0	3.95	2.0	0.015	0.668

Annular case

diffuser type	δ_o^*/δ_I^*	$N/\Delta R_1$	AR	B_1	Cp_t
15.0;15.0;0.5	1.3	5.5	1.982	0.015	0.675
15.0;15.0;0.5	1.0	5.5	1.982	0.015	0.677
15.0;15.0;0.5	0.7	5.5	1.982	0.015	0.678

The comparison of Norbury's data in Chapter 3 shows similar results for the two-dimensional case; indeed the predicted pressure recovery value did not change when the measured inlet boundary layer displacement thicknesses were replaced by an average value of the displacement thicknesses.

The above discussion indicates that for "normal" conditions the relevant parameter with respect to pressure recovery is the total value of B_1 ; the individual values of δ^* 's from which B_1 is composed are essentially irrelevant. Hence, on the performance charts only B_1 is specified.

The pressure recovery contours for each diffuser geometry have been plotted on four charts corresponding to $B_1 = 0.0075, 0.015, 0.03, \text{ and } 0.05$. These values cover the range from the thinnest boundary layer that can usually be achieved in practice to the thickest boundary layer for which the theory satisfactorily predicts pressure recovery values. In addition, the initial value of the shape parameter was chosen to be 1.4 for all calculations. The effect of different values of H_1 on pressure recovery will be considered below.

To indicate the probable inception of stall in the diffuser, contours of $\beta^* = 0.48$ have been included on every performance chart. Extrapolation of pressure recovery contours to higher values of AR at constant N is not recommended even though the pressure recovery has been predicted for some geometries with $\beta^* < 0.48$.

The contours of pressure recovery normalized on mass averaged, inlet dynamic head have been plotted on the performance charts since this is the most useful form for design. The other performance parameters described in Chapter 2 have not been plotted. However, they can be obtained from the given pressure recovery values and the relations between the parameters given by equations (28), (31), (32), and (33).

The performance charts for two-dimensional diffusers (Figures 17a, b, c, and d) have been reproduced from Reneau [1964] for completeness. The performance charts for the remainder of the class A diffusers, three-dimensional, conical, and annular, are presented in Figures 18a, b, c, d, 19a, b, c, d, and 20a, b, c, d, respectively.

B. Additional Calculated Effects

In addition to preparing the performance charts, several other effects were investigated with the diffuser flow model. These results will be considered in the following paragraphs.

1. The effect of the initial value of the shape parameter on pressure recovery was determined by Reneau [1964] for straight wall, two-dimensional diffusers; the effect is indicated in Figures 21a and b. Numerical calculations indicate that the effect is similar for the remaining class A diffusers.

2. The effect of Reynolds number on pressure recovery is small as indicated in the following table for conical diffusers with $N/R_1 = 8.0$, $AR = 2.01$, $B_1 = 0.015$, $Cp_1 = 0.752$:

Re	Cp_t
2.5×10^4	0.680
5×10^4	0.682
5×10^5	0.673

Similar results apply for the remaining class A diffusers. These results indicate the effect of Reynolds number at constant B_1 . In an experiment, B_1 may change as Reynolds number changes. In this case, pressure recovery will be altered; the effect can be determined from the changes in B_1 .

3. The effect inlet of Mach number is small as indicated in the following table for a conical diffuser with $N/R_1 = 5.5$, $AR = 1.92$, $B_1 = 0.015$, $Re = 1.33 \times 10^6$, $Cp_1 = 0.729$:

M	Cp_t
0.2	0.649
0.5	0.656
0.8	0.666

4. The effect of wall contouring on pressure recovery for a two-dimensional diffuser was calculated to be small by Reneau [1964] and measured to be small by Carlson [1965] (see Chapter 3, page 31). The theory indicates that contouring has little effect in conical diffusers with area programs given by

$$AR(x) = 1 + (AR - 1) \frac{x}{N} \left[1 + \alpha \left(1 - \frac{x}{N} \right) \right] \quad (37)^\dagger$$

For example,

with $B_1 = 0.015$, $N/R = 10.0$, $AR = 1.82$, $Cp_1 = 0.698$:

contour parameter	Cp
$\alpha = 0.5$	0.645
$= 0.0$	0.633
$= - 0.5$	0.620

Similar results are to be expected for other class A diffusers but have not been calculated.

5. The theory assumes that the boundary layers do not interact in the corners of two- and three-dimensional diffusers. A correction to account for the corner boundary layer interaction has been developed based on the study of corner boundary layers by Gersten [1959]. The development is presented in Appendix B. The calculations indicate that the effect of the corner boundary layer interaction is small. For a two-dimensional diffuser with $N/W_1 = 24.5$, $AR = 2.5$, $B_1 = 0.016$, $Cp_1 = 0.840$, the change in pressure recovery is indicated in the following table:

[†] Equation (37) is functionally the same as the wall contour equation used for the two-dimensional diffusers with the exception that $\alpha = 0$ does not correspond to a straight wall conical diffuser.

	Cp
corner boundary layer correction	0.711
no corner boundary layer correction	0.728

6. The next calculated effect to be considered is the effect of geometry on pressure recovery at fixed AR and B_1 . In the following table, pressure recovery is tabulated as a function of geometry:

geometry	\hat{N}	AR	B_1	Cp_t	Cp_1
two-dimensional	7.2	2.0	0.015	0.667	0.750
three-dimensional	3.95	2.0	0.015	0.668	0.750
conical	5.93	2.0	0.015	0.669	0.750
annular	16.75	2.0	0.015	0.661	0.750

7. The last calculated effect to be considered is the effect of B_1 on pressure recovery for class A diffusers at constant area ratio. The effect is indicated in Figure 22.

Combining the results indicated in Figure 22 with the following relationships between the B_1 's for the different diffuser inlet geometries (assuming equal displacement thicknesses on all walls) provides a basis for evaluating the design problem where the flow area and the boundary layer displacement thickness are specified:

$$\frac{B_{1,rect}}{B_{1,cir}} = \sqrt{\frac{AS}{\pi}} \left(1 + \frac{1}{AS}\right) \quad (38)$$

and

$$\frac{B_{1,ann}}{B_{1,cir}} = \sqrt{\frac{1+r}{1-r}} \quad (39)$$

The subscripts rect, cir, and ann refer to rectangular, circular, and annular inlet geometries respectively. The general conclusion, as expected, is that a conical diffuser has the highest pressure recovery for all class A diffusers with fixed inlet area and displacement thickness.

C. General Conclusions

For class A diffusers, pressure recovery depends essentially only on AR and B_1 . The dependence on Mach number, Reynolds number, wall contouring, corners, and a particular diffuser geometry, in general, appears negligible. Although this conclusion is inductive, sufficient cross-checks have been performed so that it appears extremely likely. This conclusion should lead to considerable simplification and increased understanding in modeling and in design procedures for class A diffusers.

CHAPTER 5
CONCLUSIONS

1. A successful diffuser flow model and prediction method have been developed for class A[†] diffusers.
2. Using this model and comparisons with data, the following more specific conclusions have been reached for class A diffusers:
 - a. Pressure recovery can be predicted to 5% or better.
 - b. Pressure recovery depends only on AR and B_1 ; that is, the effects of Reynolds number, Mach number, aspect ratio, wall-contouring, corners, and a particular geometry are negligible (for fixed AR and B_1).
 - c. The line of first appreciable stall, line a-a, can be correlated with β^* decreasing through the value 0.48; this provides a means to terminate calculations before class A restrictions are violated. It also provides the best indicator of appreciable stall so far available.
 - d. The assumption that the criterion, $\beta^* = 0.48$, can be applied to all class A diffusers appears consistent, but needs to be verified with additional three-dimensional, conical, and annular data.

Because conclusion 2b is particularly important to understanding, to simplifying design, and to modeling, a few experiments specifically designed as a critical test should probably be performed (see Appendix D).

[†]The restrictions on flow conditions and geometries for class A diffusers are listed on pages xii and xiii.

"Line of Appreciable Stall" is called "line a-a" for high inlet turbulence in Moore and Kline [1958].

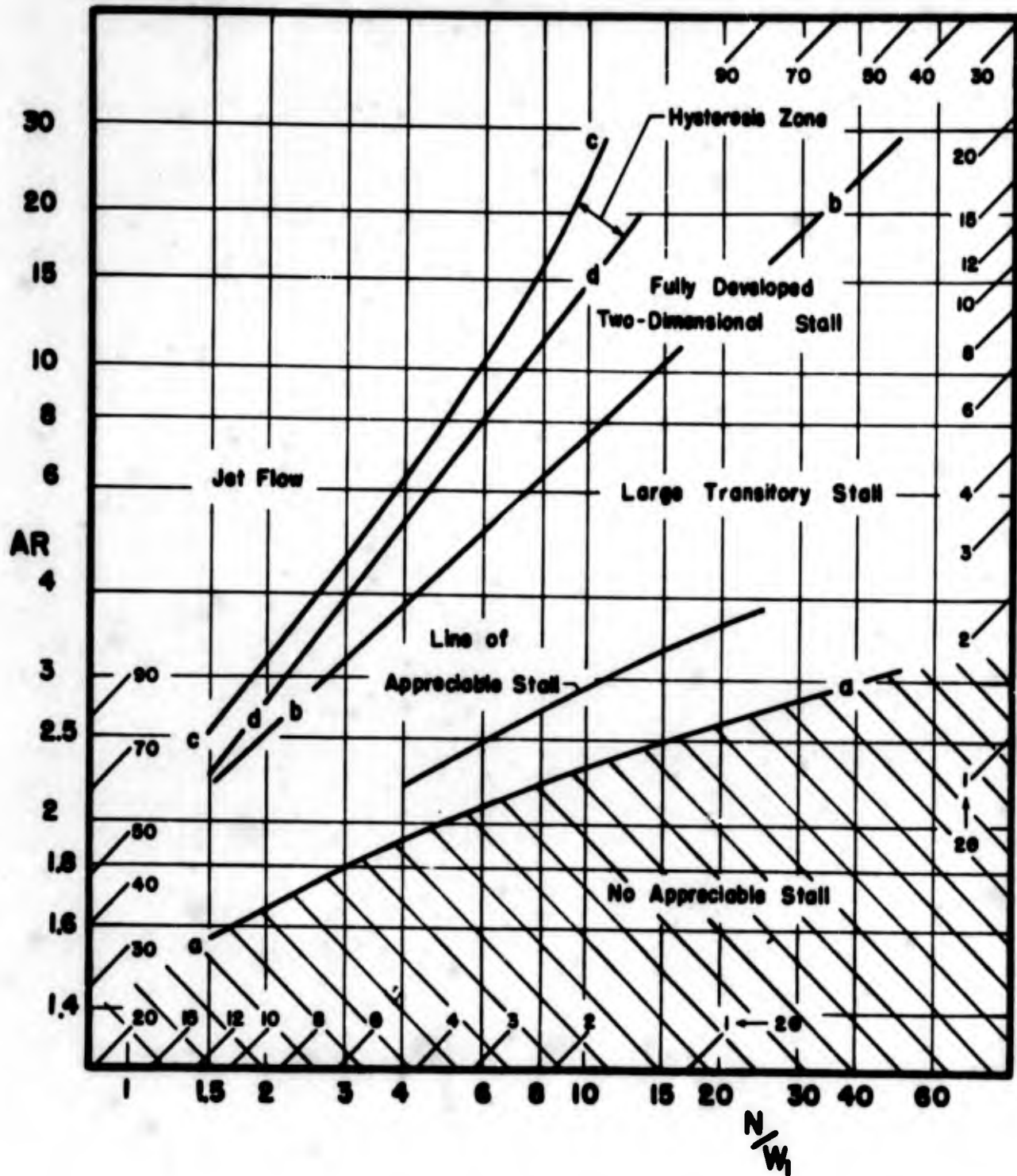
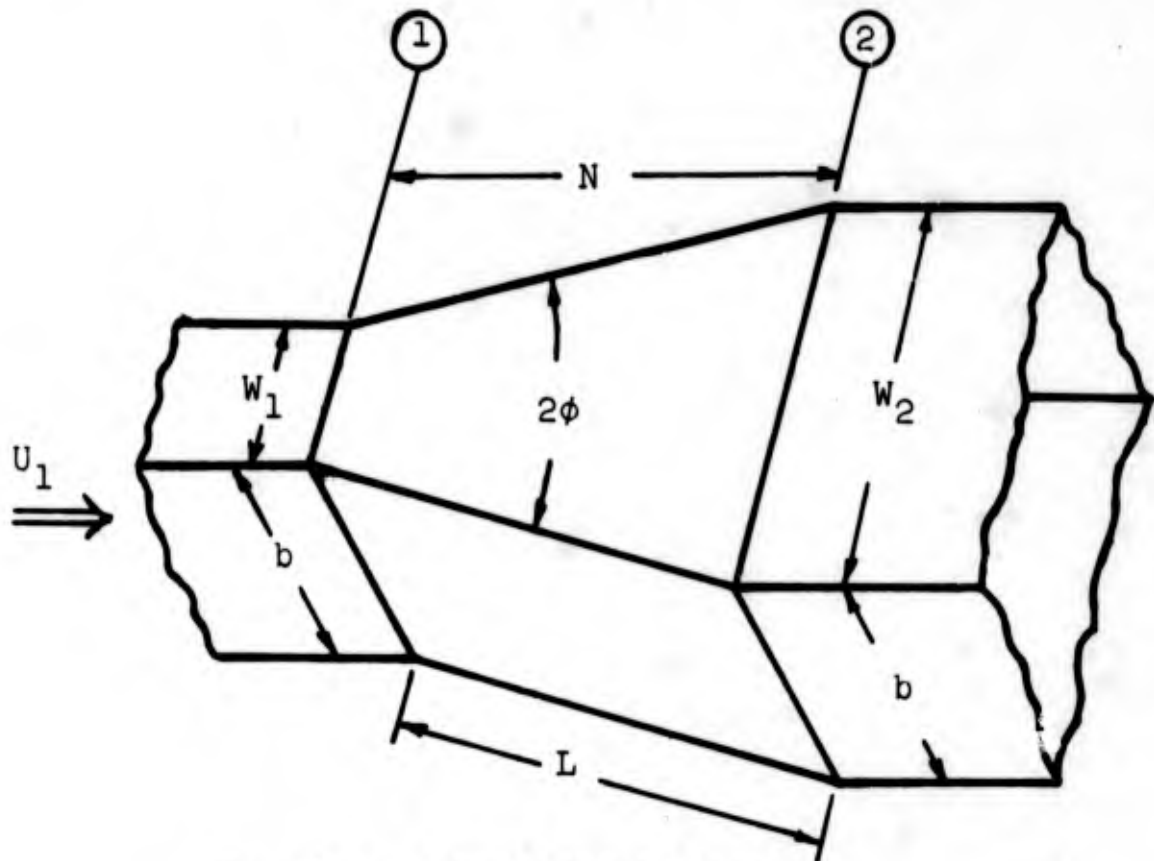
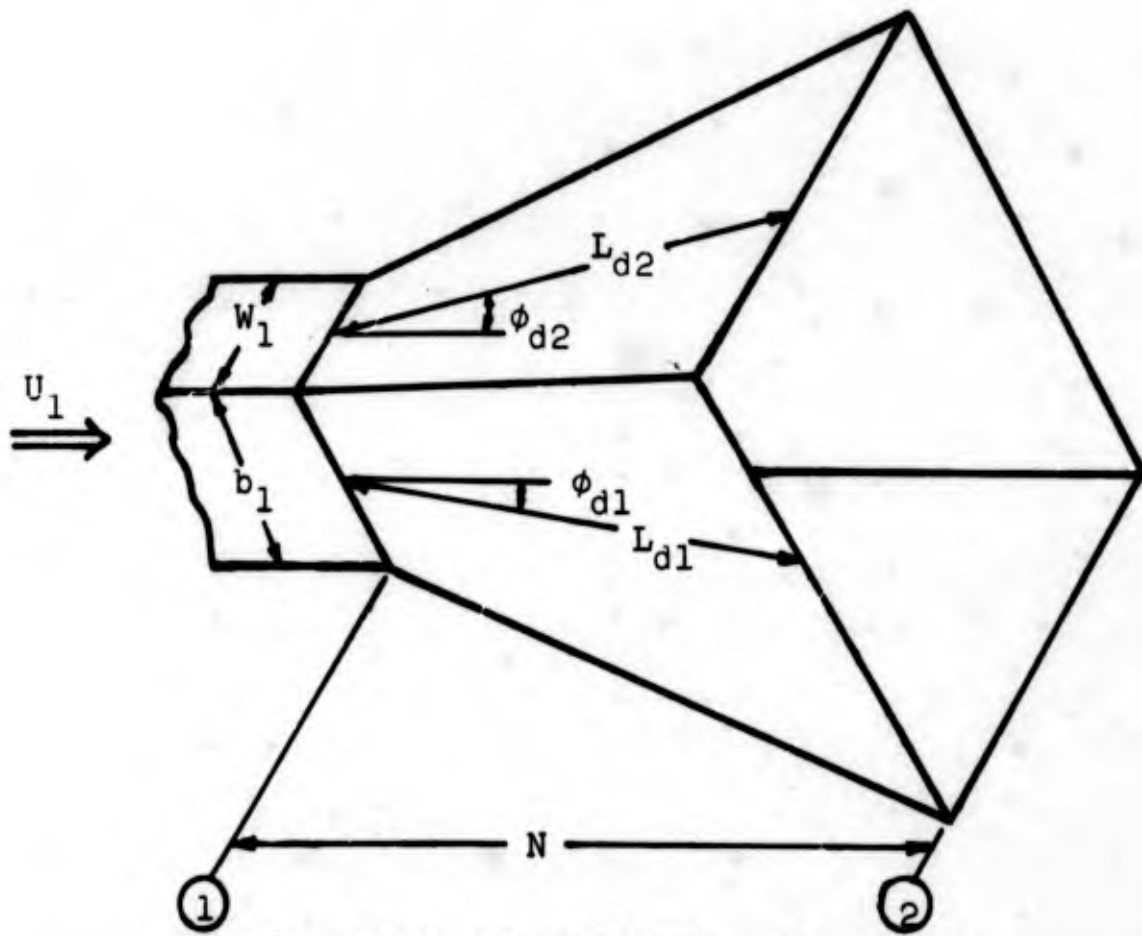


Fig. 1 Diffuser flow regimes as established by Fox and Kline [1962] for two-dimensional diffusers.

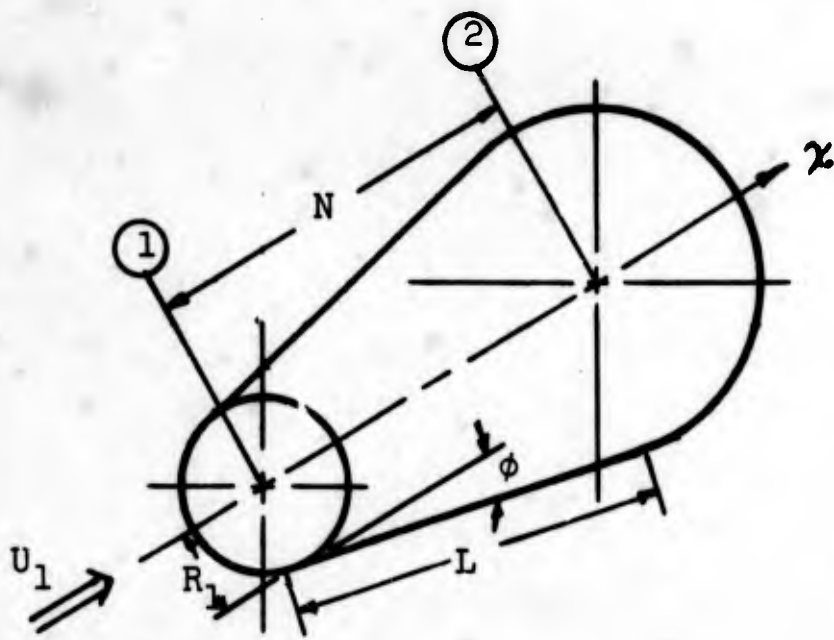


a. Two-Dimensional Diffuser

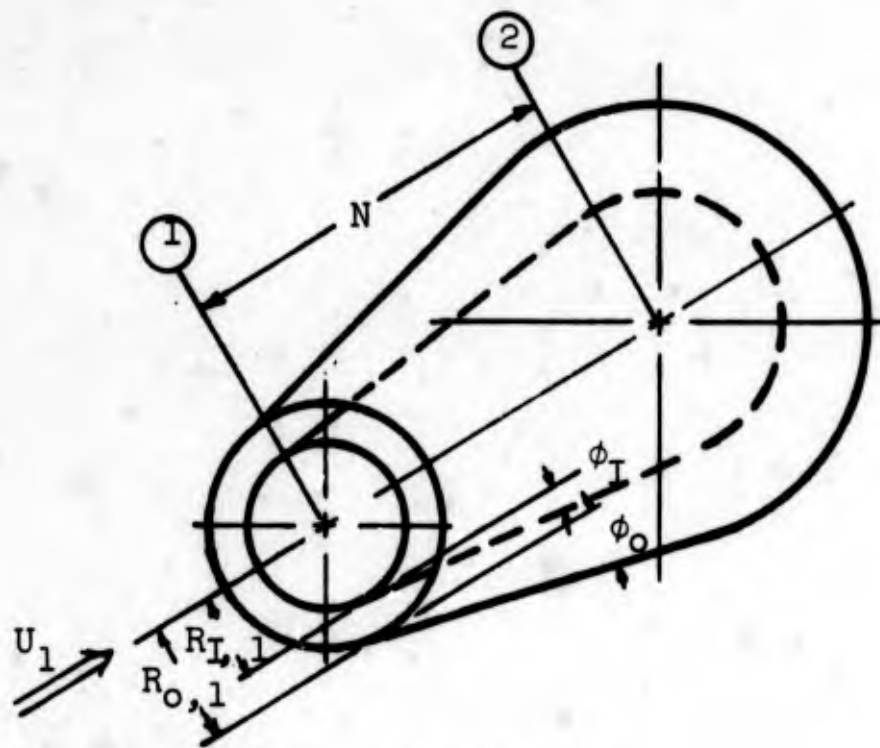


b. Three-Dimensional Diffuser

Fig. 2 Diffuser geometries with nomenclature.



c. Conical Diffuser



d. Annular Diffuser

Fig. 2 Concluded.

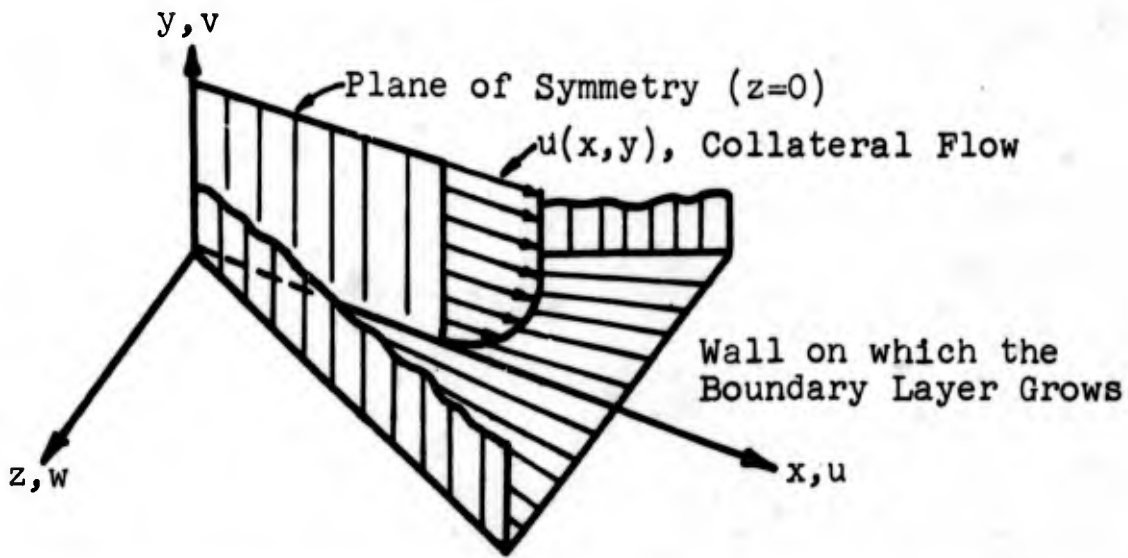


Fig. 3 Coordinate system used in developing the two-dimensional boundary layer equations.

Fig. 4 Relation of "a" to the bounding streamline.

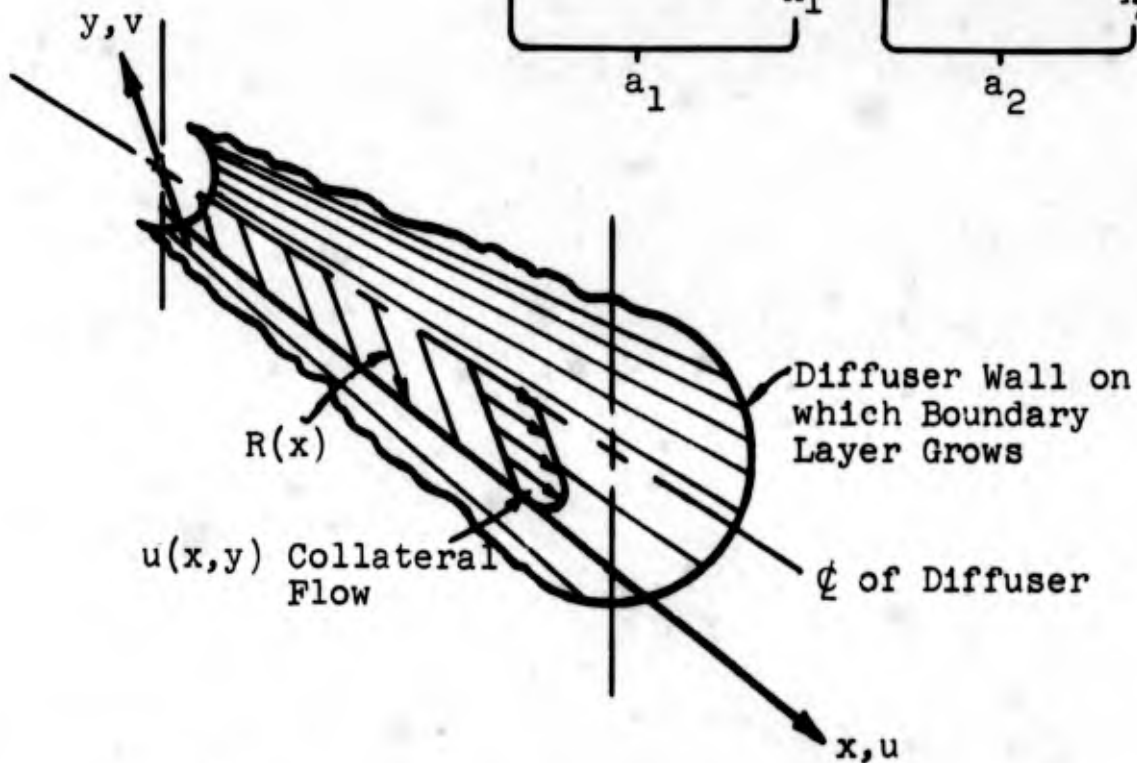
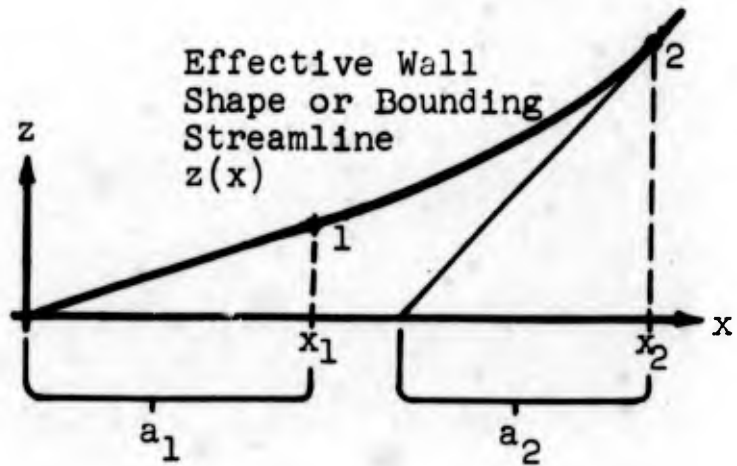


Fig. 5 Coordinate system used in developing the axisymmetric boundary layer equations.

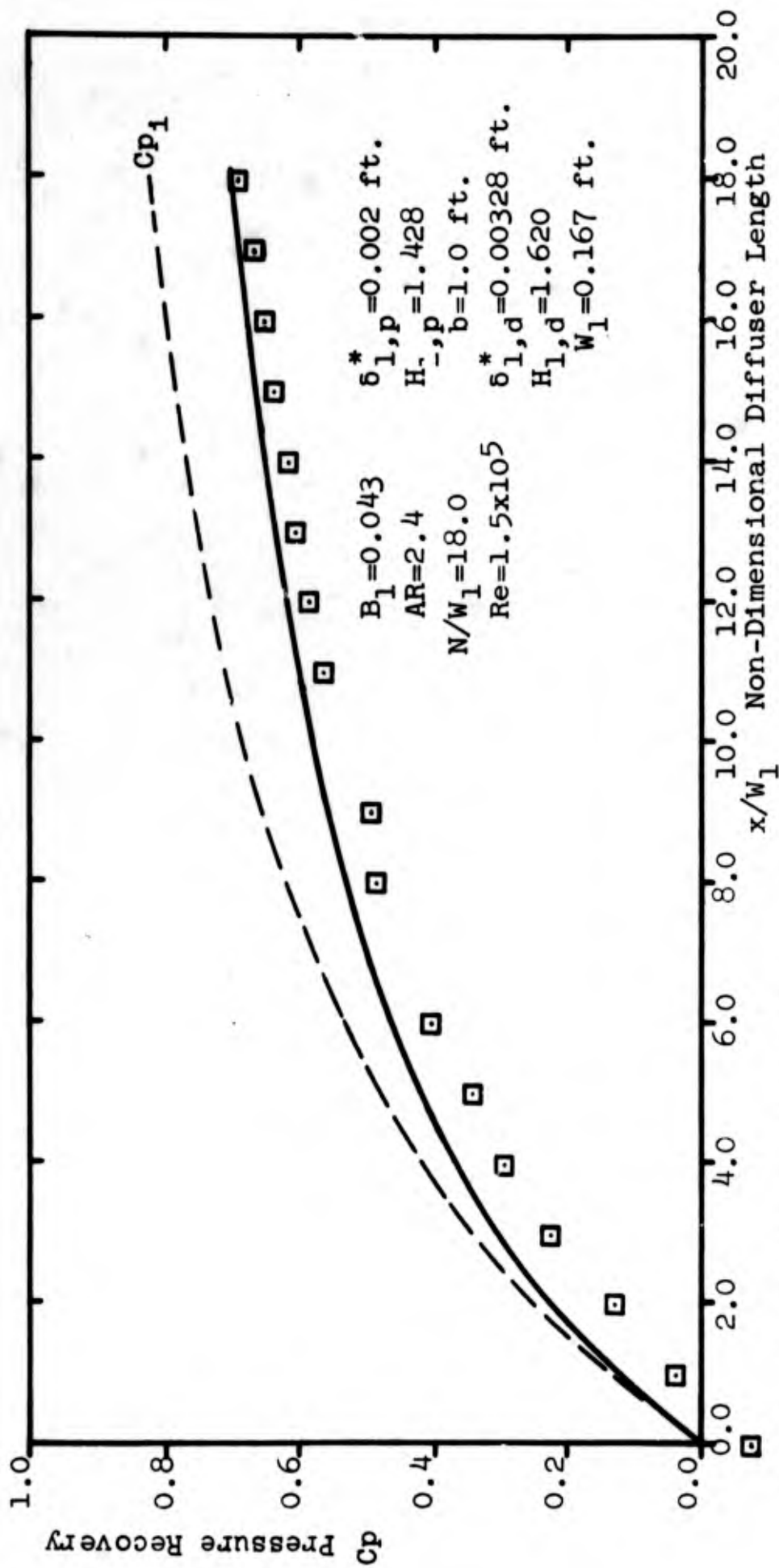


Fig. 6 Comparison between theory and Carlson's [1965] data for a two-dimensional diffuser.

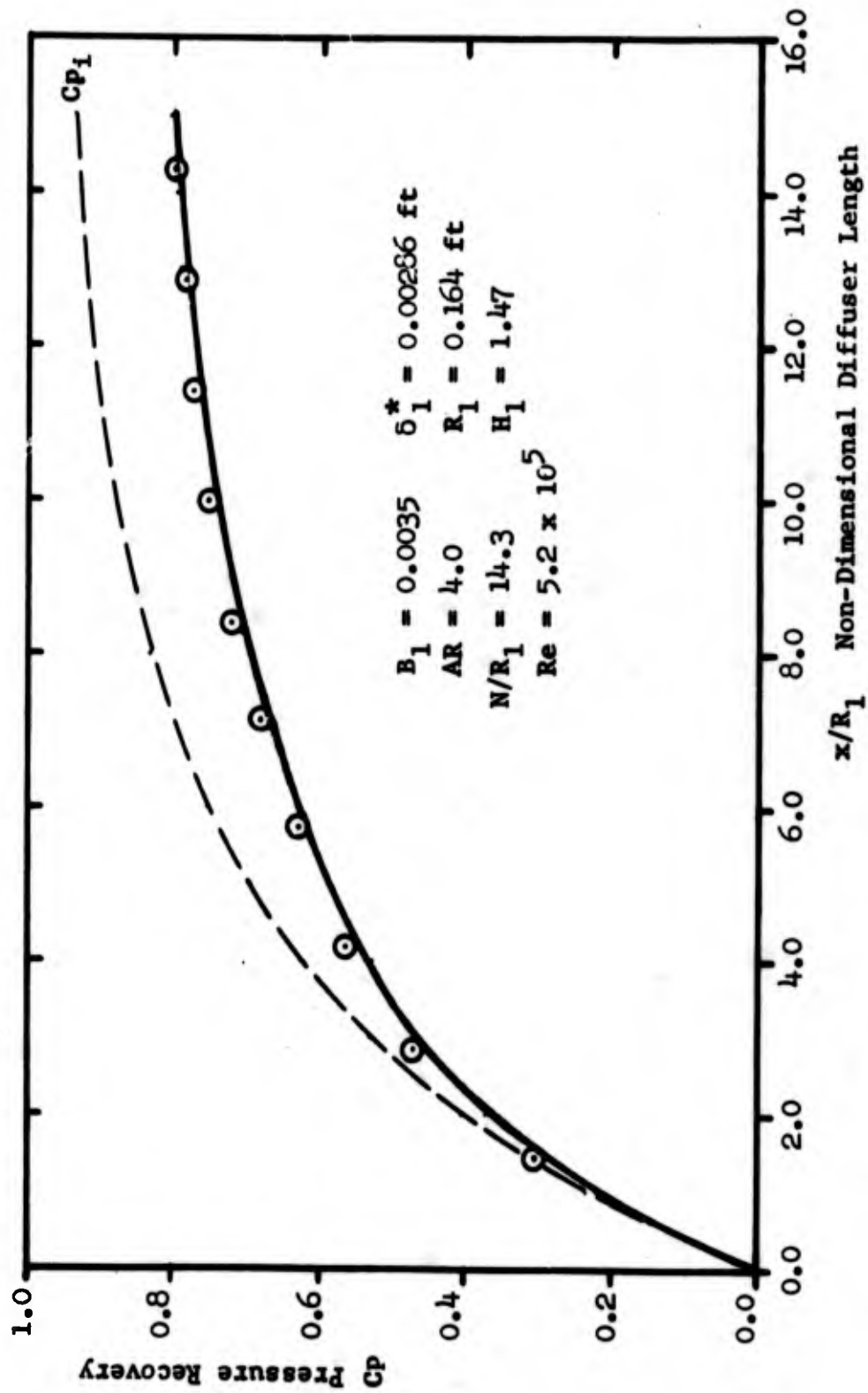


Figure 7 Comparison between theory and Sprenger's [1959] data for a conical diffuser.

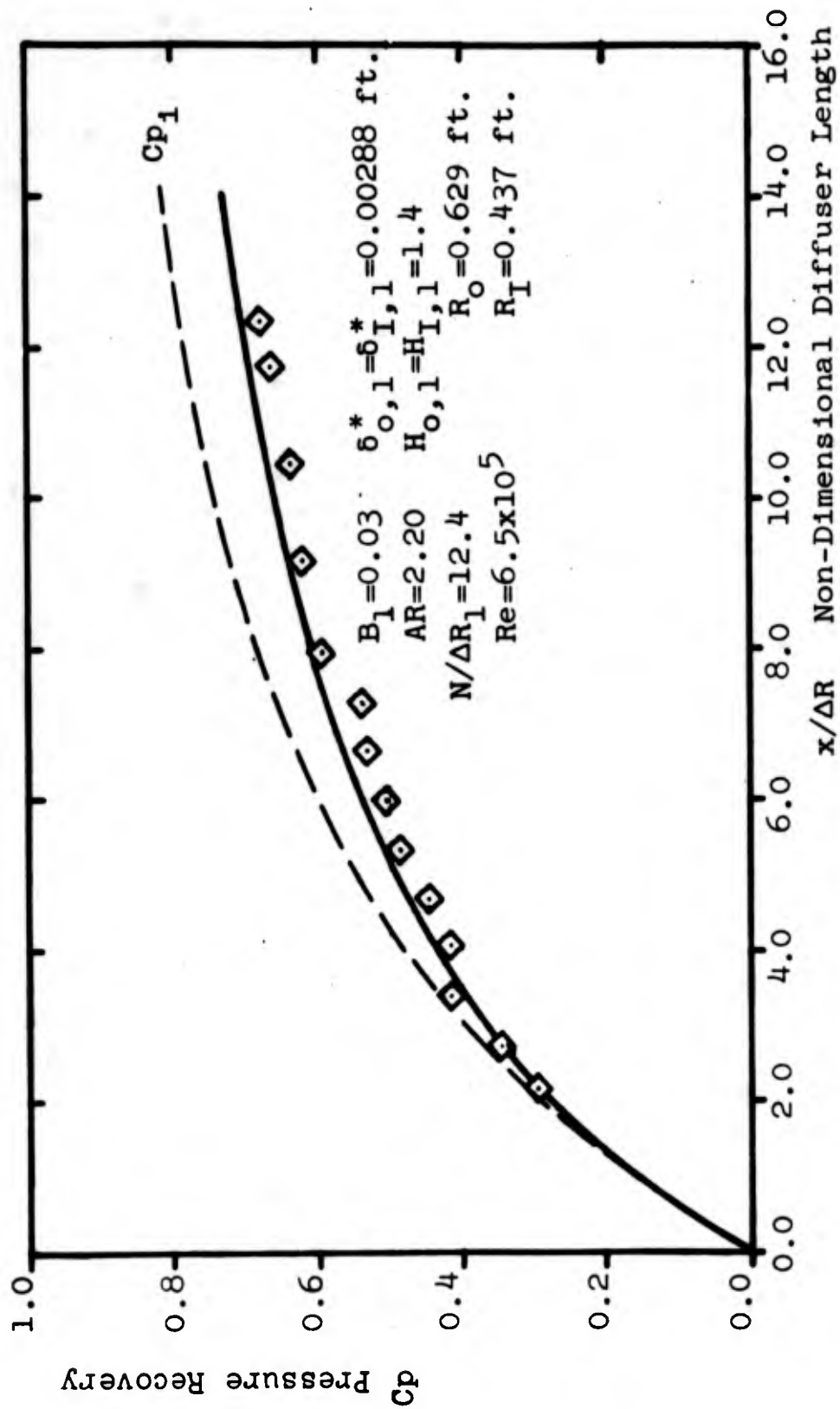


Fig. 8 Comparison between theory and Sovran and Klomp's [1964] data for an annular diffuser.

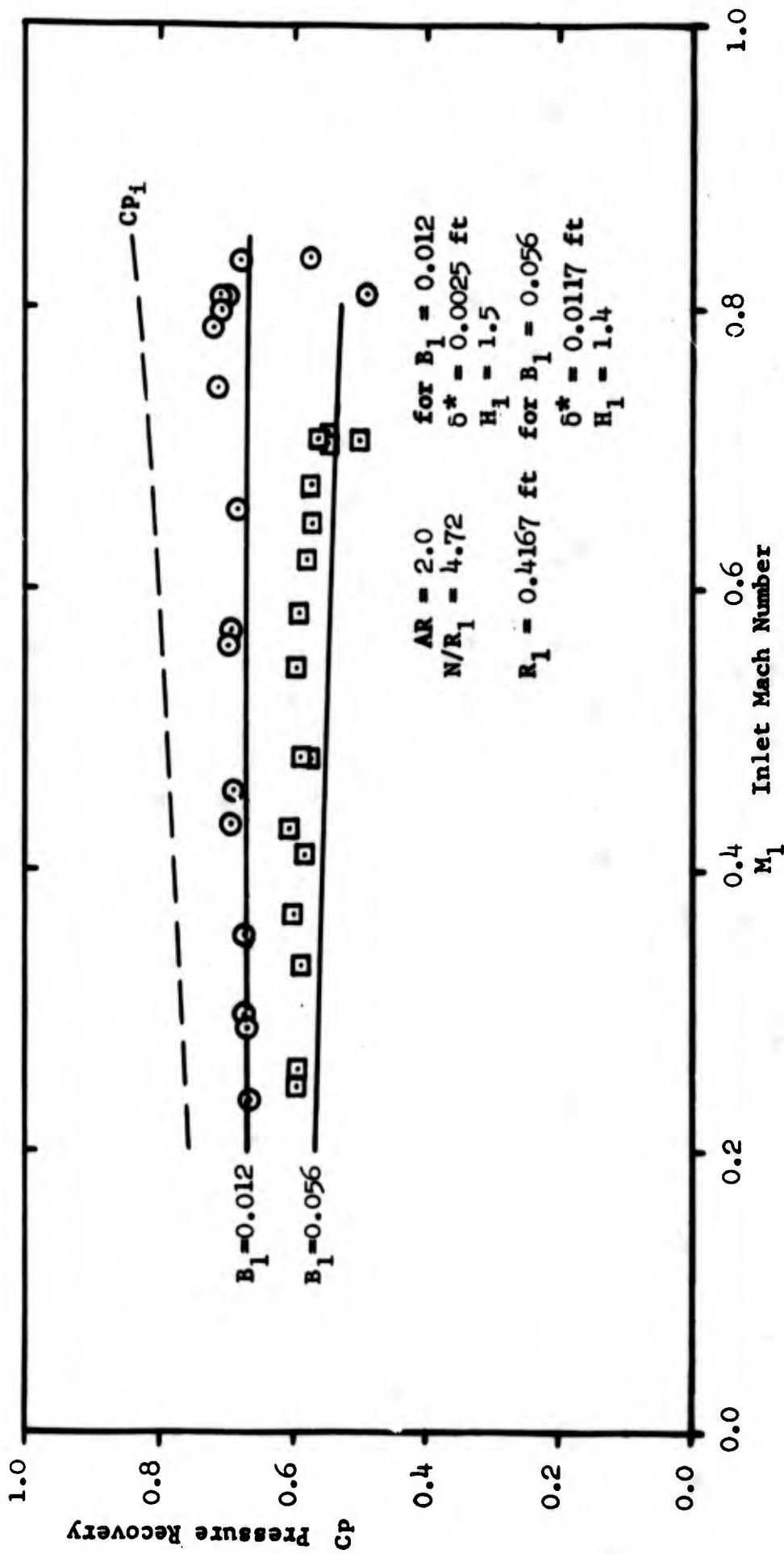
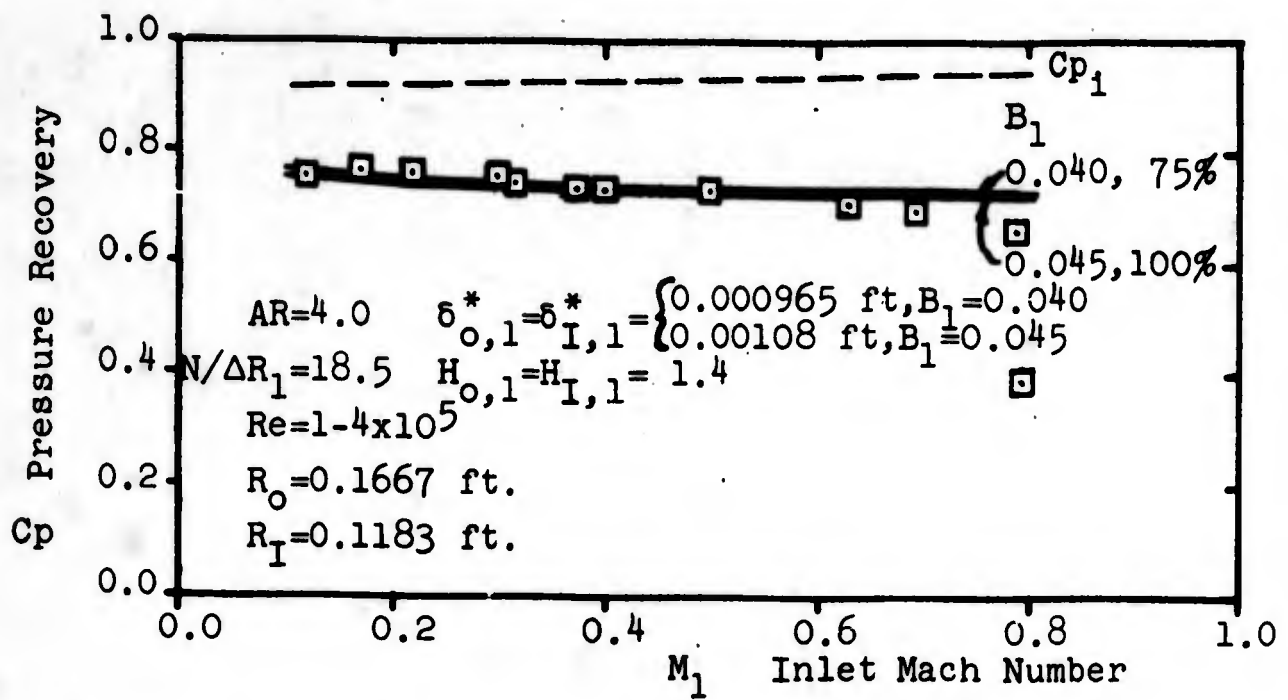
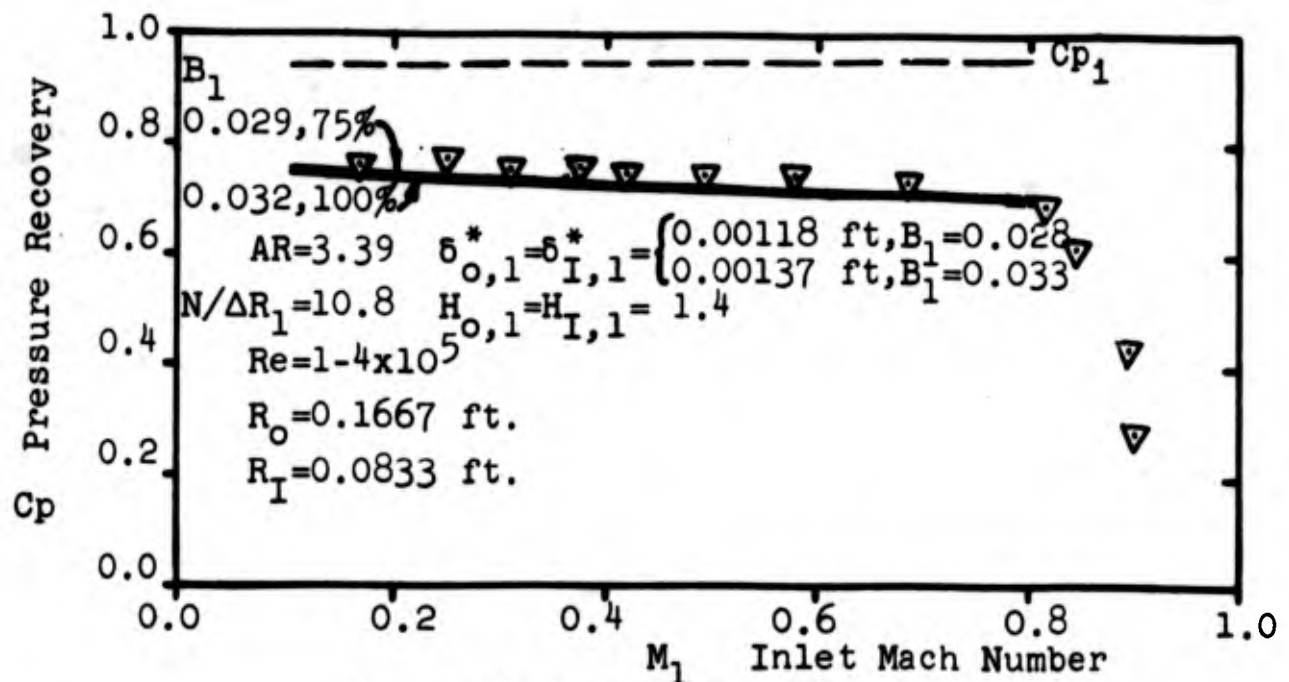


FIGURE 9 Comparison between theory and Copp's [1951] data for compressible flow in a conical diffuser.

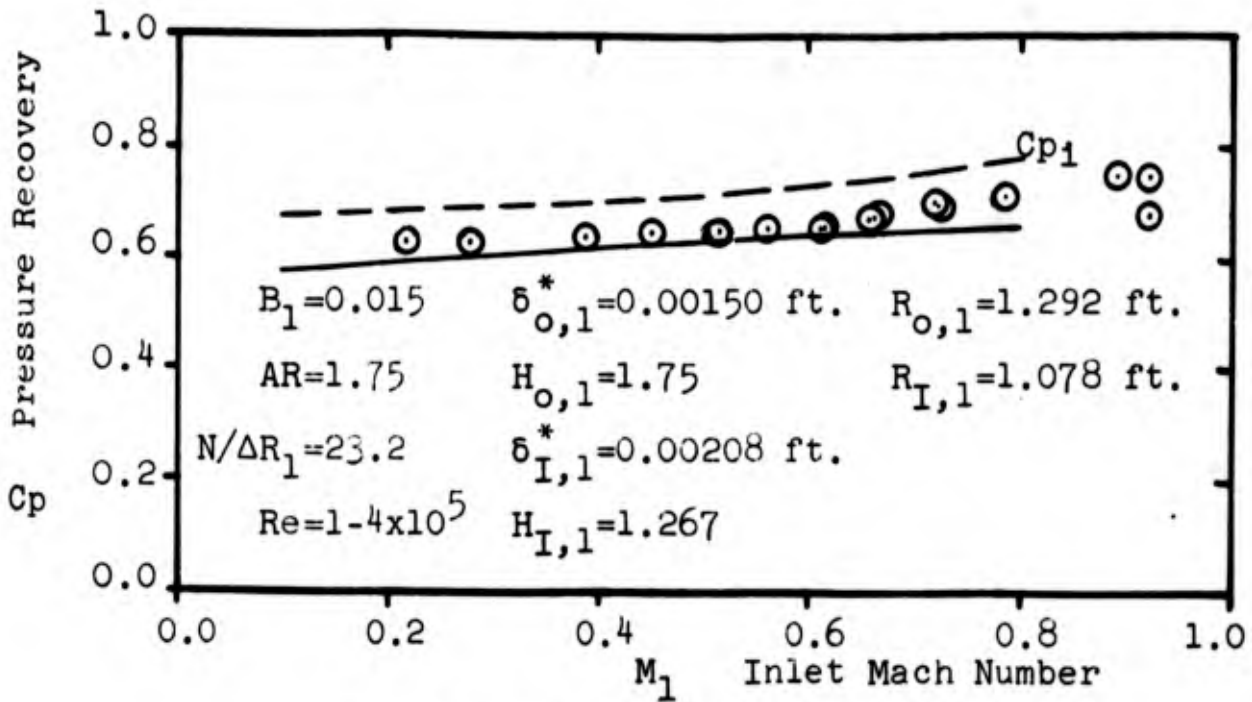


a. 10.5; 7.5; 0.71

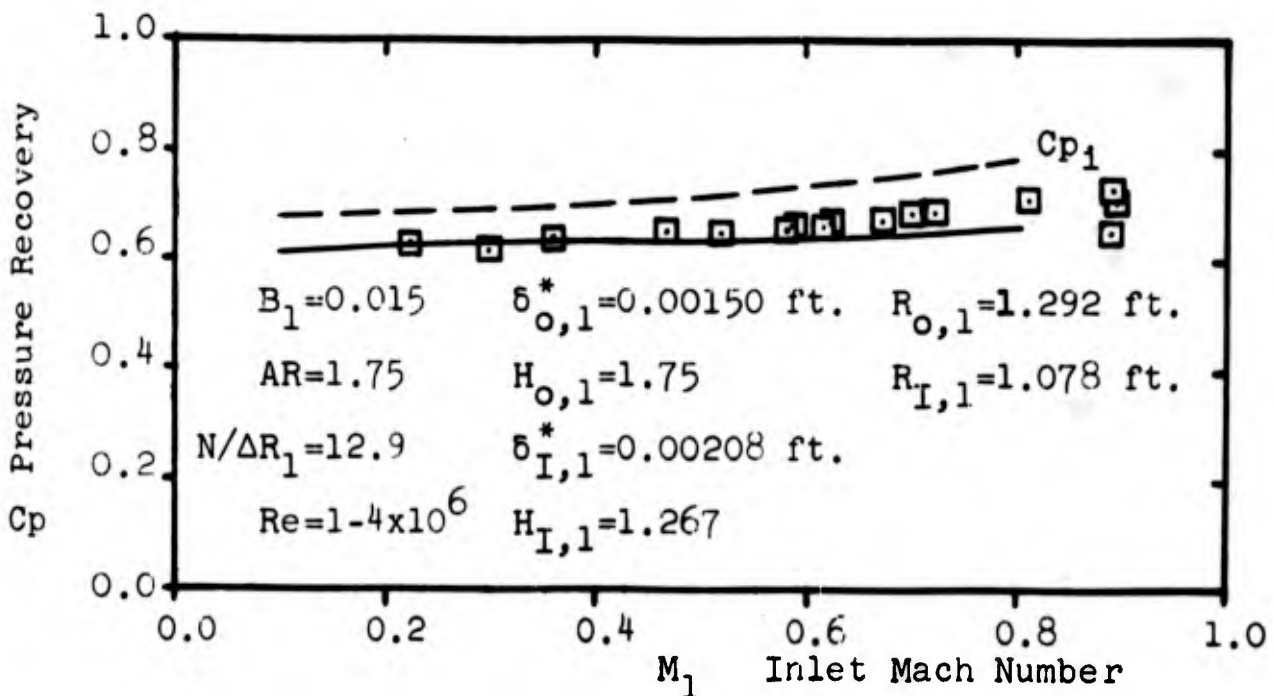


b. 10.5; 7.5; 0.50

Fig. 10 Comparison between theory and Johnston's [1959] data for compressible flow in an annular diffuser.



a. 0.0; -2.58; 0.834



b. 0.0; -5.25; 0.834

Fig. 11 Comparison between theory and Nelson and Popp's [1949] data for compressible flow in an annular diffuser.

Symbol	\hat{N}	AR	B_1	Geometry	Source	
○	18.0	2.4	0.043	2D	Carlson [1965]	$\alpha = 1.0$
◻	18.0	2.4	0.043	2D	" "	$\alpha = 0.0$
◈	18.0	2.4	0.043	2D	" "	$\alpha = -1.0$
▼	8.0	2.0	0.043	2D	Norbury [1951]	
◀	6.9	2.98	0.03	Square	Hudimoto [1952]	
◁	14.3	4.0	0.047	Conical	Sprenger [1959]	
◊	14.3	4.0	0.012	"	" "	
◊	2.8	1.44	0.010	"	" "	
◊	2.8	1.44	0.035	"	" "	
◊	2.8	1.44	0.092	"	" "	
◁	4.72	2.0	0.012	"	Copp [1951]	
◁	4.72	2.0	0.012	"	" "	
△	4.72	2.0	0.056	"	" "	
●	4.72	2.0	0.056	"	" "	
◁	28.6	4.0	0.0075	"	Squire [1953]	
◊	22.8	4.0	0.0075	"	" "	
▼	18.9	4.0	0.0075	"	" "	
◻	14.3	4.0	0.0075	"	" "	
◁	11.4	4.0	0.0075	"	" "	
◉	19.25	3.19	0.019	Annular	Ainley [1952]	
◉	14.75	3.19	0.019	"	" "	
◊	10.0	1.75	0.015	"	Nelson & Popp [1949]	
▷	20.4	1.75	0.015	"	" " "	
▽	12.4	2.20	0.03	"	Sovran & Klomp [1964]	
◻	3.43	1.68	0.03	"	" " "	
◻	3.43	2.05	0.03	"	" " "	
○	8.5	3.26	0.015	"	" " "	

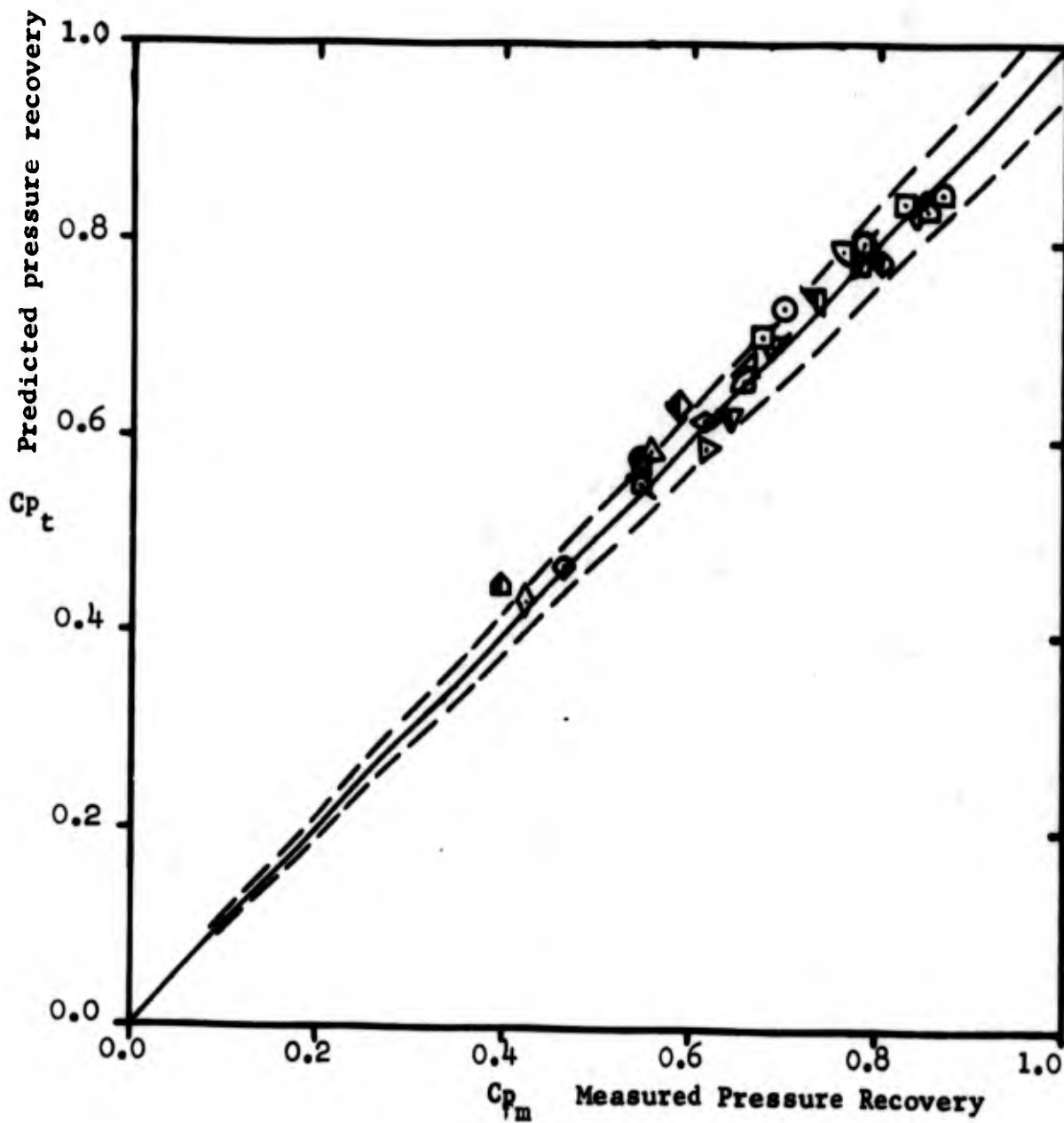


FIGURE 12 Comparison of measured and theoretical pressure recovery. The root mean square percentage difference is 3.2%.

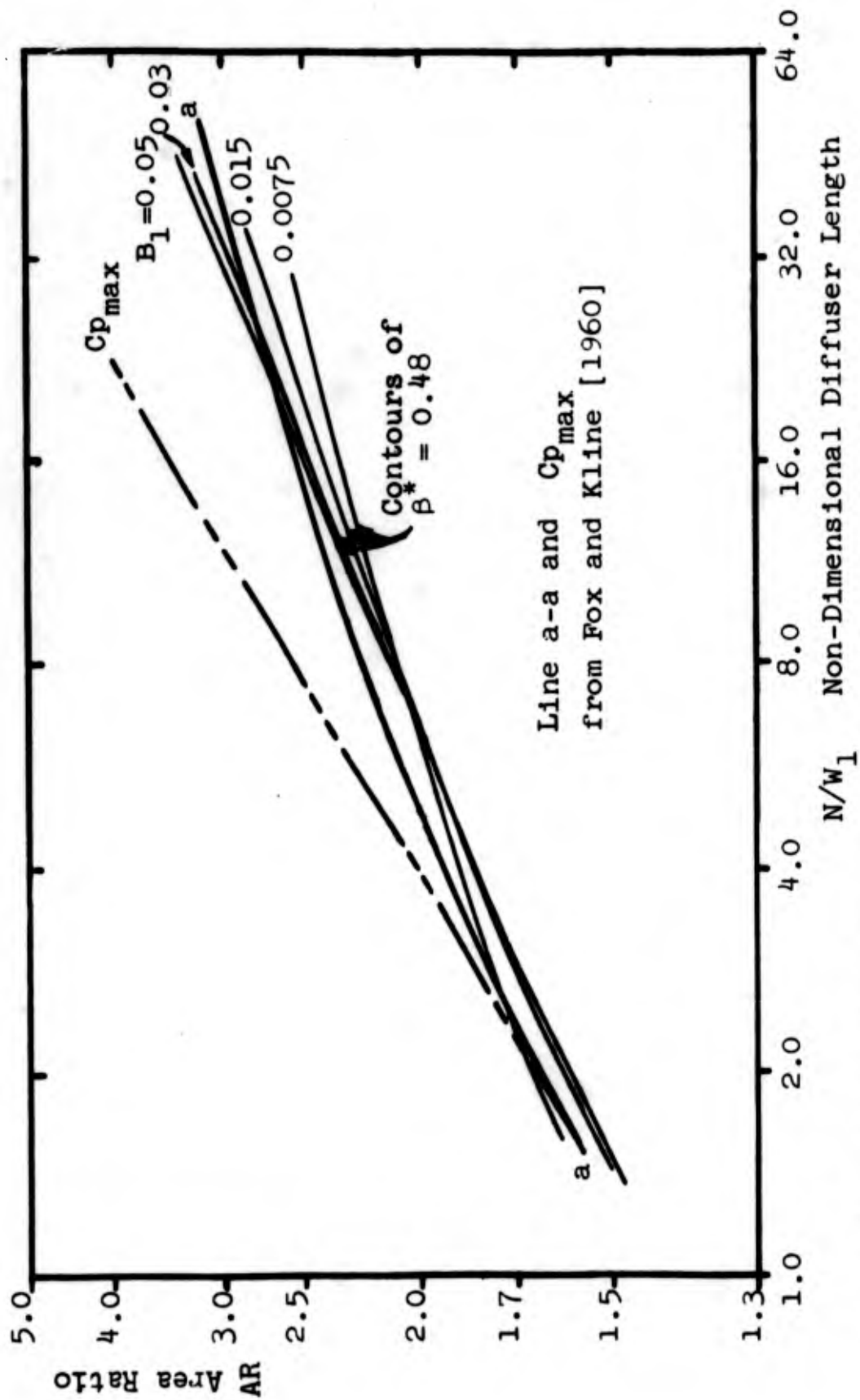


Fig. 13 Comparison among contours of $\beta^* = 0.48$, line a-a, and maximum pressure recovery for two-dimensional diffusers.

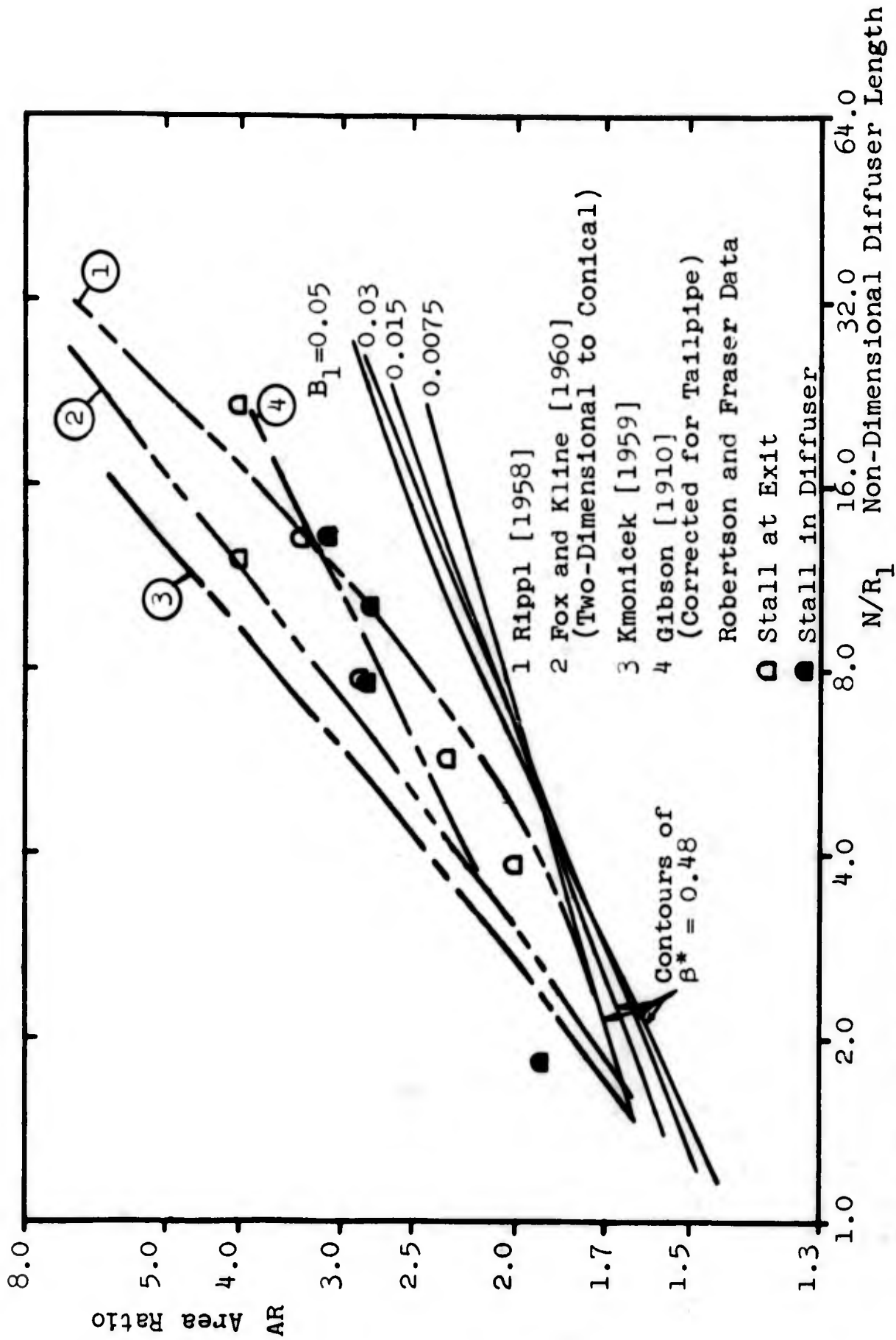


FIG. 14 Comparison between contours of $\beta^* = 0.48$ and maximum pressure recovery of several researchers for conical diffusers.

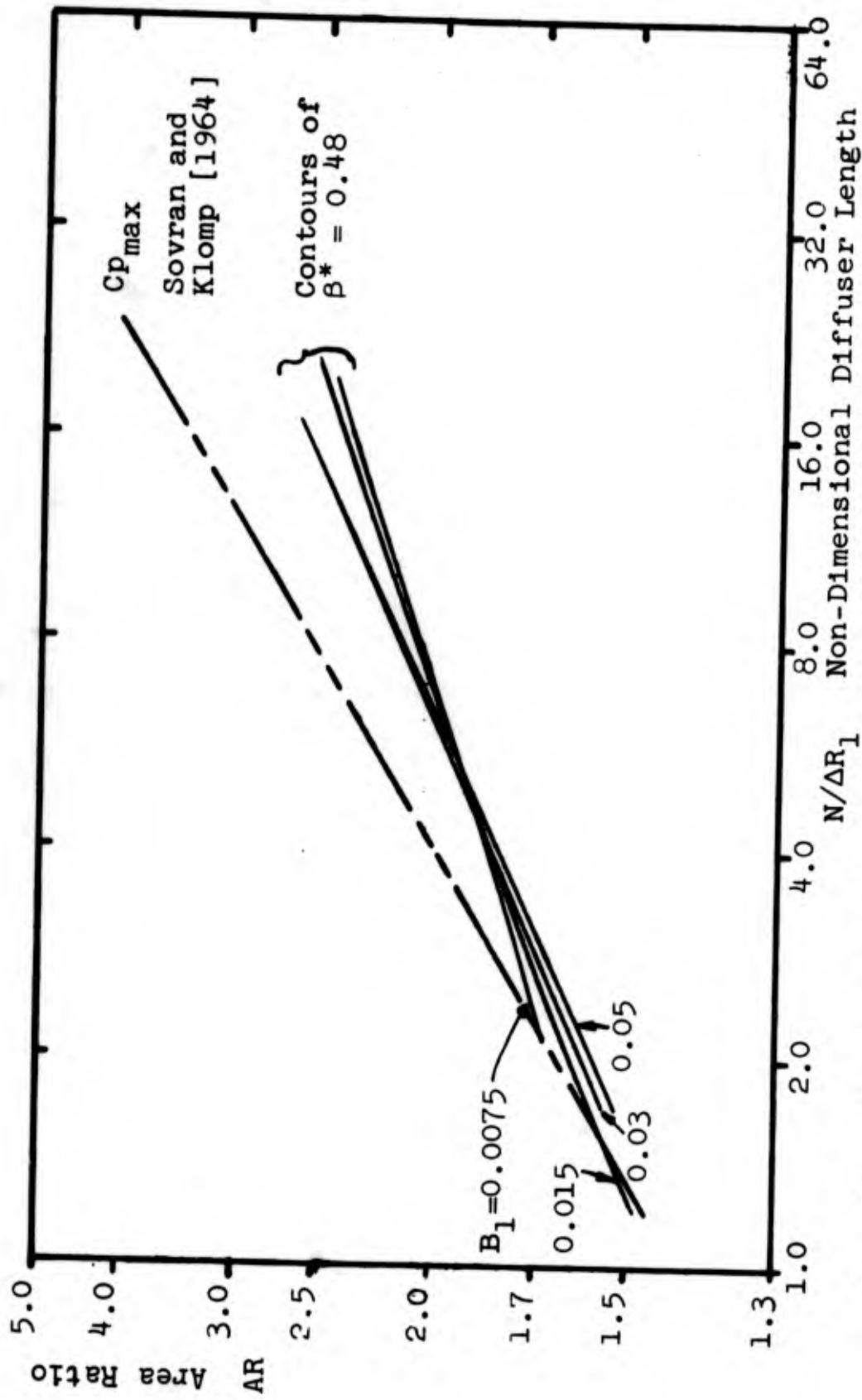


Fig. 15 Comparison between contours of $\beta^* = 0.48$ and maximum pressure recovery for annular diffusers.

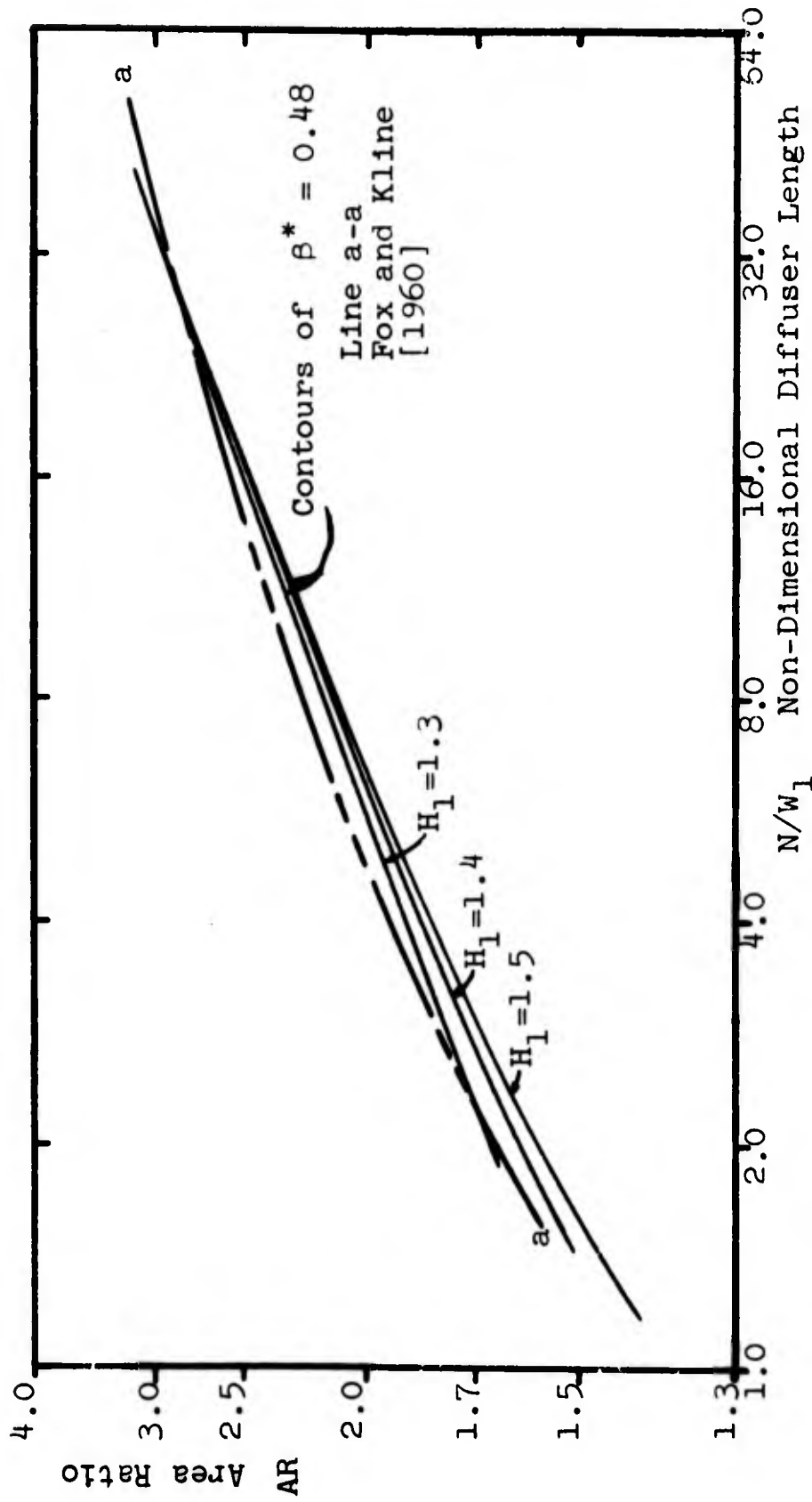
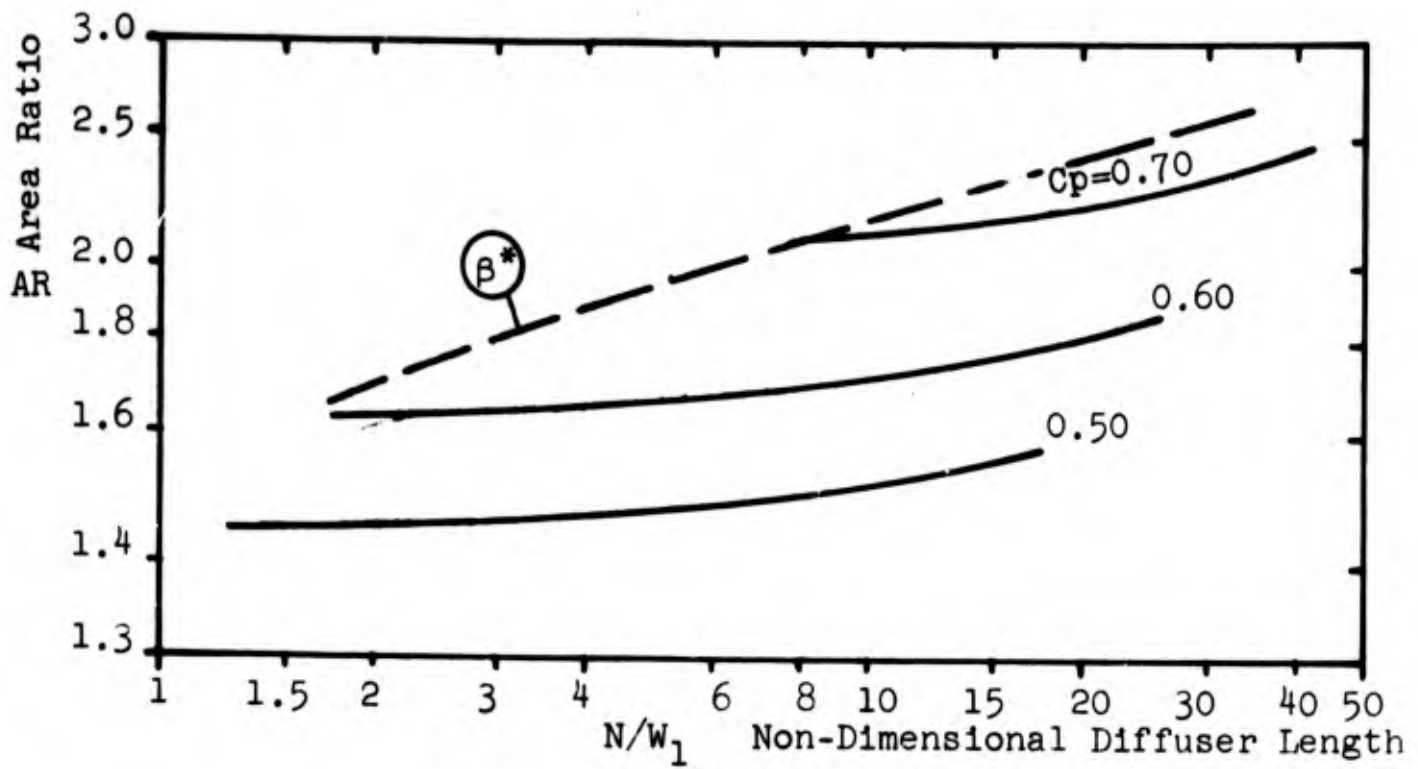
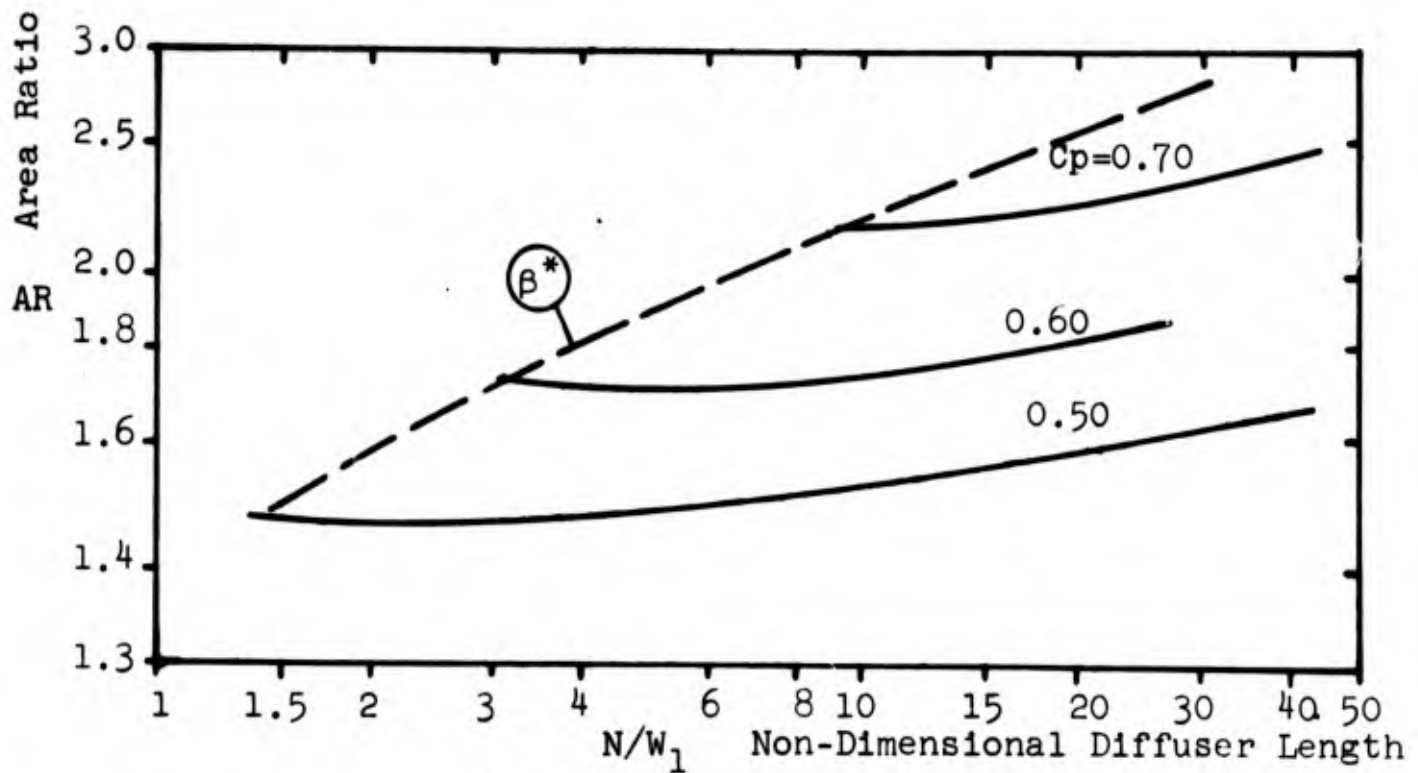


Fig. 16 The effect of H_1 on contours of $\beta^* = 0.48$ for two-dimensional diffusers.



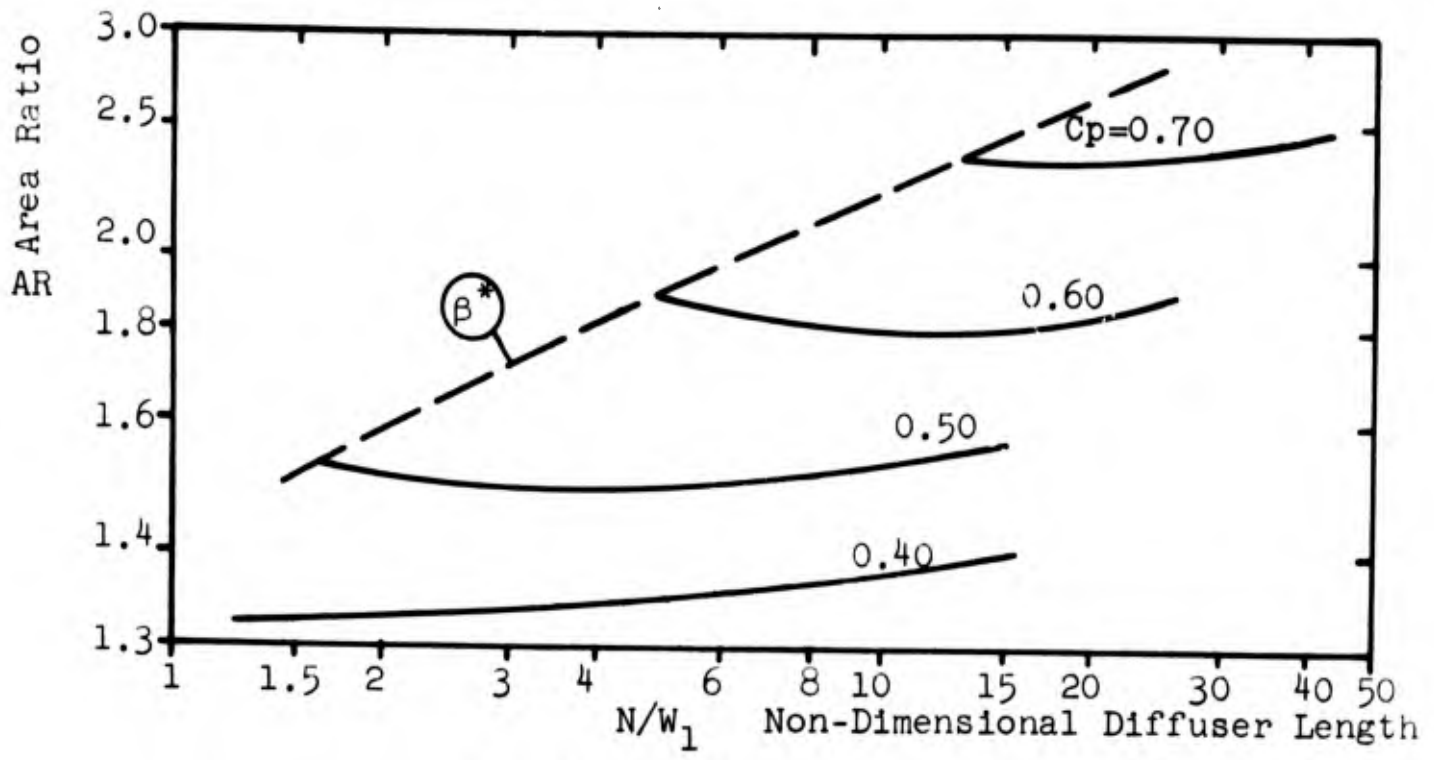
a. $B_1 = 0.0075$



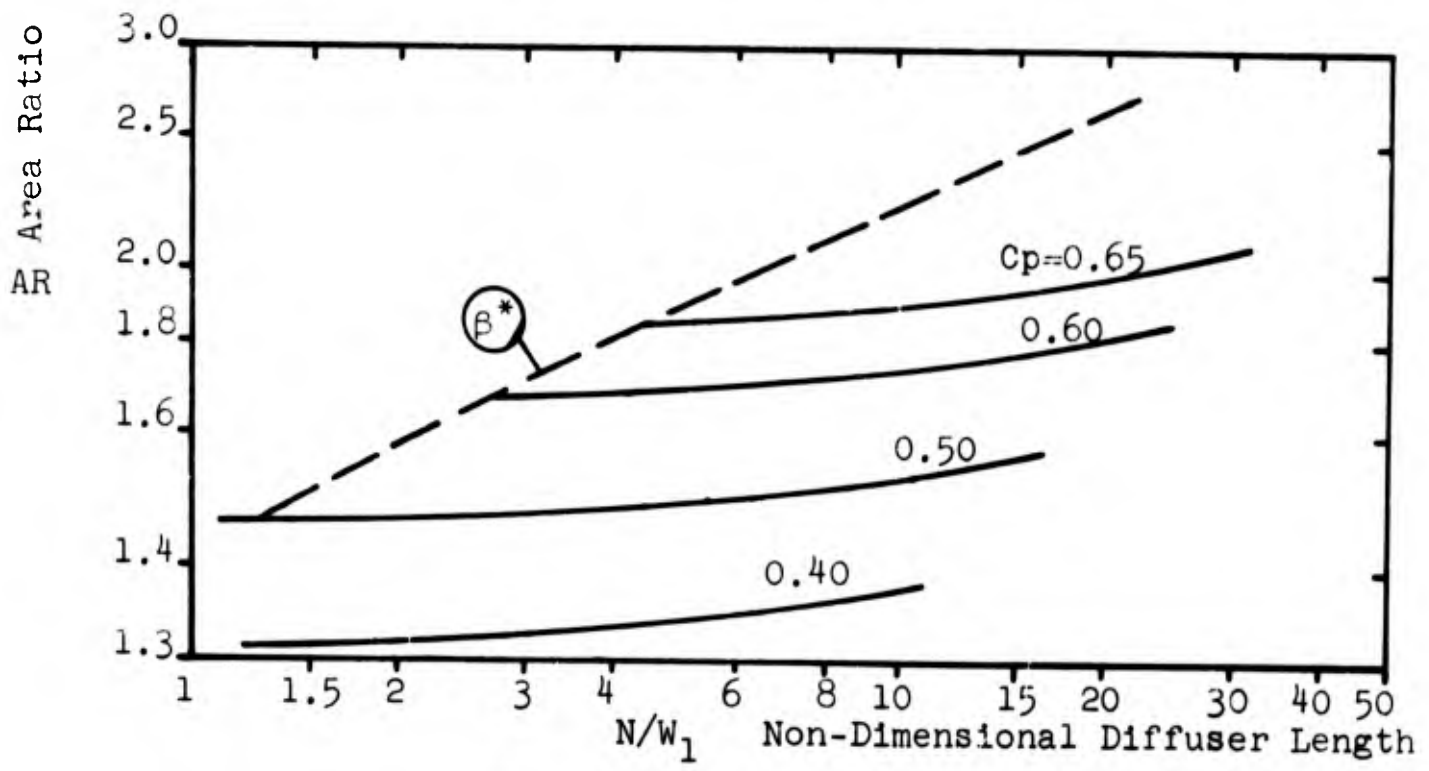
b. $B_1 = 0.015$

Fig. 17 Performance charts for two-dimensional diffusers.

β^* $\beta^* = 0.48$; indicates probable inception of appreciable stall.

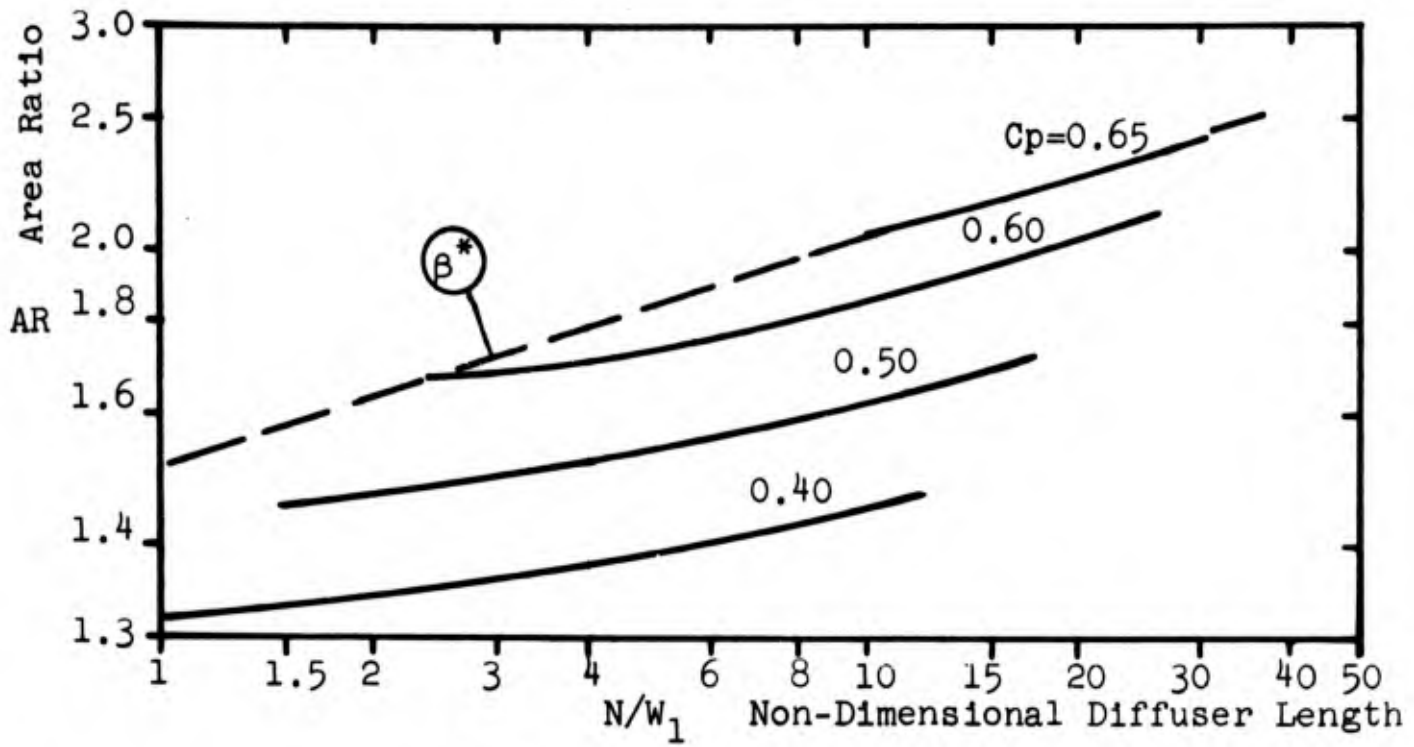


c. $B_1 = 0.03$

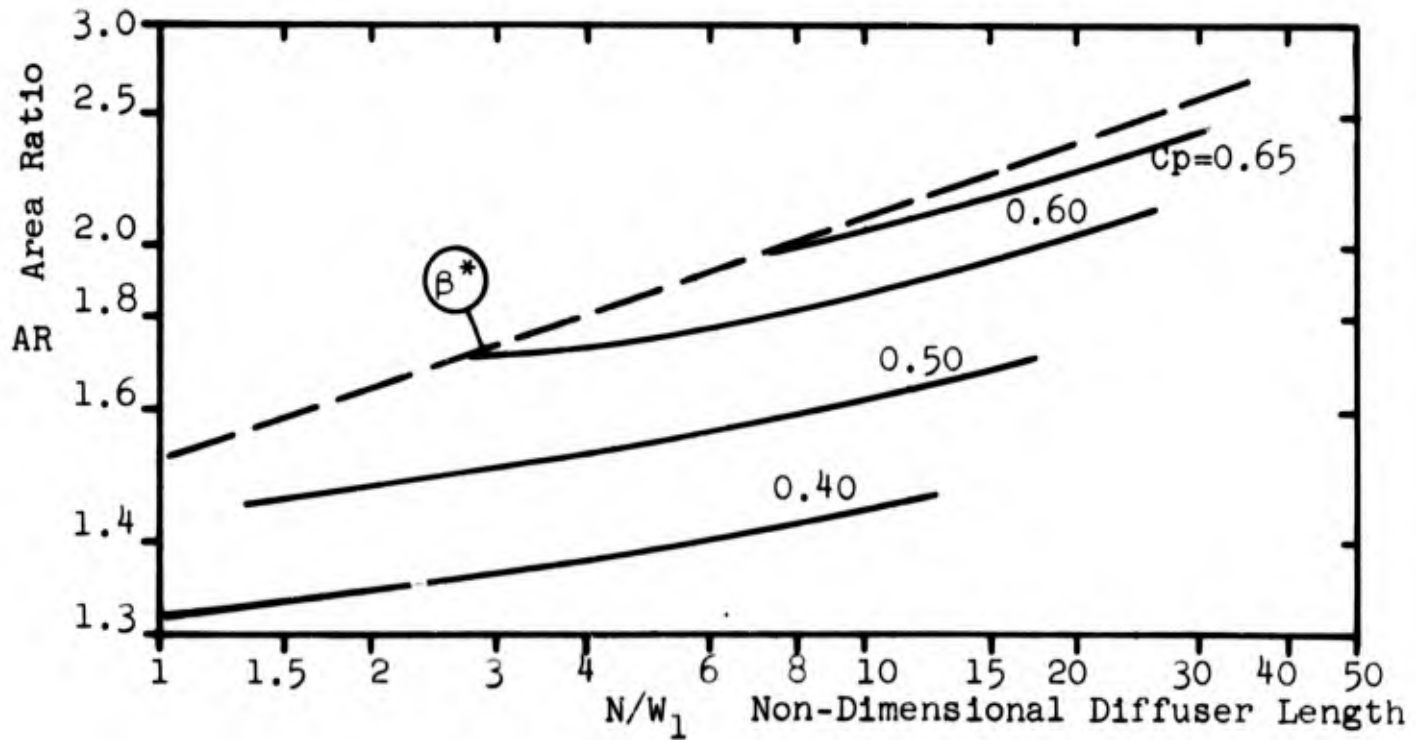


d. $B_1 = 0.05$

Fig. 17 Concluded.



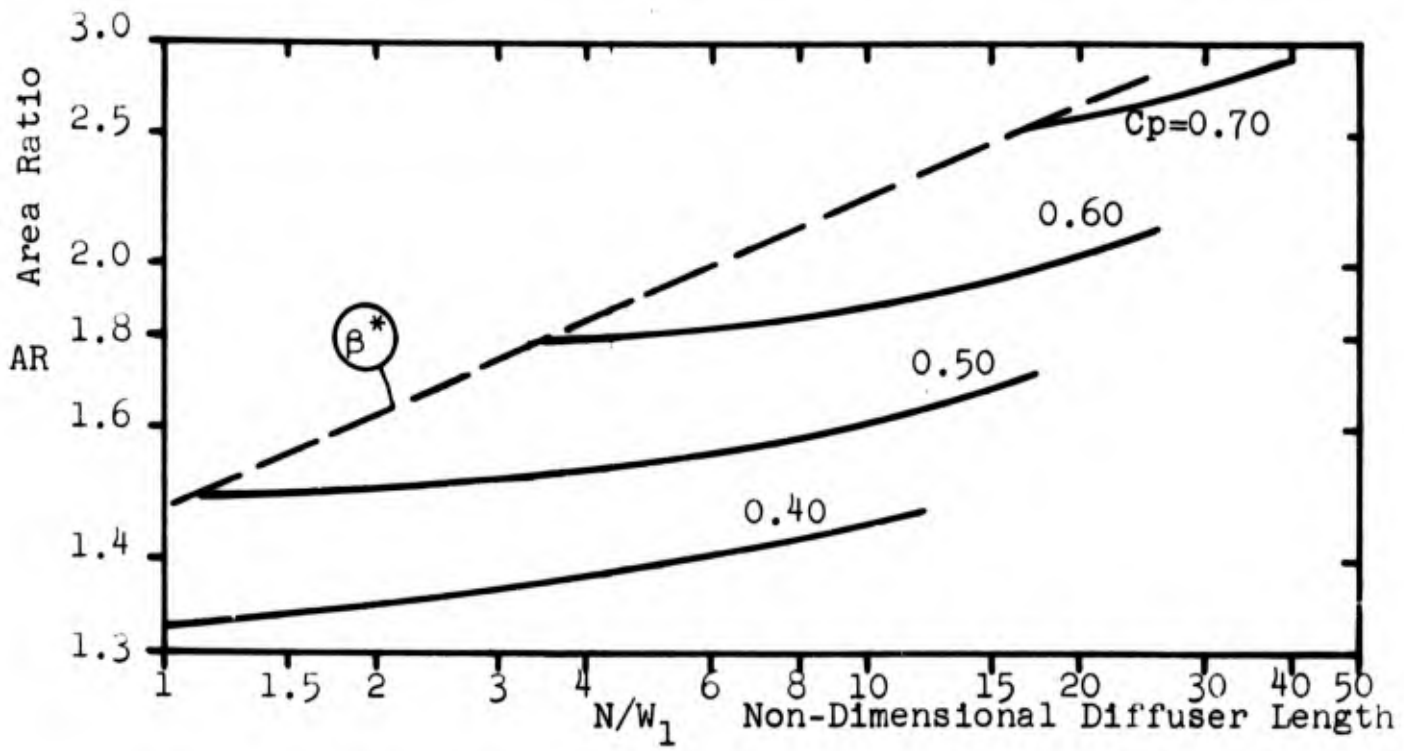
a. $B_1 = 0.0075$



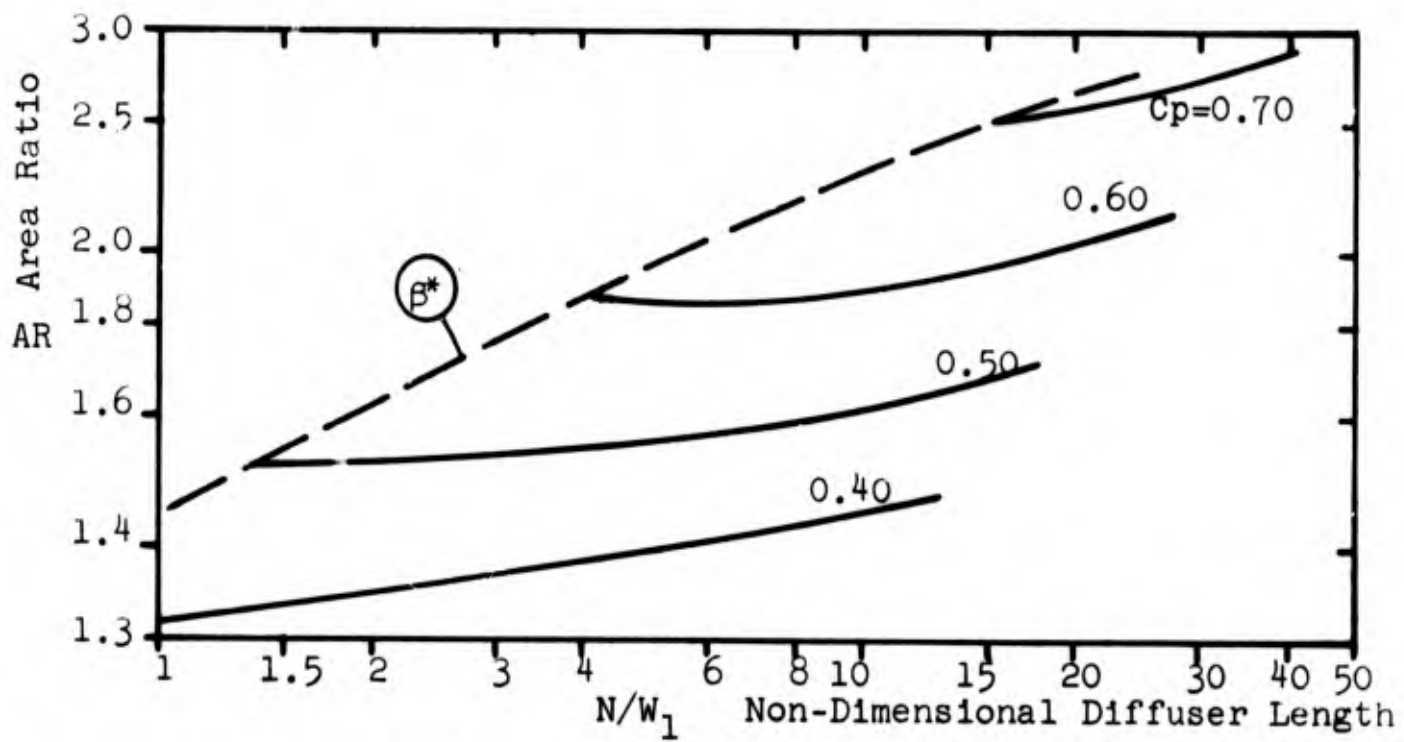
b. $B_1 = 0.015$

Fig. 18 Performance charts for three-dimensional diffusers.

β^* $\beta^* = 0.48$; indicates probable inception of appreciable stall.

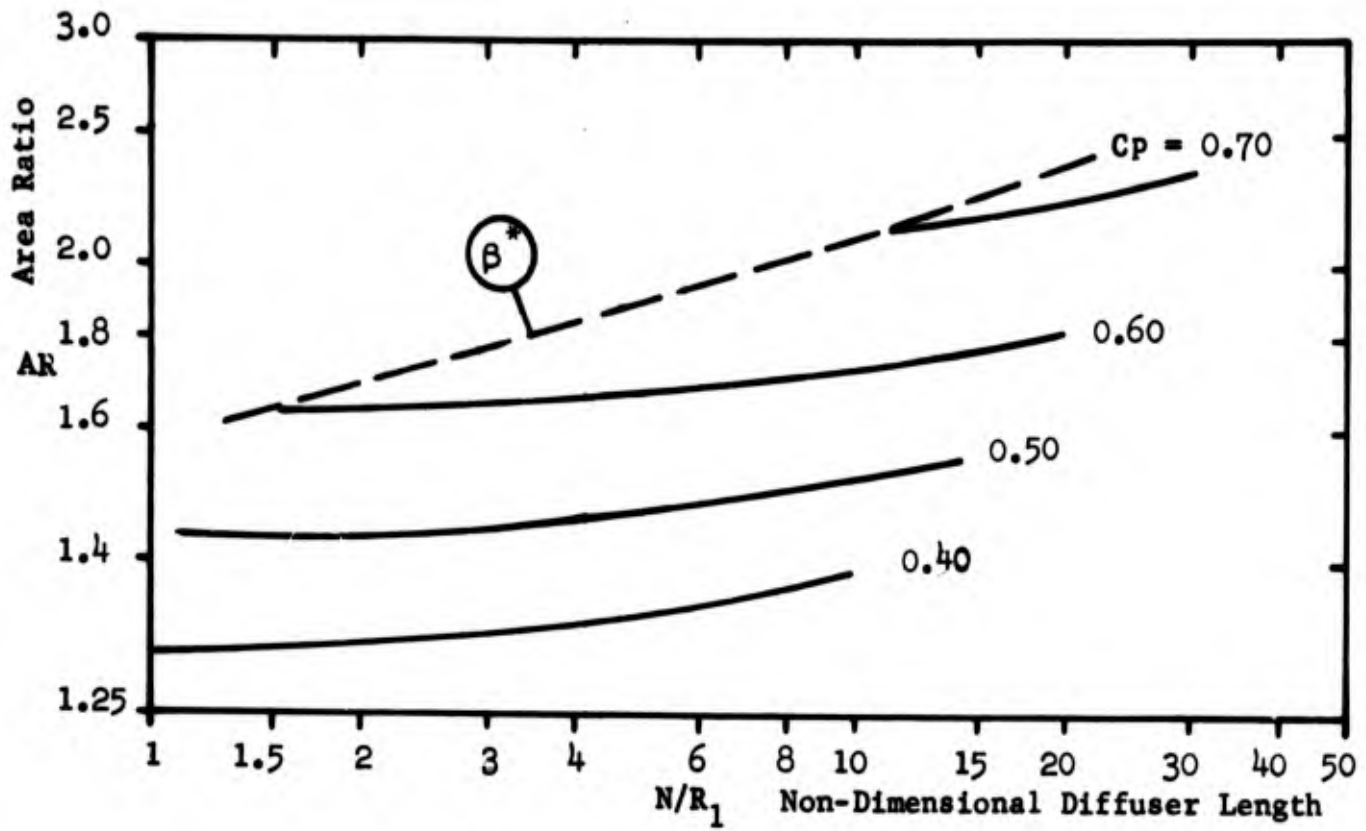


c. $B_1 = 0.03$

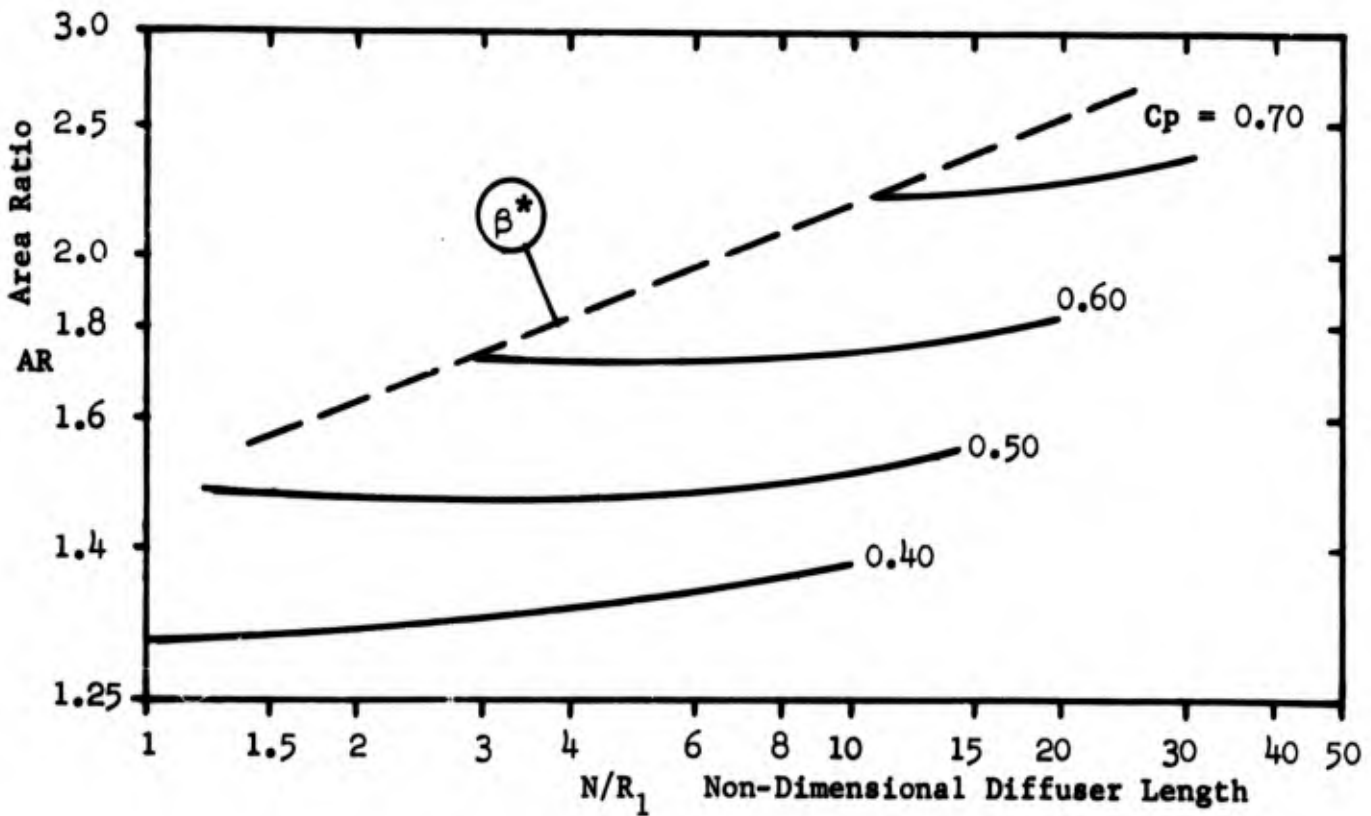


d. $B_1 = 0.05$

Fig. 18 Concluded.



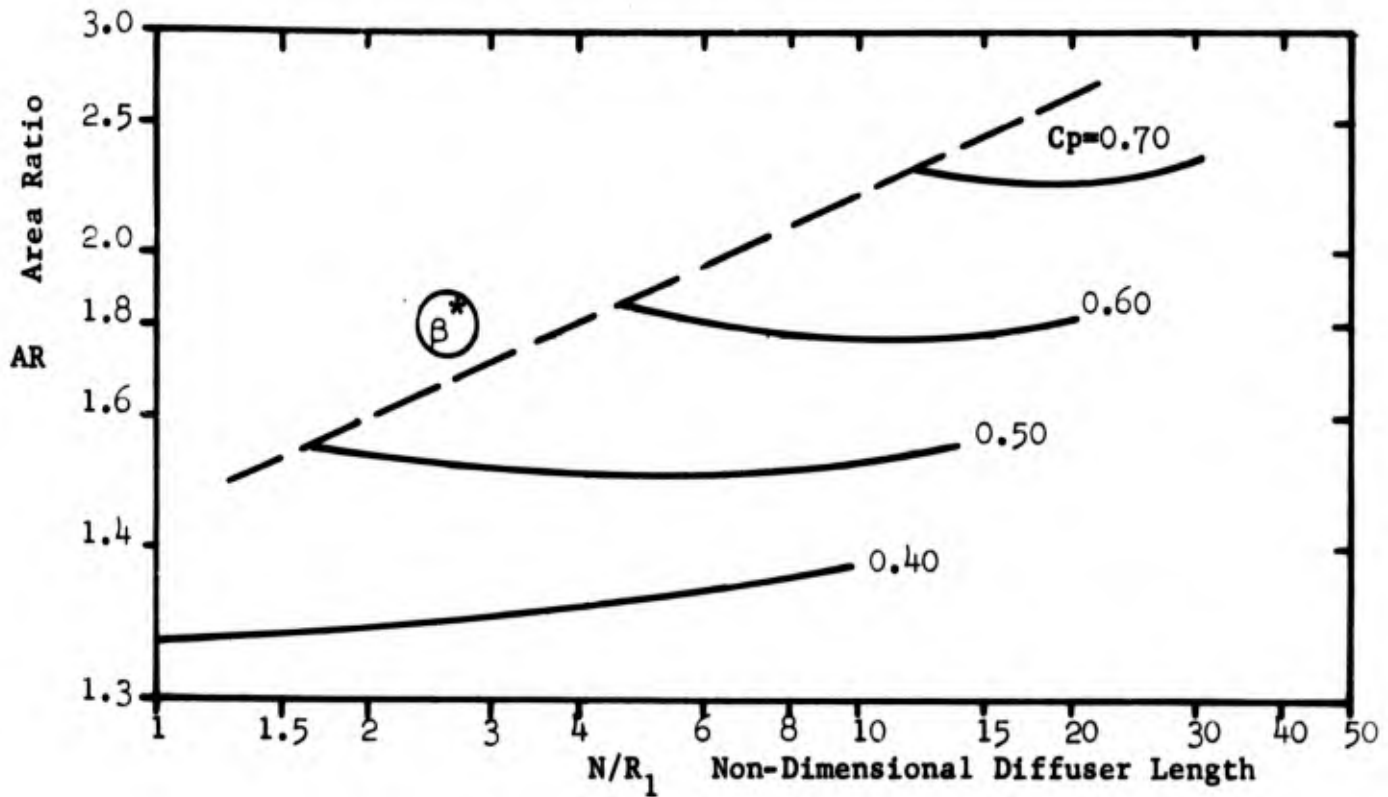
a. $B_1 = 0.0075$



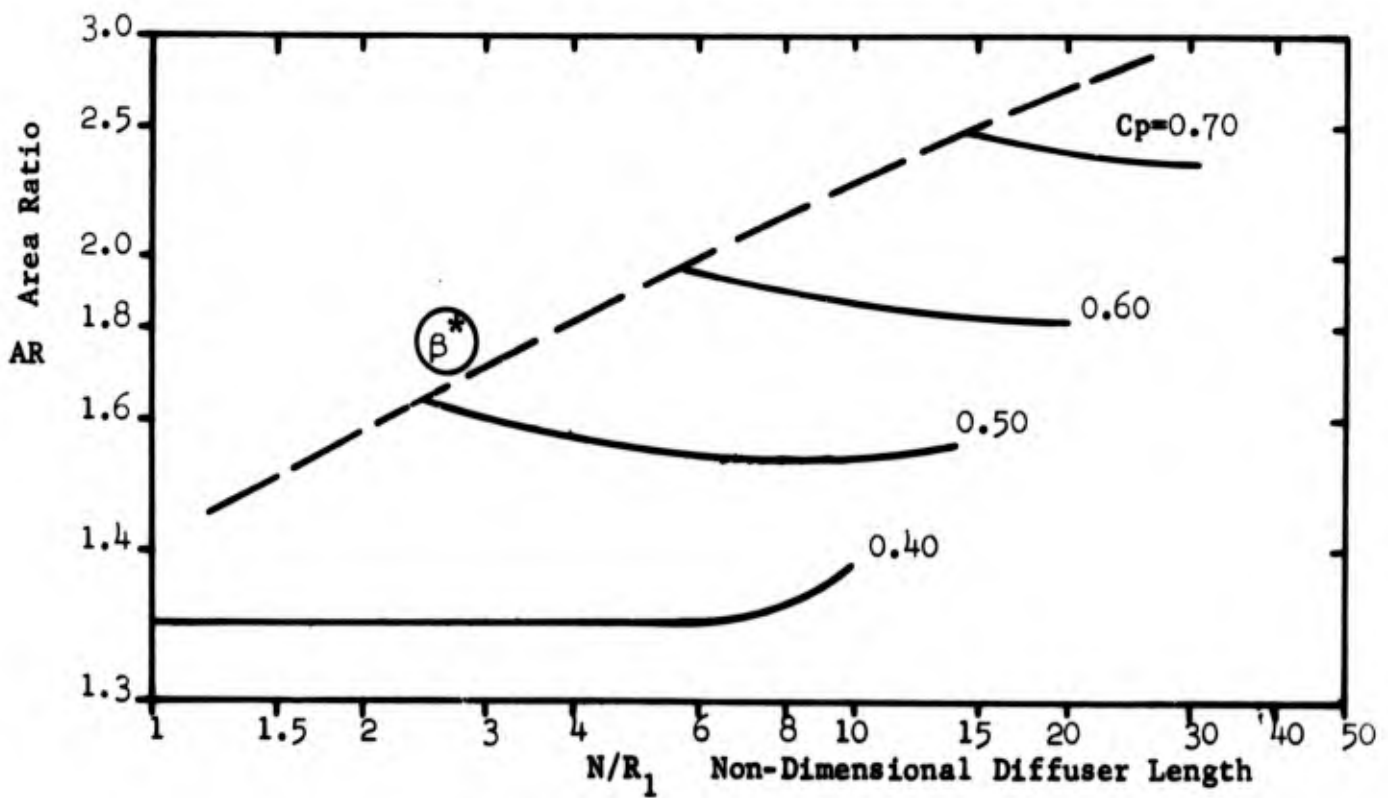
b. $B_1 = 0.015$

Fig. 19 Performance charts for conical diffusers.

β^* $\beta^* = 0.48$; indicates probable inception of appreciable stall.

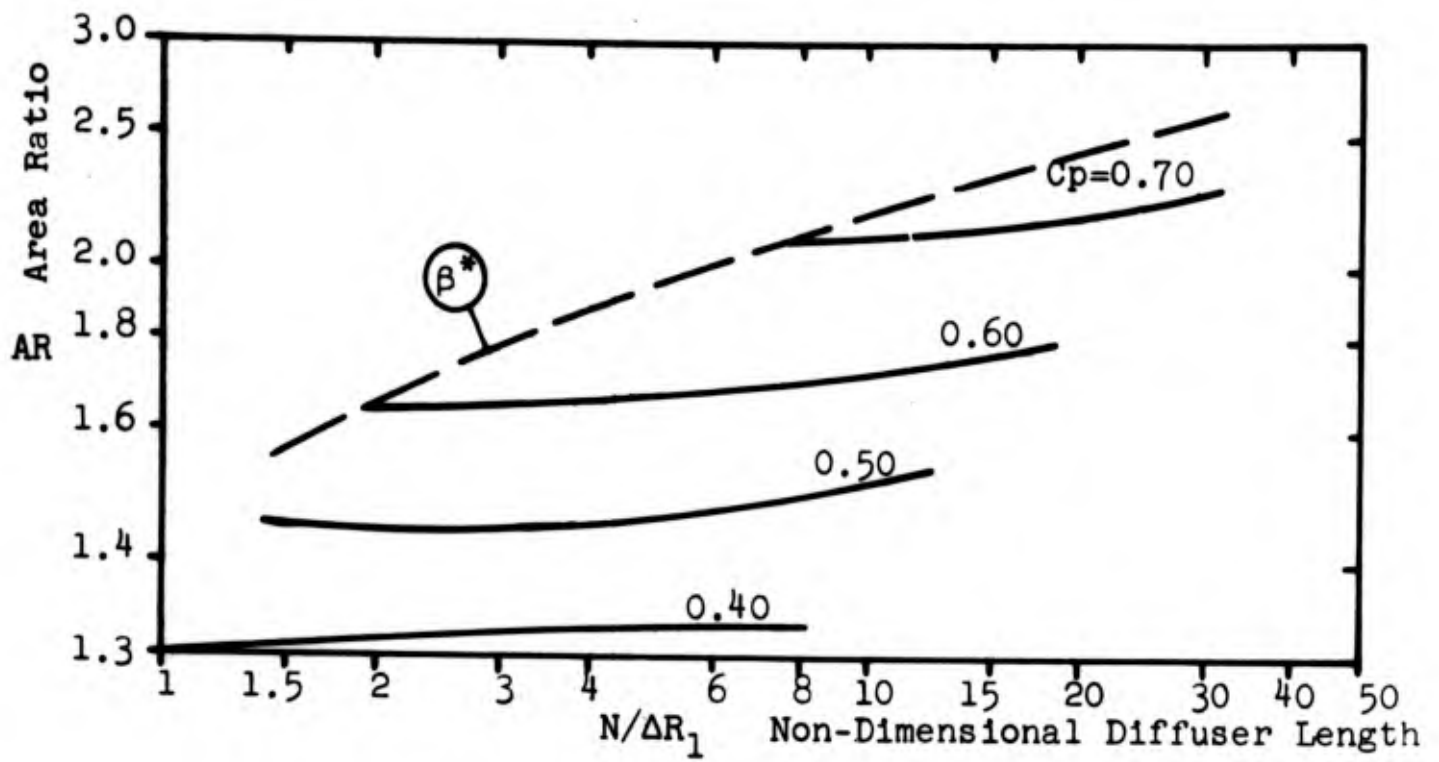


c. $B_1 = 0.03$

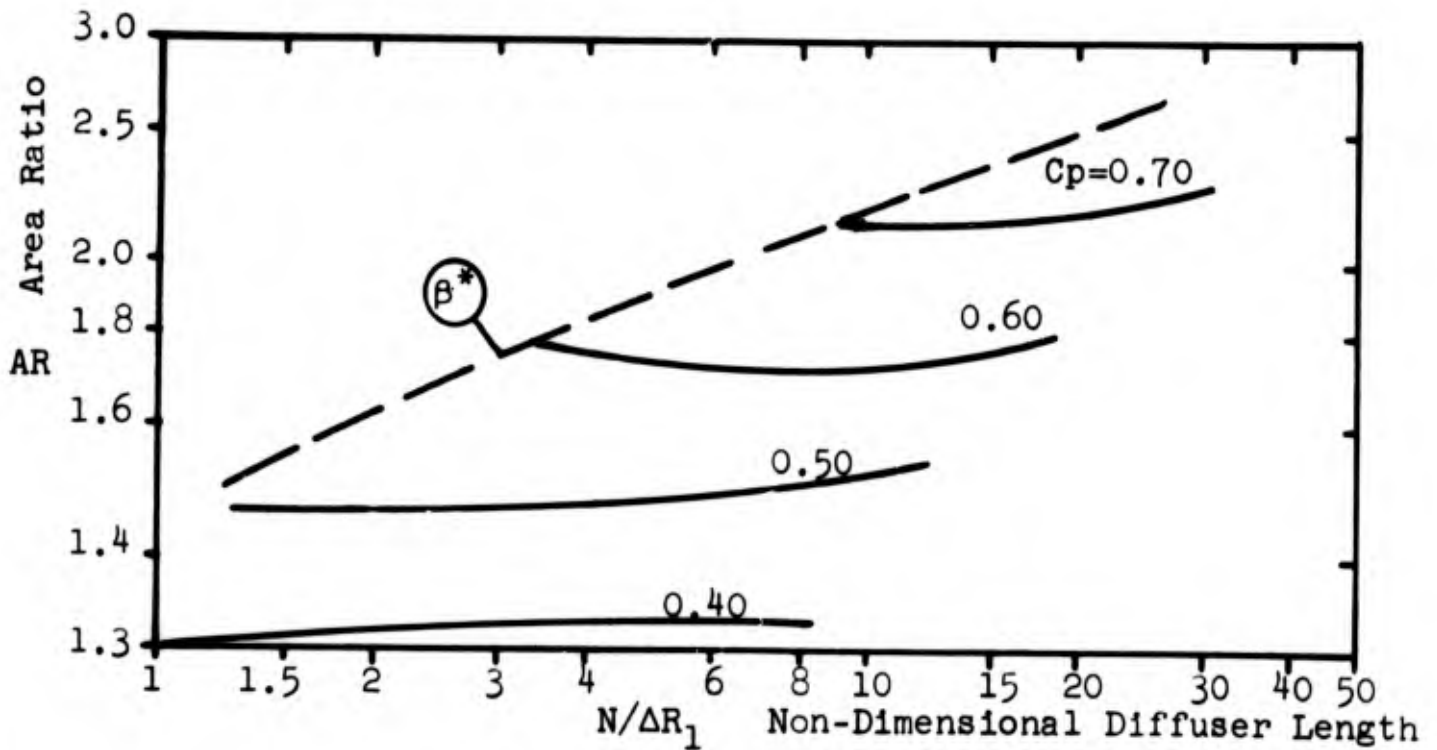


d. $B_1 = 0.05$

Fig. 19 Concluded.



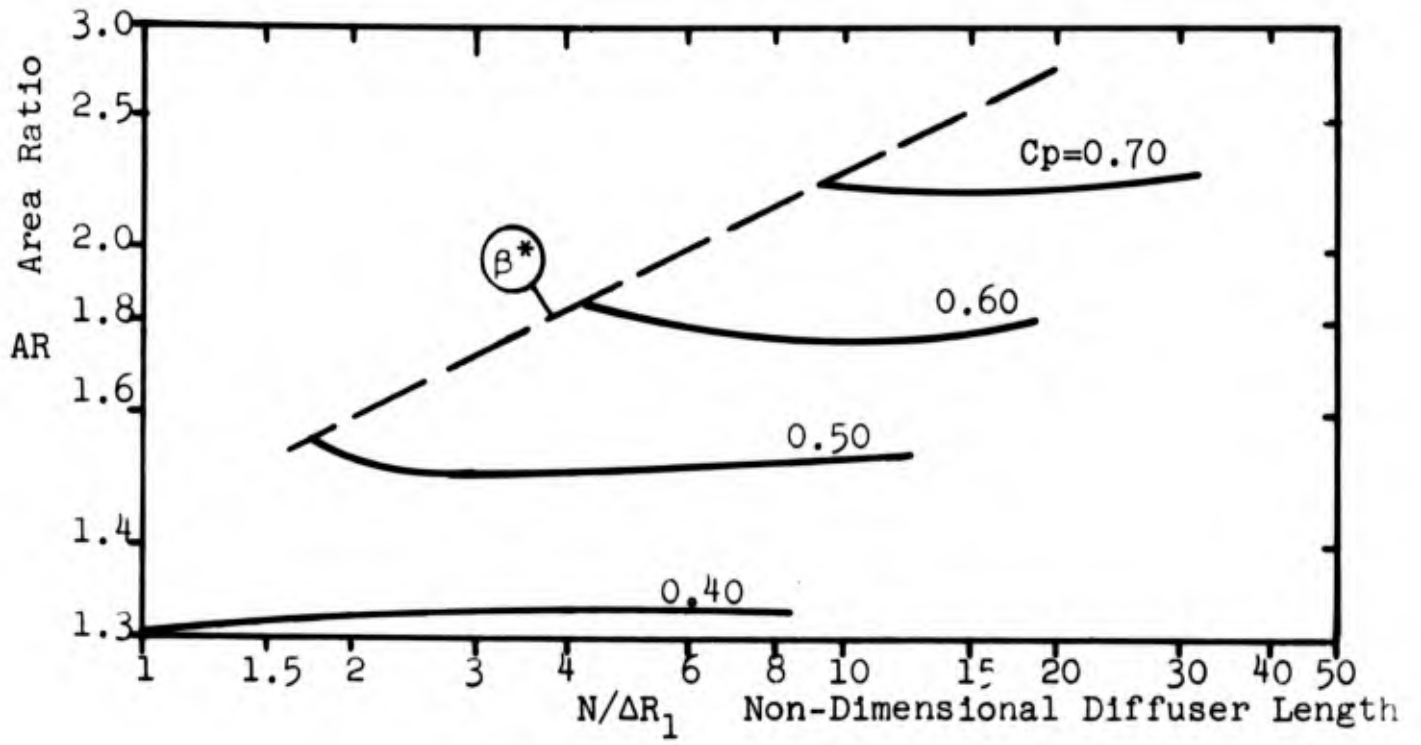
a. $B_1 = 0.0075$



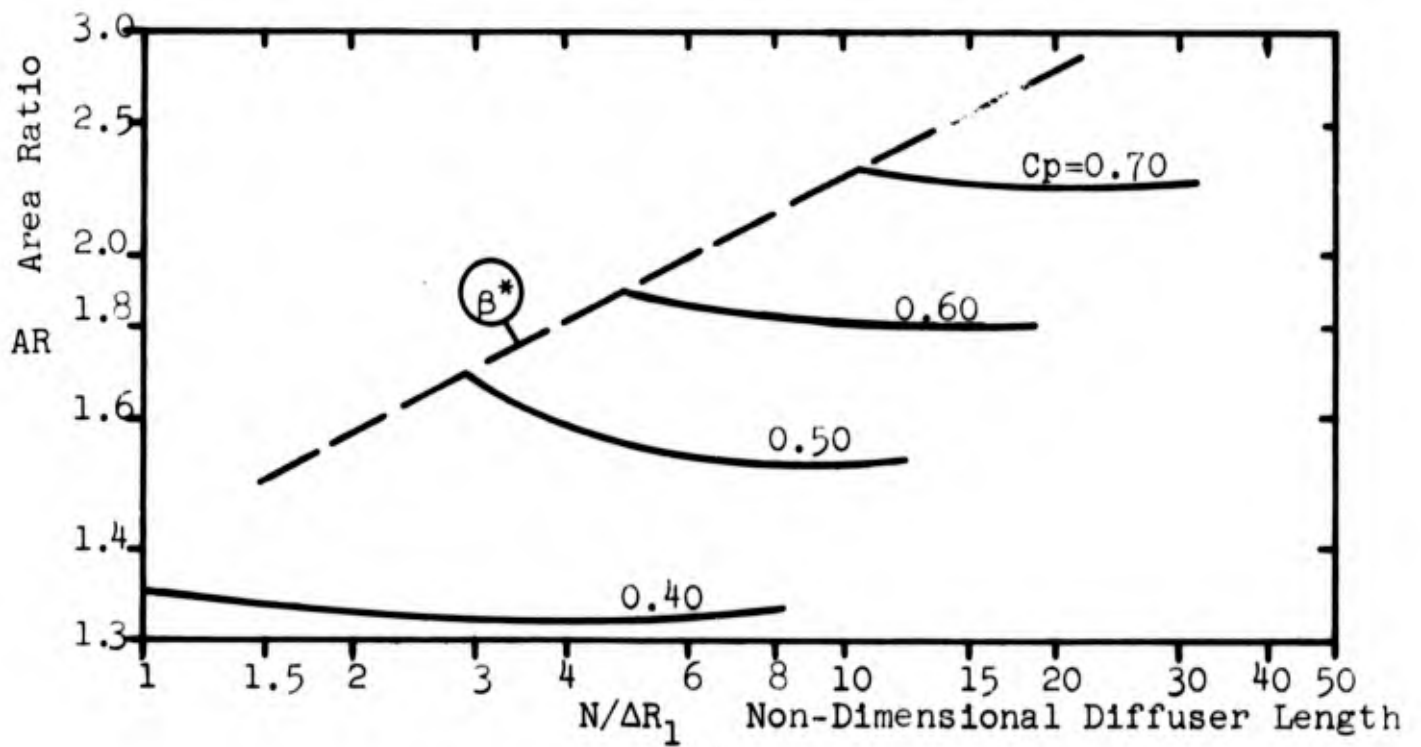
b. $B_1 = 0.015$

Fig. 20 Performance charts for annular diffusers.

β^* $\beta^* = 0.48$; indicates probable inception of appreciable stall.

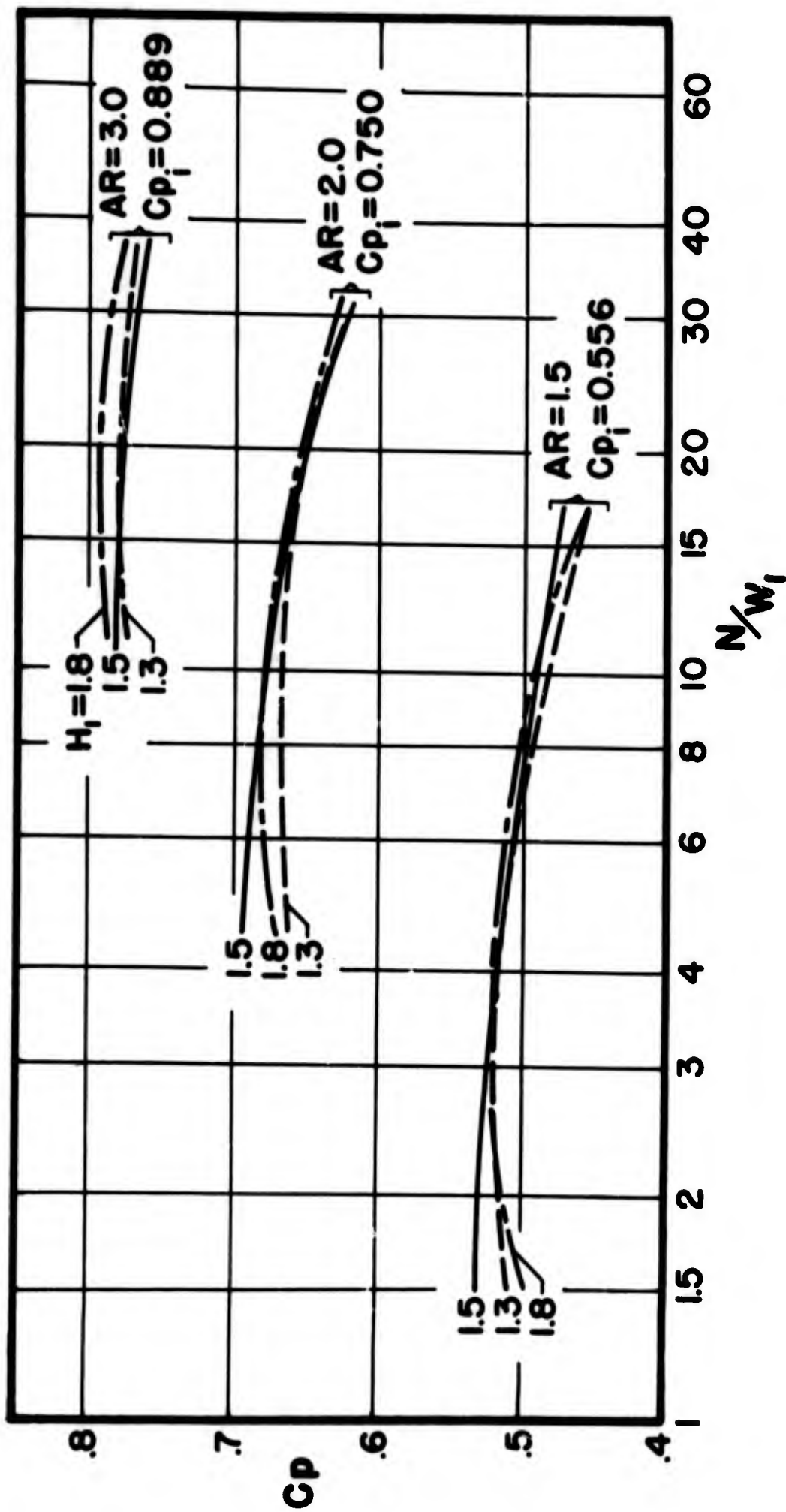


c. $B_1 = 0.03$



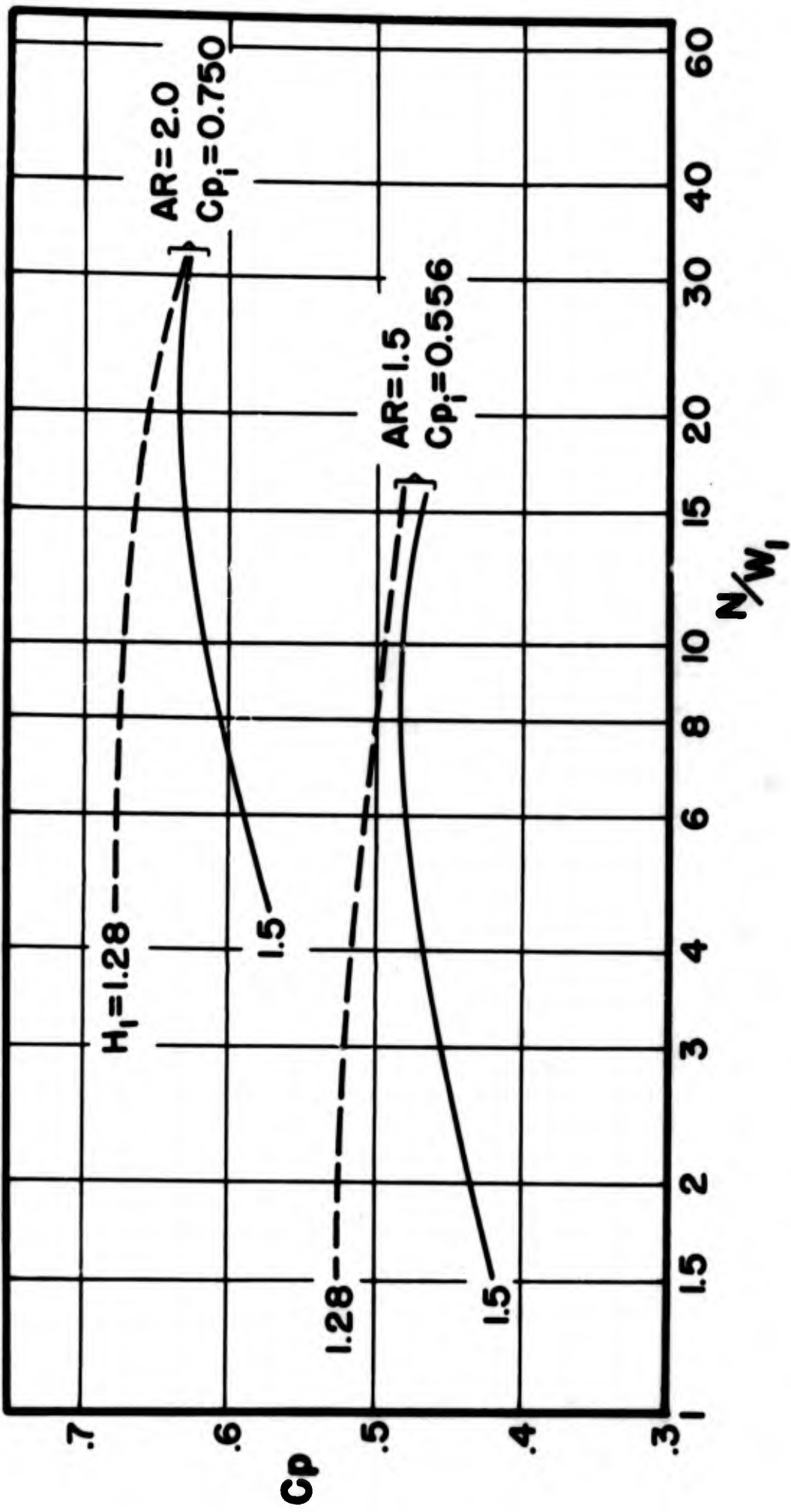
d. $B_1 = 0.05$

Fig. 20 Concluded.



a. $B_1 = 0.015$

Fig. 21 The predicted effects of inlet boundary layer shape parameter, H_1 , on two-dimensional diffuser performance. $Re = 1.45 \times 10^5$.



b. $B_1 = 0.05$

Fig. 21 Concluded.

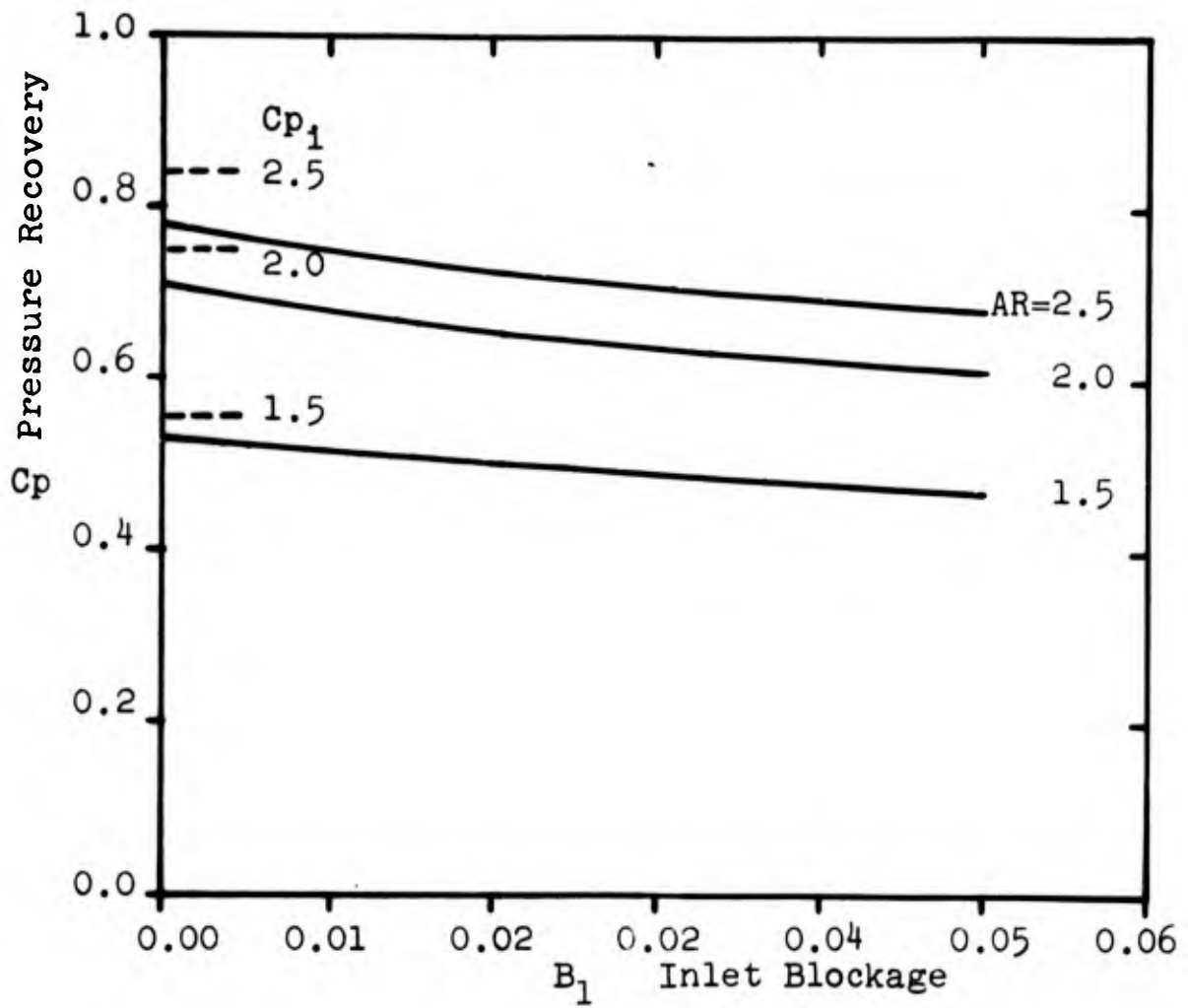


Fig. 22 The predicted effect of B_1 on pressure recovery at constant area ratios for class A diffusers.

REFERENCES

- Ackeret, J. [1958], "Grenzschichten in geraden und gekrümmten Diffusoren," (Boundary Layers in Straight and Curved Diffusers). Boundary Layer Research, IUTAM Symposium 1957, Springer-Verlag, Berlin, 1958, pp. 22-40.
- Ainley, D. G. [1952], "Investigation of Airfoil through some Annular Diffusers," Great Britain ARC Power Jets Report No. R 1151, 1952 (uncertain).
- Carlson, J. [1965], "The Effect of Wall Shape on Flow Regimes and Performance in Straight Two-Dimensional Diffusers," Engineers Thesis, Thermosciences Division, Mechanical Engineering Department, Stanford University, June 1965, (to be published).
- Copp, M. R. [1951], "Effects of Inlet Wall Contour on the Pressure Recovery of a 10° 10-inch I.D. Conical Diffuser," NACA Research Memorandum L51E11a, September 1951.
- von Doenhoff, A. E. and Tetervin, N. [1943], "Determination of General Relations for the Behavior of Turbulent Boundary Layers," NACA Report 772, 1943.
- Fox, R. W. and Kline, S. J. [1960], "Flow Regime Data and Design Methods for Curved Subsonic Diffusers," Report PD-6, Dept. of Mechanical Engineering, Stanford University, August 1960.
- Fox, R. W. and Kline, S. J. [1962], "Flow Regime Data and Design Methods for Curved Subsonic Diffusers," TASME, Jour. Basic Engineering, Vol. 84, Series D, September 1962, pp. 303-312.
- Gersten, K. [1959a], "Corner Interference Effects," AGARD Report 299, March 1959.
- Gersten, K. [1959b], "Die Grenzschichtströmung in einer rechtwinkligen Ecke," (The Boundary Layer Flow in a Right-angle Corner), ZAMM, Vol. 39, 1959, pp. 428-429.
- Gibson, A. H. [1910], "On the Flow of Water through Pipes and Passages Having Converging or Diverging Boundaries," Proc. Royal Society (London), Series A, Vol. 83, No. 563, March 1910, pp. 366-378.
- Gibson, A. H. [1912], "Conversion of Kinetic to Potential Energy in the Flow of Water through Passages Having Divergent Boundaries," Engineering, Vol. 93, 1912, pp. 205-206.

- Gibson, A. H. [1913], "On the Resistance to Flow of Water through Pipes or Passages Having Divergent Boundaries," *Trans. Royal Society (Edinburgh)*, Vol. 48, Pt. 1, art. no. 5, 1913, pp. 97-116. This reference also contains the results of the 1910 and 1912 papers.
- Hudimoto, B. [1952], "The Experimental Results of Diverging Flows," *Bulletin of the Engineering Research Institute, Kyoto Univ.*, Vol. 2, September 1952, pp. 18-23.
- Johnston, J. P. [1959], "Summary of Results of Tests on Short Conical Diffusers with Flow Control Inserts; as of June 1, 1959," *Technical Note Number 71, Advanced Engineering Department, Ingersoll-Rand Company*, June 1959.
- Kline, S. J. [1959], "On the Nature of Stall," *TASME, Jour. Basic Engineering*, Vol. 81, Series D, September 1959, pp. 305-320.
- Kline, S. J., Abbott, D. E., and Fox, R. W. [1959], "Optimum Design of Straight-Walled Diffusers," *TASME, Jour. Basic Engineering*, Vol. 81, Series D, September 1959, pp. 321-329.
- Kmonicek, V. [1959], "Unterschallstromung in Kegeldiffusoren," *Acta Technica (Czechoslovakia) No. 5*, 1959.
- Ludwig, H. and Tillman, W. [1949], "Untersuchungen über die Wandschubspannung in turbulenten Reibungsschichten," *Ing. Arch.* 17, 288-299, 1949; (Translation: "Investigation of the Wall Shearing Stress in Turbulent Boundary Layers," *NACA TM 1285*, May 1950).
- Moore, C. A. and Kline, S. J. [1958], "Some Effects of Vanes and of Turbulence on Two-Dimensional Wide-Angle Subsonic Diffusers," *NACA TN 4080*, June 1958. Essentially the same material was originally published under the same title as *Final Report on NACA Contract NAW-6317 and Progress Report on NACA Contract NAW-6404*, Dept. of Mechanical Engineering, Stanford University, September 1955.
- Nelson, W. J. and Popp, E. G. [1949], "Performance Characteristics of Two 6° and Two 12° Diffusers at High Flow Rates," *NACA Research Memorandum L9H09*, October 1949.
- Nikuradse, J. [1929], "Untersuchungen über die Strömungen des Wassers in Konvergenten und Divergenten Kanälen," (Research on the Flow of Water in Converging and Diverging Channels), *Forschungsarbeiten des VDI*, No. 289, 1929.
- Norbury, J. F. [1959], "Some Measurements of Boundary-Layer Growth in a Two-Dimensional Diffusers," *TASME, Jour. Basic*

Engineering, Vol. 81, Series D, No. 3, September 1959, pp. 285-294.

Patterson, G. N. [1938], "Modern Diffuser Design," Aircraft Engineering, Vol. 10, No. 115, September 1938, pp. 267-273.

Peters, H., "Conversion of Energy in Cross-Sectional Divergences under Different Conditions of Inflow," NACA Technical Memorandum No. 737, 1934.

Pierce, F. J. [1961], "The Turbulent Flow at the Plane of Symmetry of a Three-Dimensional Collateral Boundary Layer," Ph.D. Thesis, Cornell University, 1961.

Pierce, F. J. [1964], "The Turbulent Flow at the Plane of Symmetry of a Collateral Three-Dimensional Boundary Layer," TASME, Jour. Basic Engineering, Vol. 86, Series D, No. 2, June 1964, pp. 227-233.

Polzin, J. [1940], "Strömungsuntersuchungen an einen ebenen Diffusor," (Flow Investigations in a Two-Dimensional Diffuser), Ing.-Arch., Vol. 11, October 1940, pp. 361-385; also Min. Aircraft Prod. RTP transl. 1286.

Reneau, L. R. [1964], "Performance and Design of Straight Two-Dimensional Diffusers," Ph.D. Thesis, Stanford University, 1964.

Reneau, L. R., Johnston, J. P. and Kline, S. J. [1964], "Performance and Design of Straight Two-Dimensional Diffusers," Report PD-8, Thermosciences Division, Mechanical Engineering Department, Stanford University, September 1964.

Rippl, E. [1958], "Experimental Investigations Concerning the Efficiency of Slim Conical Diffusers and Their Behavior with Regards to Flow Separation," Monthly Technical Review, Vol. 2, No. 3, March 1958, pp. 64-70; (translated from Maschinenbautechnik, Vol. 5, No. 5, 1956, pp. 241-246).

Robertson, J. M. and Fraser, H. R. [1960], "Separation Prediction in Conical Diffusers," TASME, Jour. Basic Engineering, Vol. 82, Series D, March 1960, pp. 201-209.

Rotta, J. C. [1962], "Turbulent Boundary Layers in Incompressible Flow," Progress in Aeronautical Sciences, Vol. 2, Pergamon Press, Inc., 1962, pp. 1-221.

Schlichting, H. and Gersten, K. [1961], "Berechnung der Strömung in rotationssymmetrischen Diffusoren mit Hilfe der Grenzschichttheorie," (Calculation of the Flow in Rotationally Symmetric Diffusers with the Aid of Boundary Layer Theory),

Zeit. für Flugwissenschaften, Vol. 9, No. 4-5, April-May 1961, pp. 135-140.

Schubauer, G. B. and Tchen, C. M. [1961], "Turbulent Flow," Number 9, Princeton Aeronautical Paperbacks, Princeton University Press, Princeton, New Jersey, 1961.

Sovran, G. and Klomp, E. [1964], "Proposed Selection Chart for Straight-Walled Annular Diffusers with Non-Swirling Inlet Flow," General Motors Corporation Research Laboratories Technical Memorandum, Report No. 38-1376, May 1964.

Sprenger, H. [1959], "Experimentelle Untersuchungen an geraden und gekrümmten Diffusoren," (Experimental Research on Straight and Curved Diffusers), Mitteilung aus dem Institute für Aerodynamik an der ETH, Zurich, No. 27, 1959; (translated by Ministry of Aviation, Gt. Brit.).

Squire, H. B. [1950], "Experiments on Conical Diffusers," Great Britain ARC Reports and Memoranda No. 2751, November 1950.

Squire, H. B. and Young, A. D. [1938], "The Calculations of the Profile Drag of Aerofoils," Great Britain ARC Reports and Memoranda No. 1838, 1938.

Venturi, G. B. [1797], "Recherches Experimentales sur le Principe de Communication Lateral dans les Fluides," (Experimental Research on the Principle of Diffusion of Fluids), Paris, 1797, (translation in Nicholson's Journal of Natural Philosophy, Vol. 3, London, 1802).

Waitman, B. A., Reneau, L. R., and Kline, S. J. [1960], "Effects of Inlet Conditions on Performance of Two-Dimensional Diffusers," Report PD-5, Dept. of Mechanical Engineering, Stanford University, March 1960.

Waitman, B. A., Reneau, L. R. and Kline, S. J. [1961], "Effects of Inlet Conditions on Performance of Two-Dimensional Diffusers," TASME, Jour. Basic Engineering, Vol. 83, Series D, September 1961, pp. 349-360.

Young, A. D. and Green, G. L. [1944], "Tests of High-Speed Flow in Diffusers of Rectangular Cross-Section," Aero. Research Council, Tech. Report 2201, 1944.

APPENDIX A
DETAILED FLOW EQUATIONS

In Chapter 1, the generalized equations that model the flow in class A diffusers were developed. The detailed equations that must be solved for each of the cases in the following outline will be presented in this appendix.

A. INCOMPRESSIBLE

1. Two-dimensional
 - a. straight walls, Reneau [1964]
 - b. contoured walls, Reneau [1964]
 - c. correction for corner boundary layer
 - d. inlet boundary layer of unequal thickness on opposite walls (asymmetric inlet velocity distribution)
2. Three-dimensional, straight walls
3. Conical
 - a. straight walls
 - b. contoured walls
4. Annular, straight walls

B. COMPRESSIBLE FLOW

1. Two-dimensional, straight walls
2. Conical, straight walls
3. Annular, straight walls

For notational convenience, the following additional nomenclature will be defined:

$$\begin{aligned} \bar{\alpha} &= 0.123 e^{-1.56H} \left(U \frac{\theta}{v} \right)^{-0.268} \\ \zeta &= -2e^{4.68(H-2.975)} \left[2.558 \ln \left(4.075 \frac{U\theta}{v} \right) \right]^2 \\ \gamma &= -e^{4.68(H-2.975)} (H - 1.286) \frac{2.035}{6} \end{aligned} \tag{A1}$$

A. INCOMPRESSIBLE FLOW

1. a. Two-dimensional, straight walls

$$\frac{d\theta_p}{dx} = \bar{\alpha}_p - \theta_p \left[\frac{2}{\epsilon} \Gamma_d + (H_p + 2) \frac{1}{U} \frac{dU}{dx} \right]$$

$$\frac{d\theta_d}{dx} = \bar{\alpha}_d - \theta_d \left[\frac{-2}{\kappa} \Gamma_p + (H_d + 2) \frac{1}{U} \frac{dU}{dx} \right]$$

$$\frac{dH_p}{dx} = \zeta_p \frac{1}{U} \frac{dU}{dx} + \gamma_p$$

$$\frac{dH_d}{dx} = \zeta_d \frac{1}{U} \frac{dU}{dx} + \gamma_d$$

$$\frac{dH_p}{dx} = \theta_p \frac{d\delta_p^*}{dx} + \delta_p^* \frac{d\theta_p}{dx}$$

$$\frac{dH_d}{dx} = \theta_d \frac{d\delta_d^*}{dx} + \delta_d^* \frac{d\theta_d}{dx}$$

$$\frac{1}{U} \frac{dU}{dx} = - \frac{2}{\epsilon} \Gamma_d + \frac{2}{\kappa} \Gamma_p$$

$$U = \frac{\lambda}{\epsilon \kappa} .$$

(A2)

where

$$\epsilon = W_1 + 2(x \tan \phi - \delta_d^*)$$

$$\kappa = b - 2\delta_p^*$$

$$\lambda = U_1 (W_1 - 2\delta_{d,1}^*) (b - 2\delta_{p,1}^*)$$

$$\Gamma_d = \tan \phi - \frac{d\delta_d^*}{dx} ; \Gamma_p = \frac{d\delta_p^*}{dx} \quad (A3)$$

b. Two-dimensional, contoured walls

For contoured walls, equations (A2) and (A3) apply with the change

$$\begin{aligned}\epsilon &= W(x) - 2\delta_d^* \\ \Gamma_d &= \frac{dW}{dx} - 2 \frac{d\delta_d^*}{dx}\end{aligned}\quad (A4)$$

For the case where

$$AR(x) = 1 + (AR - 1) \frac{x}{N} \left[1 + \alpha \left(1 - \frac{x}{N} \right) \right] \quad (A5)$$

then

$$\begin{aligned}\epsilon &= W_1 AR(x) \\ \Gamma_d &= \frac{W_1}{N} (AR - 1) \left[1 - \alpha \left(1 - \frac{2x}{N} \right) \right]\end{aligned}\quad (A6)$$

c. Two-dimensional, correction for corner boundary layer

For the corner boundary layer correction, equations (A2) and (A3) apply with the change

$$U = \frac{\lambda}{\epsilon \kappa - (\delta_3^*)^2} \quad (A7)$$

where δ_3^* is an additional displacement thickness resulting from the corner boundary layer interference; the relation between the flow variables and δ_3^* will be developed in Appendix B.

d. Two-dimensional, inlet boundary layers of unequal thickness on opposite walls

$$\begin{aligned}\frac{d\theta_{p_a}}{dx} &= \bar{\alpha}_{p_a} - \theta_{p_a} \left[\frac{1}{\epsilon} \Gamma_d + (H_{p_a} + 2) \frac{1}{U} \frac{dU}{dx} \right] \\ \frac{d\theta_{p_b}}{dx} &= \bar{\alpha}_{p_b} - \theta_{p_b} \left[\frac{1}{\epsilon} \Gamma_d + (H_{p_b} + 2) \frac{1}{U} \frac{dU}{dx} \right]\end{aligned}$$

$$\frac{d\theta_{d_a}}{dx} = \bar{\alpha}_{d_a} - \theta_{d_a} \left[-\frac{1}{\kappa} \Gamma_p + (H_{d_a} + 2) \frac{1}{U} \frac{dU}{dx} \right]$$

$$\frac{d\theta_{d_b}}{dx} = \bar{\alpha}_{d_b} - \theta_{d_b} \left[-\frac{1}{\kappa} \Gamma_p + (H_{d_b} + 2) \frac{1}{U} \frac{dU}{dx} \right]$$

$$\frac{dH_{p_a}}{dx} = \zeta_{p_a} \frac{1}{U} \frac{dU}{dx} + \gamma_{p_a}$$

$$\frac{dH_{p_b}}{dx} = \zeta_{p_b} \frac{1}{U} \frac{dU}{dx} + \gamma_{p_b}$$

$$\frac{dH_{d_a}}{dx} = \zeta_{d_a} \frac{1}{U} \frac{dU}{dx} + \gamma_{d_a}$$

$$\frac{dH_{d_b}}{dx} = \zeta_{d_b} \frac{1}{U} \frac{dU}{dx} + \gamma_{d_b}$$

$$\frac{dH_{p_a}}{dx} = \theta_{p_a} \frac{d\delta_{p_a}^*}{dx} + \delta_{p_a}^* \frac{d\theta_{p_a}}{dx}$$

$$\frac{dH_{p_b}}{dx} = \theta_{p_b} \frac{d\delta_{p_b}^*}{dx} + \delta_{p_b}^* \frac{d\theta_{p_b}}{dx}$$

$$\frac{dH_{d_a}}{dx} = \theta_{d_a} \frac{d\delta_{d_a}^*}{dx} + \delta_{d_a}^* \frac{d\theta_{d_a}}{dx}$$

$$\frac{dH_{d_b}}{dx} = \theta_{d_b} \frac{d\delta_{d_b}^*}{dx} + \delta_{d_b}^* \frac{d\theta_{d_b}}{dx}$$

$$\frac{1}{U} \frac{dU}{dx} = -\frac{1}{\epsilon} \Gamma_d + \frac{1}{\kappa} \Gamma_p$$

$$U = \frac{\lambda}{\epsilon \kappa}$$

(A8)

where

$$\begin{aligned}\Gamma_p &= \frac{d\delta_{p_a}^*}{dx} + \frac{d\delta_{p_b}^*}{dx} \\ \Gamma_d &= 2 \tan\phi - \frac{d\delta_{d_a}^*}{dx} - \frac{2\delta_{d_b}^*}{dx} \\ \epsilon &= W_1 + 2x \tan\phi - \delta_{d_a}^* - \delta_{d_b}^* \\ \kappa &= b - \delta_{p_a}^* - \delta_{p_b}^* \\ \lambda &= U_1 \left(W_1 - \delta_{d_{a,1}}^* - \delta_{d_{b,1}}^* \right) \left(b - \delta_{p_{a,1}}^* - \delta_{p_{b,1}}^* \right) \quad (A9)\end{aligned}$$

2. Three-dimensional, straight walls

For three-dimensional diffusers, equations (A2) apply with equations (A3) replaced by

$$\begin{aligned}\Gamma_d &= \tan\phi_1 - \frac{d\delta_d^*}{dx} \\ \Gamma_p &= -\tan\phi_2 + \frac{d\delta_p^*}{dx} \\ \epsilon &= W_1 + 2(x \tan\phi_1 - \delta_d^*) \\ \kappa &= b_1 + 2(x \tan\phi_2 - \delta_p^*) \\ \lambda &= U_1 (W_1 - 2\delta_{d,1}^*) (b_1 - 2\delta_{p,1}^*) \quad (A10)\end{aligned}$$

3. a. Conical, straight walls

$$\begin{aligned}\frac{d\theta}{dx} &= \xi \bar{\alpha} - \theta \left[\frac{\Gamma}{\epsilon} + (2 + H) \frac{1}{U} \frac{dU}{dx} \right] \\ \frac{dH}{dx} &= \zeta \frac{1}{U} \frac{dU}{dx} - \gamma \xi \\ \frac{dH}{dx} &= \theta \frac{d\delta^*}{dx} + \delta^* \frac{d\theta}{dx}\end{aligned}$$

$$\frac{1}{U} \frac{dU}{dx} = \frac{-2}{\kappa} \left(\Gamma - \frac{d\delta^*}{dx} \right)$$

$$U = \frac{\lambda}{\kappa^2} \quad (A11)$$

where

$$\Gamma = \tan\phi$$

$$\epsilon = R_1 + x \tan\phi$$

$$\xi = 1/\cos\phi \quad (\text{This term represents a length correction since the boundary layer grows on a diverging wall while the coordinate, } x, \text{ is measured on the center-line.})$$

$$\kappa = \epsilon - \delta^*$$

$$\lambda = U_1 (R_1 - \delta_1^*)^2 \quad (A12)$$

b. Conical, contoured walls

For contoured walls where the change in area ratio is given by

$$AR(x) = 1 + (AR - 1) \frac{x}{N} \left[1 + \alpha \left(1 + \frac{x}{N} \right) \right]$$

equations (A11) apply with

$$\Gamma = \frac{R_1 (AR - 1) \left(1 + \alpha \left(1 - 2x/N \right) \right)}{2N \sqrt{AR(x)}}$$

$$\epsilon = R_1 \sqrt{AR(x)}$$

$$\xi = \sqrt{\Gamma^2 - 1}$$

$$\kappa = \epsilon - \delta^*/\xi \quad \lambda = U_1 (R_1 - \delta_1^*)^2 \quad (A13)$$

4. Annular, straight walls

$$\frac{d\theta_o}{dx} = \frac{\bar{\alpha}_o}{\cos\phi_o} - \theta_o \left[\frac{\tan\phi_o}{\epsilon_o} + (2 + H) \frac{1}{U} \frac{dU}{dx} \right]$$

$$\frac{d\theta_I}{dx} = \frac{\bar{\alpha}_I}{\cos\phi_I} - \theta_I \left[\frac{\tan\phi_I}{\epsilon_I} + (2 + H) \frac{1}{U} \frac{dU}{dx} \right]$$

$$\frac{dH_o}{dx} = \zeta_o \frac{1}{U} \frac{dU}{dx} - \frac{\gamma_o}{\cos\phi_o}$$

$$\frac{dH_I}{dx} = \zeta_I \frac{1}{U} \frac{dU}{dx} - \frac{\gamma_I}{\cos\phi_I}$$

$$\frac{dH_o}{dx} = \theta_o \frac{d\delta_o^*}{dx} + \delta_o^* \frac{d\theta_o}{dx}$$

$$\frac{dH_I}{dx} = \theta_I \frac{d\delta_I^*}{dx} + \delta_I^* \frac{d\theta_I}{dx}$$

$$\frac{1}{U} \frac{dU}{dx} = -2 \frac{\kappa_o \left[\tan\phi_o - \frac{d\delta_o^*}{dx} \right] - \kappa_I \left[\tan\phi_I + \frac{d\delta_I^*}{dx} \right]}{\kappa_o^2 - \kappa_I^2}$$

$$U = \frac{U_1 \left[(R_{o,1} - \delta_{o,1}^*)^2 - (R_{I,1} + \delta_{I,1}^*)^2 \right]}{\kappa_o^2 - \kappa_I^2} \quad (A14)$$

where

$$\epsilon_o = R_{o,1} + x \tan\phi_o$$

$$\epsilon_I = R_{I,1} + x \tan\phi_I$$

$$\kappa_o = \epsilon_o - \delta_o^*$$

$$\kappa_I = \epsilon_I + \delta_I^* \quad (A15)$$

B. COMPRESSIBLE FLOW

1. Two-dimensional, straight walls

For the compressible case, equations (A2) and (A3) apply with the change

$$\frac{1}{U} \frac{dU}{dx} = -\left(\frac{2}{\epsilon} \Gamma_d + \frac{2}{k} \Gamma_p\right) \left[\frac{1}{1 - M^2} \right]$$

$$U = \frac{\lambda}{\epsilon k} \left[\frac{1 + 0.2 M^2(x)}{1 + 0.2 M_1^2} \right] ; k = 1.4 \quad (A16)$$

2. Conical, straight walls

For the compressible case, equations (A11) and (A12) apply with the change

$$\frac{1}{U} \frac{dU}{dx} = -\frac{2}{k} \left(\Gamma - \frac{d\delta^*}{dx} \right) \frac{1}{1 - M^2}$$

$$U = \frac{\lambda}{k^2} \left[\frac{1 + 0.2 M^2(x)}{1 + 0.2 M_1^2} \right] ; k = 1.4 \quad (A17)$$

3. Annular, straight walls

For the compressible case, equations (A14) and (A15) apply with the change

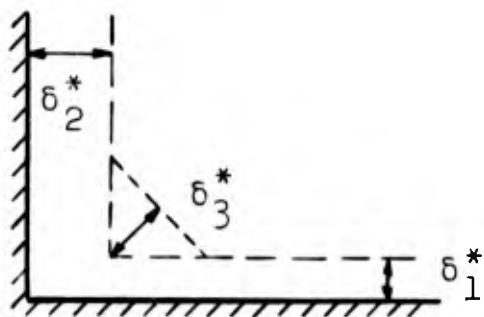
$$\frac{1}{U} \frac{dU}{dx} = -2 \frac{\kappa_o \left[\tan\phi_o - \frac{d\delta_o^*}{dx} \right] - \kappa_I \left[\tan\phi_I + \frac{d\delta_I^*}{dx} \right]}{\kappa_o^2 - \kappa_I^2} \left[\frac{1}{1 - M^2} \right]$$

$$U = \frac{U_1 \left[(R_{o,1} - \delta_{o,1}^*)^2 - (R_{I,1} + \delta_{I,1}^*)^2 \right]}{\kappa_o^2 - \kappa_I^2} \left[\frac{1 + 0.2 M^2(x)}{1 + 0.2 M_1^2} \right] ;$$

$$k = 1.4 \quad (A18)$$

APPENDIX B
CORNER BOUNDARY LAYER CORRECTION

The effect of boundary layer interference in a corner can be described by an additional displacement thickness, δ_3^* , as indicated in the following sketch:



Flow into paper; δ_1^* and δ_2^* are the displacement thicknesses far from the corner; δ_3^* is the corner interference displacement thickness.

Gersten [1959a] experimentally determined a correlation for δ_3^* to be

$$\frac{\delta_3^*}{l} = \frac{7.0}{\sqrt{\text{Re}_l}} f_3 [\text{Eu}] \quad (\text{B1})$$

where l is an entry length and

$f_3[\text{Eu}]$ was given graphically by Gersten and has been approximated by a polynomial to be (fitted by a least squares technique)

$$f_3[\text{Eu}] = 1.0 - 3.083 \text{Eu} - 57.83 \text{Eu}^2 - 526.7 \text{Eu}^3 - 866.7 \text{Eu}^4 \quad (\text{B2})$$

and

$$\text{Eu} = \frac{l}{U} \frac{dU}{dx}$$

The initial entry length, l_s , can be determined from

$$\frac{\delta_s^*}{l_s} = \frac{0.052}{(\text{Re}_l)^{1/5}} \quad (\text{B3})$$

as given by Gersten for a fully turbulent entry in a zero

pressure gradient. The equation (B3) can be solved for l_s giving,

$$l_s = \left(\frac{\delta_s^*}{0.052} \right)^{5/4} \left(\frac{U_s}{v} \right)^{1/4} \quad (B4)$$

the values of δ_s^* , U_s , and v are known for the inlet of the diffuser.

The length changes as the flow proceeds down the diffuser and equals

$$l = l_s + x \quad (B5)$$

where x is the centerline length measured from the diffuser inlet.

APPENDIX C

LETTER OF PERMISSION FROM INGERSOLL-RAND COMPANY

The following letter from the Ingersoll-Rand Company grants permission to use the diffuser performance data reported in their internal report TN-71:

HPE:24:012565



Ingersoll-Rand Company

Established 1871

RESEARCH AND DEVELOPMENT

BEDMINSTER, N. J. 07921

25 January 1965

Dr. James P. Johnston
Associate Professor, Thermosciences Div.
Mechanical Engineering Department
Stanford University
Stanford, California

Dear Jim:

In your letter of January 4, you are asking me for the release of information contained in TN-71, "Summary of Results of Tests in Short Conical Diffusers with Flow Control Inserts as of June 1, 1959".

I wish herewith to give permission to use this data in your student's Ph.D. thesis and in a subsequent publication. Of course, it is expected that the source will be acknowledged.

Sincerely yours,

INGERSOLL-RAND COMPANY

H. P. Eichenberger

Hans P. Eichenberger
Director of Research

HPE:gr

APPENDIX D
SUGGESTED CRITICAL EXPERIMENTS

In this appendix, a few additional experiments are suggested to check the present theory in extreme cases for which data do not presently exist. These suggested experiments and their purpose are:

1. Measure the effect of the following on the pressure recovery of class A diffusers:
 - a. Geometry for fixed area ratio and inlet blockage,
 - b. Geometry for fixed area ratio and inlet boundary layer displacement thickness,
 - c. Inlet shape parameter for fixed area ratio and inlet blockage;
2. Measure the effect of aspect ratio on the pressure recovery of two-dimensional diffusers; particularly for aspect ratio less than one;
3. Measure the pressure recovery in detail for two or three three-dimensional diffusers which satisfy class A restrictions.

In addition to the diffuser performance experiments, the assumption that the parameter, β^* , is a reliable predictor of first appreciable stall in three-dimensional, conical, and annular diffusers needs to be checked experimentally.

Associated with this check is the necessity of defining first appreciable stall for these geometries which is consistent with the two-dimensional definition.

Besides considering the basic objectives of the experiments, the experimenter must design his apparatus so that the inlet boundary layer parameters can be measured.